R. & M. No. 2975
(16,957 and 16,958)
A.R.C. Technical Report

MINISTRY OF SUPPLY

AERONAUTICAL RESEARCH COUNCIL
REPORTS AND MEMORANDA

# Investigations on an Experimental Air-Cooled Turbine

## Part I.—General Description of Turbine and Experimental Technique

*By*
D. G. AINLEY and N. E. WALDREN

## Part II.—Cooling Characteristics of Blades having a Multiplicity of Small Diameter Coolant Passages

*By*
D. G. AINLEY, N. E. WALDREN and K. HUGHES



LONDON: HER MAJESTY'S STATIONERY OFFICE
1957
EIGHTEEN SHILLINGS NET

# Investigations on an Experimental Air-Cooled Turbine

COMMUNICATED BY THE PRINCIPAL DIRECTOR OF SCIENTIFIC RESEARCH (AIR), MINISTRY OF SUPPLY

*Reports and Memoranda No.* 2975*
*March,* 1954

## PART I

## General Description of Turbine and Experimental Technique

*By*
D. G. AINLEY and N. E. WALDREN

*Summary*.—Tests on internally air-cooled turbine blades operating under realistic conditions are required to determine (*a*) the degree of cooling achievable and (*b*) the effects of cooling on the overall turbine performance. This requirement has led to the manufacture and installation of an experimental air-cooled turbine specially designed for testing internally air-cooled nozzle and rotor blades. This part of the report records a general description of the turbine, the first set of cooled blades to be tested, and the associated instrumentation. It also records some results of early tests made to check the cooling of the turbine structure (excluding blades).

1. *Introduction*.—The possible advantages to be derived from the development of cooled turbines are several-fold. Cooled blades might be constructed of a heat resistant material, as in the present instance, and be employed in an engine operating with the highest possible gas temperature to secure simply a high specific power output. In addition the engine cycle might include heat exchanges and intercooling to take full advantage of the high peak cycle temperature for securing a high overall thermal efficiency. Alternatively, the cooled blades might be constructed from low-alloy steels and used in place of high-alloy uncooled blades in order to minimize the use of expensive and strategically important metals.

Adoption of turbine cooling with any of these applications in mind raises a number of problems for which both theoretical and experimental research is required with several objectives in view. Broadly, the objectives may be summarised as follows :

(*a*) Determination of gas to blade and blade to coolant heat transfer coefficients for a variety of blade shapes and cooling systems

(*b*) Determination of blade metal temperature distributions for a variety of blade shapes and cooling systems

(*c*) Determination of the influence of metal temperature distributions, in relation to blade material properties, on the strength and life of the blades. This is necessary because of the thermal stresses created by non-uniformity in blade metal temperature, these stresses being additional to the centrifugal, gas bending, and vibratory stresses currently encountered in uncooled turbine blades. In addition local hot spots on the blade may lead to excessive local oxidation of the blade material

(*d*) Determination of the effects of cooling on the turbine performance characteristics and, in particular, on the associated engine performance.

*N.G.T.E. Reports R.153 and R.154, received 30th July, 1954.

Objectives (*a*) and (*b*) have been partially covered by theoretical work and experimental work on cooled blades in stationary cascade tunnels (Ref. 1 to 4). Experimental studies of cooled blades operating in a real turbine stage are necessary to cover objectives (*c*) and (*d*) and also to qualify the validity of results obtained in stationary cascade tunnels. The latter is considered necessary since secondary flows and boundary-layer flows in a turbine stage (particularly a rotor blade) will differ from those in a cascade tunnel and may have important influences on the heat transfer coefficients as obtained in cascade tunnels.

To assist in the task of reaching an answer to these may problems an experimental single-stage air-cooled turbine has been designed, built, and operated. The turbine, together with the first set of blades to be tested, was designed and manufactured to Ministry of Supply requirements by the General Electric Company Ltd., and has been erected and operated at the National Gas Turbine Establishment.

This unit, together with a power absorption dynamometer and a group of inlet combustion chambers designed to operate with a gas temperature range of 600 to 1,200 deg C (1,100 to 2,200 deg F) provides an apparatus for obtaining overall performance characteristics and cooling characteristics of internally air-cooled rotor and stator blades and also root-cooled rotor blades.

The present Report gives a general description of the turbine, the test rig, and instrumentation. It also records some early tests made to check the cooling of components of the rig other than the blades and also tests to measure turbine inlet temperature and velocity distributions.

Part II of the Report records results relating to the cooling of the first set of cooled blades. The work recorded in Parts I and II of this Report has been summarily presented in Refs. 5 and 6.

2. *Description of the Turbine.*—A cross-section drawing of the turbine is shown in Fig. 1. It consists essentially of a single stage, the rotor of which is supported centrally between two ball journal bearings. A feature of the turbine is that no struts supporting either the bearing housings or the inner structure of the turbine pass directly through the hot gas stream. The hot gas enters the turbine through eight inlet branches, fed from eight can-type combustion chambers, and leaves the turbine through eight exhaust ducts grouped around the exhaust annulus, the main struts supporting the bearings and inner structure at entry and exit passing between adjacent inlet branches and between adjacent exhaust branches.

The turbine has a rotor blade tip diameter of 24 in. and a blade height of 2·5 in. This size was dictated largely by the maximum delivery of the service compressor plant which supplied compressed air for the operation of the test rig. The design tip speed is 943 ft/sec (corresponding to 9,000 r.p.m.). The design pressure ratio of the stage is about 1·5 and the unit is intended to operate over a range of inlet pressure of 1·1 to 3·0 atmospheres—this range in pressure being desirable to achieve a range of operating Reynolds number* on the rotor blades of about $5 \times 10^4$ to $2 \times 10^5$. The high inlet pressures are achieved by throttling the turbine exhaust.

The whole turbine unit has been designed with a view to permitting operation at inlet gas temperatures up to as high as 1,200 deg C. Operation at such a temperature necessitates provision of a means of cooling for a large part of the turbine structure in addition to the blades.

At the turbine inlet the annulus walls are formed of sheet metal liners (fabricated from Nimonic 75 sheet), cooling air being passed underneath the liners (*see* Fig. 2). On the outer diameter wall the cooling air passes beneath the liner and is discharged into the main gas stream from an annular gap just ahead of the nozzle guide vanes and provides a small degree of film cooling over the nozzle blade platforms. On the inner diameter wall a portion of the cooling air is discharged into the gas stream through a row of holes in the liner to provide additional film cooling for the liner.

*$R_e$ defined by outlet gas velocity relative to the blade, outlet gas kinematic viscosity, and blade chord.

The remainder of the inner wall cooling air passes underneath a nozzle shroud liner to be finally discharged into the gas stream through an annular gap downstream of the nozzle blades. This discharged air provides additionally a small measure of film cooling over the rotor blade platform. Cooling air to the nozzle blades is fed in at the roots from an annular header surrounding the nozzle roots and is discharged from the nozzle blade tips into the main gas stream.

Thus the cooling air introduced into the turbine inlet (*a*) cools the sheet metal walls (*b*) provides a heat insulating layer between the sheet metal walls and the adjacent turbine structure and (*c*) discharges eventually into the main gas stream to expand through the turbine rotor, carrying with it most of the heat picked up in the course of its cooling duty. In this way there is very little net heat loss in the cycle resulting from cooling the turbine inlet, although, of course, the influence of introducing the cooling air into the main gas stream in reducing the mean effective inlet gas temperature must be taken into account. The actual quantities of cooling air involved and the relevant metal temperatures achieved are discussed later in section 5.

The turbine rotor blade roots are clamped between twin discs and the rotor blade cooling air is passed from the rotor shaft to the blade roots between the two discs. Leads from thermocouples inserted in the blades also pass radially inwards between the discs and are led along the shaft to a slip ring unit mounted at the free end of the shaft. The rotor thermocouple installation, which introduces certain novelties, is described in greater detail in section 4.3.4. Cooling air is fed into the rotor shaft from a small ' header ' surrounding the shaft on the upstream side of the rotor discs. This header is provided with labyrinth gland seals (A and B) on either side to minimise leakage of coolant. Air pressures are measured on either side of these seals, which have been carefully calibrated in order that leakage losses may be estimated. Rotor blade cooling air is eventually discharged from the blade tips into the main gas stream.

The outer faces of the rotor discs are provided with cover plates and a substantial amount of cooling air can be passed radially outwards between disc and cover plate on the turbine inlet side of the disc, axially through holes bored through the disc rims and across the blade roots, and radially inwards between disc and cover plate on the turbine outlet stream side of the disc, to be finally discharged from the turbine through a specially provided exhaust duct. This arrangement was included for the special purpose of providing substantial quantities of cooling air for root-cooling of blades if it should be wished to test root-cooled blades in the future. During the current series of tests only a small quantity of rotor disc cooling air was used simply to protect the discs and rims from possible excessive heating. Leakage of some of this cooling air through glands C and D served to fill the spaces between the rotor disc assembly and the adjacent stationary turbine structure, thus excluding hot gases from this region.

Since the turbine consists only of one stage providing only a relatively small gas temperature drop it is necessary in the rig to cool the exhaust ducting. The exhaust is provided with two or more ' skins ' of sheet metal between which quantities of cool air are passed. This cool air is discharged in the main exhaust gas stream through rows of holes in the main stream annulus walls. However, since exhaust cooling is not at present considered to be a fundamental necessity in practical engine applications of a cooled turbine, no attempt is made on the experimental rig to achieve economy in the use of the exhaust cooling air. On the contrary large proportions of cool air are employed in order to partially cool the main exhaust gas stream as well as to maintain reasonably low metal temperatures. When operating at very high gas temperatures the exhaust gas may be further cooled by injection of a spray of water, this water having the additional use of cooling the rakes of pitot tubes situated downstream of the turbine stage. It has been found, however, that unless treated water is used for this purpose, spray jets and exhaust liner cooling holes are quickly fouled by deposit.

Cold pressurised air is fed to the inlet and outlet bearing housings to prevent oil leaking past seals into either the hot parts of the turbine or, in particular, to the blade cooling air and also to prevent hot gases or rotor cooling air (100 to 200 deg C) entering the bearings. This cold air also serves to cool the bearing housings and is discharged with the oil through appropriate vents (Fig. 1). Leakage of oil or oil mist from the bearing housings to the outside of the turbine (and hence on to the hot gas ducts) is prevented by the use of air-pressurised labyrinth seals on the drive shaft between the turbine and the brake.

The main static structure of the turbine, excluding the sheet metal parts, is fabricated mainly from nickel cast iron and H.R. Crown Max. The rotor discs and shaft are forged in Jessop's G.18(b) and R.20 respectively.

2.1. *Description of Cooled Blades.*—The first set of air-cooled nozzle and rotor blades (Code number A.C.I., S. & R.) tested in the turbine are illustrated in Figs. 3 and 4. The blades, which are untwisted and of constant section (*i.e.*, untapered), are internally cooled by passing the coolant spanwise from root to tip through a multiplicity of small diameter holes within the blade. Cooling air is ejected from the unshrouded blade tips into the main gas stream. The 45 nozzle blades are each provided with 53 cooling holes of approximately 0·039 in. diameter. The rotor blades, of which there are 99, are each provided with 38 holes of approximately 0·028 in. diameter.

The blades are fabricated by a sintering technique (developed by the General Electric Company, Ltd.), employing a Tungsten-Vitallium type powder (64 per cent Co, 30 per cent Cr, 6 per cent W), in which the holes are formed by embodying cadmium wires within the compacted blocks of powder. During the sintering process the cadmium wires are volatilised leaving holes in the block. This fabrication technique is described in further detail in Ref. 5. It will be observed that as a result of the high pressure used to cold-compress the powder blocks the cadmium wires are slightly flattened with the result that the holes are approximately elliptical in cross-section, the ratio of major to minor axes being roughly 1·3 : 1.

The powder is compressed and sintered in the form of rectangular bars, in order to obtain a uniform density of material (approximately 98·8 per cent of theoretical value, *i.e.*, 1·2 per cent porosity), from which the final blade and root shapes are formed by machining and grinding.

Vitallium was selected as the blade material since, at the time the work was planned, more experience in the field of powder metallurgy had been gained on this material than on other available heat resistance materials. The creep and fatigue properties of the sintered Vitallium are considerably lower than cast Vitallium, the stress-to-rupture in 100 hours at 750 deg C of the sintered material being 20 to 30 per cent lower than for a cast material.

The influence of this reduction in material properties upon the permissible operating conditions for the blades is discussed in more detail in Part II of this Report, dealing with the performance of the cooled blades.

3. *Description of Test Rig.*—Pressurised air is supplied to the rig from a service compressor. Referring to Fig. 5 the main air supply is fed into the eight combustion chambers from a large pre-entry chamber. The hot products of combustion then pass through the turbine and are exhausted through eight short exhaust pipes into an exhaust collector box, from which the exhaust gas is finally discharged at right-angles to the axis of the rig through a single exhaust duct. This main air supply is controlled by a throttle valve on the upstream side of the test rig and is metered by means of a British Standard orifice plate situated in a long length of straight duct between the throttle valve and the turbine. Cooling air to the test rig is also taken from the service compressor air line but is separately ducted and metered to the various cooled regions of the turbine. The individual regions are :

(*a*) The nozzle blades

(*b*) The rotor blades

(*c*) Outer diameter annulus wall at the turbine inlet (*d*) Inner diameter annulus wall at the turbine inlet

(*e*) Turbine exhaust ducting

(*f*) Rotor discs and disc rim

(*g*) Bearings.

Thus the cooling air delivered to any one of these individual regions may be varied and metered independently of the remainder. This is a very desirable feature of the rig, considering its experimental nature, although it makes the assembly of the turbine with its surrounding cooling ducts, etc., somewhat complex, as will appear evident from Fig. 5. Such complexity would not, of course, be necessary on a cooled turbine installation in a practical engine design.

The power output from the turbine is transmitted to a high-speed water brake through a drive shaft on the exhaust side of the turbine. Output torque is measured on the brake and the rotational speed is measured by an aircraft-type Engine Speed Indicator for approximate values and by a Hasler tachometer for more exact values.

The free end of the turbine rotor (on the inlet side of the turbine) is connected to an overspeed trip gear and a slip ring unit. The overspeed trip gear will, in the event of the turbine overspeeding, break an electric circuit which simultaneously closes an emergency butterfly valve in the air supply line and a valve in the fuel line to the combustion chambers. This trip system may also be operated manually. Fire risk is covered by a fixed system which, by the operation of an emergency switch will envelop the entire rig, both externally and internally, in a cloud of $CO_2$.

The combustion system is fed by kerosine and the fuel quantity is metered by means of a carefully calibrated Avery-Hardoll displacement-type flow meter.

3.1. *The Combustion System.*—The high turbine inlet temperatures envisaged necessitated the development of a combustion system especially suited to the rig. The form of the turbine inlet, in which support struts do not pass through the hot gas stream, led to the adoption of a group of eight straight-through can-type combustion chambers. The diameter of the chambers was largely dictated by dimensional considerations imposed by the turbine inlet and the chamber length (there being no dimensional limitation) was chosen to give a suitable compromise between combustion intensity and area of chamber wall to be cooled. The major design requirements were to achieve a good range of outlet temperature (600 deg C to 1,200 deg C) over a fairly wide flow and pressure range (1·0 to 3·0 atmospheres) with reasonable combustion efficiency and without deterioration of the sheet metal components of the chamber. This last requirement was particularly important since there must be no danger of burnt out or torn pieces of the combustion chamber passing into the turbine and breaking the cooled blades. This necessitated very careful attention to the cooling of the combustion chamber walls—a difficulty accentuated by the fact that the high outlet temperatures demand a high proportion of the incoming air to be passed directly to the primary zone of the chamber, thereby making a lower proportion of secondary mixing air available for cooling the flame-tube wall and outlet chamber liner than in current chamber designs.

A sketch of the chamber finally evolved by the Combustion Department of the N.G.T.E. is given in Fig. 6. The flame tube is cooled (*a*) by an annular film of cool air between the flame zone and the tube, this cool air being introduced by the annular air passage formed between the inner and outer shrouds of the inlet baffle and (*b*) by the secondary and tertiary cooling air passing between the flame tube and the outer casing. The outlet of the combustion chamber is cooled by perforating the outlet liner with a large number of holes through which cool air is passed at low velocity (and hence low penetration into the gas stream) to continually replenish a cold boundary layer of air on the gas side of the liner wall. This system is successful in maintaining the liner and the outlet end of the combustion chamber casing at a safe temperature. At the same time the method of cooling the flame tube and liner, the quantities of cooling air, and the rate of mixing with the hot gas stream are such that the final temperature distribution into the turbine is relatively poor as compared with current aircraft engine chambers. When operating at a mean outlet gas temperature of 1,100 deg C, peak temperatures approaching 1,300 deg C are encountered in the centre regions of the combustion chamber outlet segments.

The distance between adjacent chambers in the vicinity of the primary zones is too great to permit the use of interconnectors between chambers, so that it is necessary to provide separate ignition for all chambers. Ignition with minimum time-lag and maximum repeatability is essential to avoid a danger of accumulating and firing unburnt fuel in the turbine. It was found that although all chambers when tested individually would ignite satisfactorily with conventional sparking plugs the ignition when all chambers were operated in unison was very spasmodic. Eventually a system of igniting by means of a hydrogen pilot flame was adopted. This is found to be reliable and permits rapid and satisfactory ignition at a high air/fuel ratio (about **65 : 1**) and a relatively low air flow rate—these being ideal lighting-up conditions for an experimental rig of the type in hand.

4. *Instrumentation.*—In testing the turbine the following primary measurements are required :

(*a*) Turbine inlet gas temperature, both a mean value and a knowledge of the distribution of temperature
(*b*) Turbine inlet and outlet total pressure
(*c*) Gas mass flow
(*d*) Cooling air mass flows to the various cooled regions
(*e*) Nozzle blade metal temperatures
(*f*) Rotor blade metal temperatures
(*g*) Turbine speed
(*h*) Turbine output power.

Temperature measurements in various parts of the turbine structure are desirable to guard against overheating of the structure and also measurements of bearing temperatures, etc. Further measurements of air pressure and temperature in the coolant systems are also required in order to assess the pressure ratios required to force desired flows of coolant through such components as the nozzle and rotor blades and also to assess leakage flows of coolant from seals, etc.

Methods adopted for measuring air mass flows and turbine speed and power output have been mentioned in section 3. Methods of making other measurements are described in the following paragraphs.

4.1. *Measurement of Turbine Inlet Gas Temperature.*—This is one of the most important measurements required and at the same time is one of the most difficult to make on account of (*a*) the non-uniformity of the temperature distribution and (*b*) the high peak temperatures envisaged (possibly 1,400 deg C at some points) which preclude the use of a multiplicity of temperature sensitive instruments since these introduce an attendant danger of breakage at high temperatures and possible damage to the turbine blades. An alternative procedure is therefore adopted of measuring air flow and fuel flow to the combustion chambers and making a careful calibration of the combustion efficiency of the chambers over a suitable range of inlet pressures and air : fuel ratios. The calibration of combustion efficiency was performed, using the gas sampling technique, by mounting rakes (radial) of gas sampling tubes on to a dummy rotor disc and, by slowly rotating the dummy disc, traversing the entire annulus of the turbine. No blades, either rotor or nozzle, were inserted in the turbine during these calibrations. A rake of five pitot-tubes, two static-pressure tubes, and a rake of five total-head temperature tubes were also mounted on to the dummy rotor disc (Fig. 7) and used to examine velocity, pressure, and temperature distributions in the turbine annulus. The total-head temperature tubes (Fig. 7) consisted of double-shielded chromel/alumel couples, the inner shield being made of platinum foil having a low emissivity. Use of this inner platinum foil shield was found to be necessary to reduce radiation errors in temperature measurement (the traverses were done at mean gas temperatures of about 850 deg C) to negligible proportions. Integration of mass mean values of gas temperature from the traverse were found to agree well with estimated mean temperatures deduced from fuel flow, air flow, and combustion efficiency measurements.

Typical velocity and temperature distributions in the turbine annulus downstream of two of the combustion chambers are illustrated in Figs. 8 and 9. The calibration of combustion efficiency for a range of air : fuel ratios and inlet pressure is shown in Fig. 10.

4.2. *Measurement of Turbine Inlet Total Pressure.*—For low temperature testing two rakes of three pitot-tubes are positioned in the outlet sections of two of the combustion chambers. Traverses have shown that the total pressure is substantially uniform in the outlet sections of the combustion chambers and that the pressure loss between the plane where the total pressure is measured and the plane of the nozzle blades is negligible. A static-pressure tapping is also provided in two of the nozzle blade platforms in the nozzle blade passage about 10 per cent of the passage length from the leading edge (*see* Fig. 2). Using this static pressure a calibration between $P_i/P_{\text{stat. (nozzle)}}$ and $W_N\sqrt{T_i}/P_{\text{stat. (nozzle)}}$ has been determined at low temperatures

NOTE :

$W_N$ total mass flow entering nozzle row (lb/sec)

$T_i$ mass mean total temperature of flow leaving nozzle blades

$P_i$ mean total pressure at combustion chamber outlet (lb/in.$^2$ (absolute))

$P_{\text{stat. (nozzle)}}$ static pressure measured in nozzle passage (lb/in.$^2$ (absolute)).

When testing at high inlet temperatures the pitot-tubes are withdrawn and the inlet total pressure is deduced from measured flow, inlet temperature, and nozzle static pressure using the above mentioned relationship (plotted in Fig. 11). Theoretically this relationship should be slightly adjusted for variation in gas specific heat at different temperatures but at the ratios of $P_{\text{inlet}}/P_{\text{stat. (nozzle)}}$ involved the necessary correction is negligible as compared with the small experimental scatter in the calibration.

Outlet total pressure is measured by eight rakes of four pitot-tubes in a plane about two inches downstream of the rotor row. Corresponding tubes in all the rakes at each individual radius are connected to a common manifold. The stems of the rakes of pitot-tubes used for high temperature testing are surrounded by a water jacket and the cooling water is ejected from the jackets rearwards into the gas stream to assist in cooling the hot exhaust gas as it passes into the outlet duct.

4.3. *Measurement of Metal Temperatures.*—4.3.1. *Measurement of temperatures in the general turbine structure.*—Measurements of metal temperature are made at a number of points in the structure, such as the nozzle blade root clamping ring, rotor shroud ring, nozzle shroud ring, etc., to check the effectiveness of the structure cooling arrangements. In most instances these measurements are made by means of chromel/alumel thermocouples inserted and spring-loaded into holes drilled into the appropriate metal component. In some instances a more complete picture was obtained by using temperature sensitive paints.

4.3.2. *Measurement of sheet metal liner temperatures.*—An attempt was made to obtain these temperatures by the use of thermocouples. Unfortunately, difficulties associated with assembly and dismantling of the turbine prevent the adoption of couples welded or peened into the sheet metal and it is only possible to spring load the beads on to the cooling air side of the liners. Due to the passage of cooling air directly over the couple beads or, in some instances, over a shield surrounding the bead (*see* Fig. 2) the measurements of liner temperature made by this method are artificially low. Alternative and more reliable results are achieved by use of temperature sensitive paints and by use of small plugs of a variety of fusible metal alloys which fuse at different temperatures. The fusible metal is ' flush rivetted ' into holes drilled through the sheet metal liners. The primary objection to these latter methods is that the unit has to be dismantled after each test to inspect the paint and metal plugs. The temperature sensitive paints may be calibrated during each test by inserting a tapered copper rod, which is cooled at one end to produce a temperature gradient along the rod, into the exhaust gas stream. This rod may be coated externally with temperature sensitive paint and true metal temperatures measured by a number of thermocouples embedded at points along the rod.

4.3.3. *Measurement of nozzle blade temperatures.*—Chromel/alumel thermocouples are inserted in specially provided holes in the blade to nine selected points within the blades. The positions of these points are indicated in Fig. 12 from which it will be seen that temperatures are measured in three chordwise positions (*a*) close to the blade root, (*b*) at the mid-span of the blade and (*c*) close to the blade tip. Couple wires are nominally 0·010-in. diameter and each wire is sheathed in single-hole refractory insulators of about 0·020-in. to 0·025-in. outer diameter. The holes especially provided in a number of blades to accept each pair of wires and insulators are approximately elliptical in cross-section and size being about 0·043 in. × 0·030 in. These holes are blocked at the location point of the couple and cannot pass cooling air. The thermocouple beads are spring-loaded against the blocking metal at the end of the holes to give reasonable thermal contact.

4.3.4. *Measurement of rotor blade temperature.*—Elliptic shaped holes of size about 0·038 in. × 0·030 in. are provided in a number of the rotor blades to accept specially prepared chromel/alumel thermocouples. These holes are blocked at the points of location of the couple beads to prevent passage of cooling air and to allow the bead to bear against the blade metal. Since the disc and blades rotate at speeds up to 9,000 r.p.m. the thermocouple junction and leads must be capable of withstanding high centrifugal loading. Furthermore a reliable and robust thermocouple assembly is essential due to the difficulties and valuable time lost in completely dismantling the rig to service or modify these important thermocouples. For these reasons an elaborate but very strong thermocouple assembly was developed with the assistance of the General Electric Company, Ltd. This thermocouple is illustrated in Fig. 13. Each lead of the couple consists of chromel or alumel wire of 0·005-in. diameter coated with a covering of alumina about 0·004 in. thick over which is drawn a nickel tube, the final outside diameter of the tube, after drawing, being 0·019 in. At the actual junction of the thermocouple the chromel and alumel wires are bared from the nickel sheath tubes and welded together to form a small bead. The bead and the ends of the sheath tubes are then brazed solidly together. After cutting the assembly to a suitable length the terminal end is formed by welding stouter connector wires to the fine wires protruding from the ends of the sheaths and embedding this joint and the end of the sheaths in Sauereisen cement. This in turn is firmly embedded in a split head of brass, the split parts of the head being soldered together. This type of terminal head is necessary to avoid any possibility of shorting the thermocouple wire to the nickel sheath at the particularly vulnerable point where the wire emerges from the sheath.

These thermocouple assemblies are pushed into the special holes provided in the blades and the nickel-sheathed leads bent to conform to the surface of the rotor disc and firmly anchored to the disc at intervals by means of small tags brazed to the wires and spot welded to the disc surface. Fig. 14 shows the rotor blades located to one half of the disc assembly and also shows the sheathed pairs of thermocouple leads passing in groups of three from some of the cooled blades to a multiple terminal block, formed of tufnol, in the disc hub. Insulated chromel and alumel leads of heavier gauge wire, connecting this junction box to a slip-ring unit at the end of the shaft, pass through a tube located on the shaft centre line. In all, twenty-seven thermocouples are installed in the rotor, the measurements at each of the nine location points in the blades being repeated in three separate blades. In any one blade a maximum of three thermocouples are installed, these three couples being located in the same spanwise position but in different chordwise positions.

The slip ring unit (Ref. 7) has twelve rings and thus, since all the thermocouples are 'earthed' at the beads, only six of the rotor thermocouples may be used during any one test. Any six thermocouples may be selected and connected to the slip-ring unit with only a minor dismantling operation on the rig in the vicinity of the trip gear and slip-ring unit.

The slip-ring unit, illustrated in Fig. 15, is made up of silver-morganite brushes spring-loaded on to phosphor-bronze rings. The rings are cooled by jets of cold air. During running the rings are easily accessible, and may be lightly brushed at intervals with carbon-tetrachloride to preserve a clean surface and good brush contact. The thermocouple e.m.f's are recorded by means of a calibrated self-balancing and recording potentiometer.

Over a period of about 100 hours testing the rotor thermocouple assembly has given reliable and consistent readings of blade temperatures, and up to the time of writing only one of the twenty-seven couples has failed.

5. *Test to Determine Effectiveness of the Cooling of the Turbine Structure.*—An early series of tests was carried out to determine the degree of cooling achieved on the main components of the turbine structure, excluding the cooled blades. During these tests the rotor disc had no blades fitted and the nozzle ring was fitted with a set of solid uncooled blades. Hot gas, up to 900 deg C, was then passed from the combustion chambers through the turbine annulus while measurements of structure temperature were made for a variety of cooling air quantities to the various cooled regions of the unit.

Some results of these tests are tabulated in Table 1 (Appendix I). This Table lists measured metal temperatures when the gas temperature is 900 deg C (limit of tests) and when the quantities of cooling air, expressed as a ratio of the main stream mass flow, are adjusted to optimum values. Also listed are values of metal temperatures which may be anticipated if the gas temperature attains the maximum design value of 1,200 deg C.

The variations of the annulus wall liner temperatures in the turbine inlet with cooling air quantities are plotted in Fig. 16. The liners showed considerable peripheral variations of local temperature and also were generally hotter towards the downstream edges than at the upstream ends. The temperatures plotted correspond roughly to the maximum local values.

As mentioned in section 4.3.2. it will be noted that the liner temperatures measured by the inadequate thermocouple installations are falsely low. On the other hand a fairly good agreement exists between temperatures indicated by the fusible alloy plugs and the temperature sensitive paint.

It is to be noted that to keep the inlet annulus wall liners and the surrounding turbine structure adequately cool at a gas temperature of 1,200 deg C, a total quantity of cooling air amounting to 2 to $2\frac{1}{2}$ per cent of the main stream mass flow is required to cool the turbine inlet annulus walls and the nozzle shroud liner. The pressure required to pass this quantity of cooling air is only slightly greater than the total-head pressure in the main gas stream and, in an aircraft jet engine having a combustion chamber loss of about 5 per cent of the combustion chamber inlet pressure, the pressure required would be slightly less than the compressor delivery total pressure. As mentioned in section 2 this cooling air passes into the main gas stream ahead of the turbine stage and expands through the turbine. Providing that the introduction of this cool air into the main gas stream is taken into account when computing the mean effective turbine inlet temperature the provision of this part of the cooling system does not theoretically produce a loss of net power from an engine. On the other hand there are a number of features associated with the inlet cooling system which may slightly reduce the aerodynamic efficiency of the turbine stage. These are (*a*) the non-uniformity in inlet gas temperature produced by the film of cool air on the inlet liners (*b*) a portion of the inlet annulus cooling air (about 2/3 )passes into the gas stream between the nozzle row and the rotor row without any swirl component of velocity and may ' spoil ' the flow over the roots of the rotor blades, and (*c*) the injection of the cooling air upstream of the nozzle row into the main gas stream though holes and annular gaps may create high turbulence and eddies in the flow adjacent to the annulus walls and as a consequence increase the secondary flow losses in the turbine stage.

On the exhaust side of the turbine quantities of cooling air amounting to 10 to 20 per cent of the main stream flow are fed to the liners and thence to the gas stream. These relatively large quantities are used to serve the double purpose of both cooling the exhaust end structure of the turbine and reducing, by dilution, the exhaust gas temperature in order to ease the high temperature problems in the design of the ducts exhausting the hot gas to atmosphere.

A quantity of cooling air amounting to about 2 per cent of the main stream mass flow is passed through the spaces between the rotor discs and cover plates. This quantity is rather higher than is believed necessary but since only a small fraction of this air passes into the main gas stream it is considered that a reduction of this particular cooling quantity would not significantly enhance the value of the tests on the cooled blades but merely jeopardise the life and safety of the rotor discs.

6. *Conclusion.*—An experimental high temperature air-cooled turbine has been described together with methods adopted for making measurements of various temperatures, pressures, etc., relevant to the purposes of the rig.

Results of some tests to determine the effectiveness of the cooling means provided in various regions of the turbine, excluding blades, are briefly stated and it is concluded from these tests that the structure (excluding blades) of the turbine is sufficiently well cooled to permit the use of inlet gas temperatures in the rig up to 1,200 deg C.

This Report is a preliminary to further Reports describing, in detail, experiments on the cooled blades and experiments to determine the overall performance of the cooled turbine stage.

## REFERENCES


| *No.* | *Author* | *Title, etc.* |
|---|---|---|
| 1 | S. J. Andrews and P. C. Bradley .. | Heat transfer to turbine blades. N.G.T.E. Memo. M.37. A.R.C. 12,078. |
| 2 | H. B. Squire .. .. .. .. | Heat transfer calculation to aerofoils. R. & M. 1986. |
| 3 | A. G. Smith .. .. .. .. | Heat flow in the gas turbine. *Proc. I.Mech.E.* Vol. 159, pp. 245 to 254. 1948. |
| 4 | A. G. Smith and R. D. Pearson .. | The cooled gas turbine. *Proc. I.Mech.E.* Vol. 163, pp. 221 to 234. 1950. |
| 5 | J. Reeman and R. W. A. Buswell .. | An experimental single stage air cooled turbine. Part I. Design of the turbine and manufacture of some experimental internally cooled nozzles and blades. *Proc. I.Mech.E.* Vol. 167. 1953. |
| 6 | D. G. Ainley .. .. .. .. | An experimental single stage air cooled turbine. Part II. Research on the performance of a type of internally air cooled turbine blade. *Proc. I.Mech.E.* Vol. 167. 1953. |
| 7 | D. Mackenzie .. .. .. .. | The development of a high speed, multi-channel, brush type slip-ring assembly. N.G.T.E. Memo. M.134. A.R.C. 14,746. |

## APPENDIX I

*Table Showing Turbine Metal Structure Temperatures*

The following Table records metal temperatures measured at various points within the turbine:

(*a*) at a mean inlet gas temperature of 900 deg C (maximum value attained during the relevant tests)

(*b*) estimated values when the mean inlet gas temperature is 1,200 deg C.

In all instances the cooling flows to the various cooled regions of the structure enter at a temperature of approximately 100 deg C and are adjusted to the following values (expressed as a percentage by weight of the main stream gas flow) :

| | |
|---|---|
| (1) Cooling air to outer annulus wall at turbine inlet .. | 1·1 per cent |
| (2) Cooling air to inner annulus wall at turbine inlet .. | 0·8 per cent |
| (2a) Cooling to nozzle shroud liner .. .. .. .. | 1·6 per cent |
| (3) Nozzle blade cooling air .. .. .. .. .. | 2·0 per cent |
| (4) Rotor disc cooling air .. .. .. .. .. | 2·0 per cent |
| (5) Rotor blade cooling air .. .. .. .. .. | 2·0 per cent |
| (6) Inlet and outlet bearing cooling and sealing air (total) .. | 1·3 per cent inlet temp. = 20 deg C |
| (7) Turbine exhaust cooling air .. .. .. .. | 15 per cent (approx.) |

In the Table below the letters indicating locations of the points of measured temperature relate to the locations lettered in Fig. 1.

TABLE 1

| Location | Metal temperature when $T_g$ (inlet) = 900 deg C | Estimated metal temperature when $T_g$ (inlet) = 1,200 deg C |
|---|---|---|
| a | 270 deg C | 330 deg C |
| b | 350 | 440 |
| c | 370 | 470 |
| d | 220 | 270 |
| e | 160 | 180 |
| f | 300 | 380 |
| g | 130 | 140 |
| h | 110 | 110 |
| i | 90 | 100 |
| j | 100 | 110 |
| k | 160 | 180 |
| l | 200 | 240 |
| m | 230 | 280 |
| n | 100 (air in header = 145 deg C | 110 |
| o | 610 | 800 |
| p | 530 | 700 |

It will be observed from the above Table that the majority of temperatures are quite low. In particular it should be noted that the cooling air quantities metered to the outer annulus liner at the turbine inlet and to the nozzle shroud liners are considerably larger than are required to maintain the sheet metal liners at a safe temperature (about 900 deg C maximum). These quantities may apparently be reduced to approximately 0·25 per cent and 1 per cent respectively without leading to excessive heating. In practice the larger quantities were used since the extra cooling insured against possible distortion of the liner and furthermore the main experimental investigations on the cooled nozzle and rotor blades were not affected to any important degree by a slight excess of cooling flows in these regions.

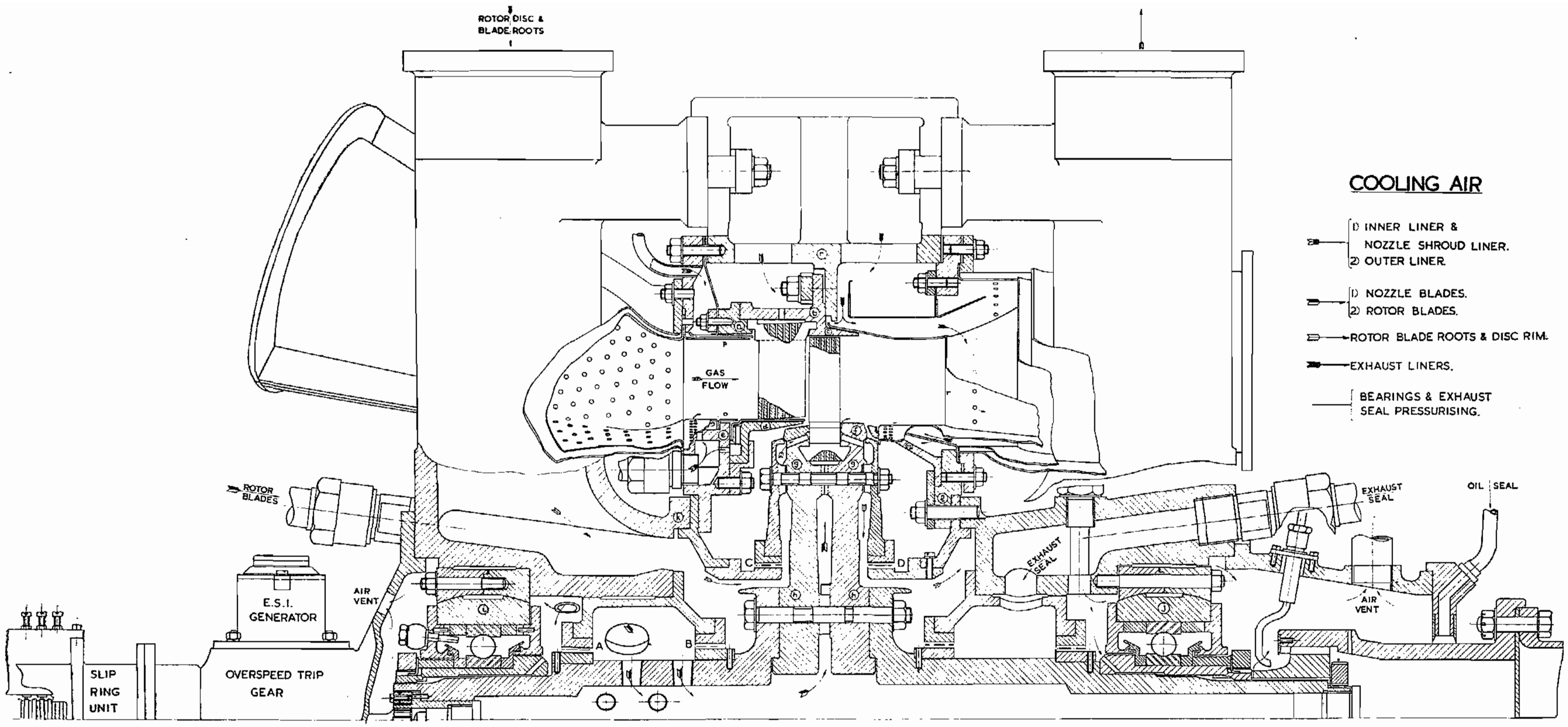


FIG. 1. Experimental single-stage air-cooled turbine.

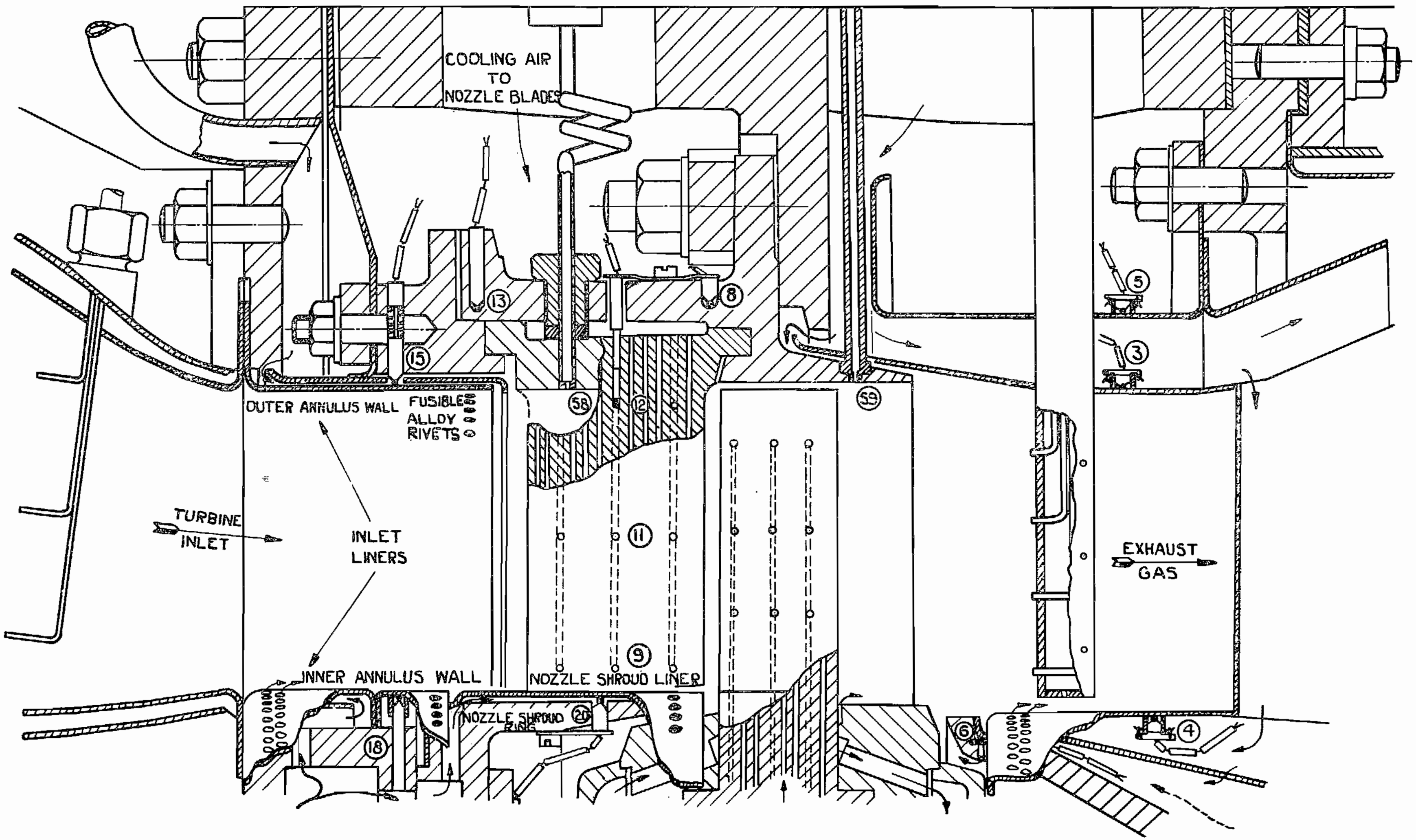


Fig. 2. Cross-section of the turbine annulus.

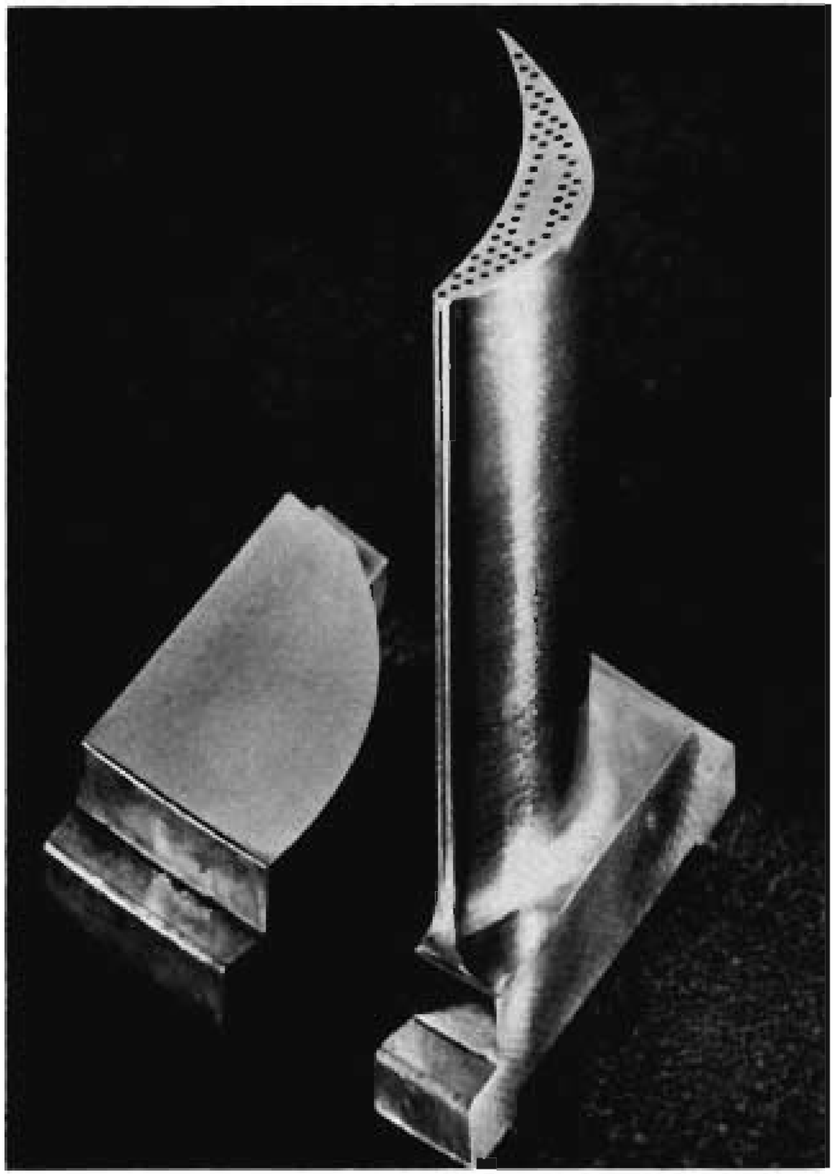

FIG. 3. Air-cooled nozzle blade (A.C.I.S.).

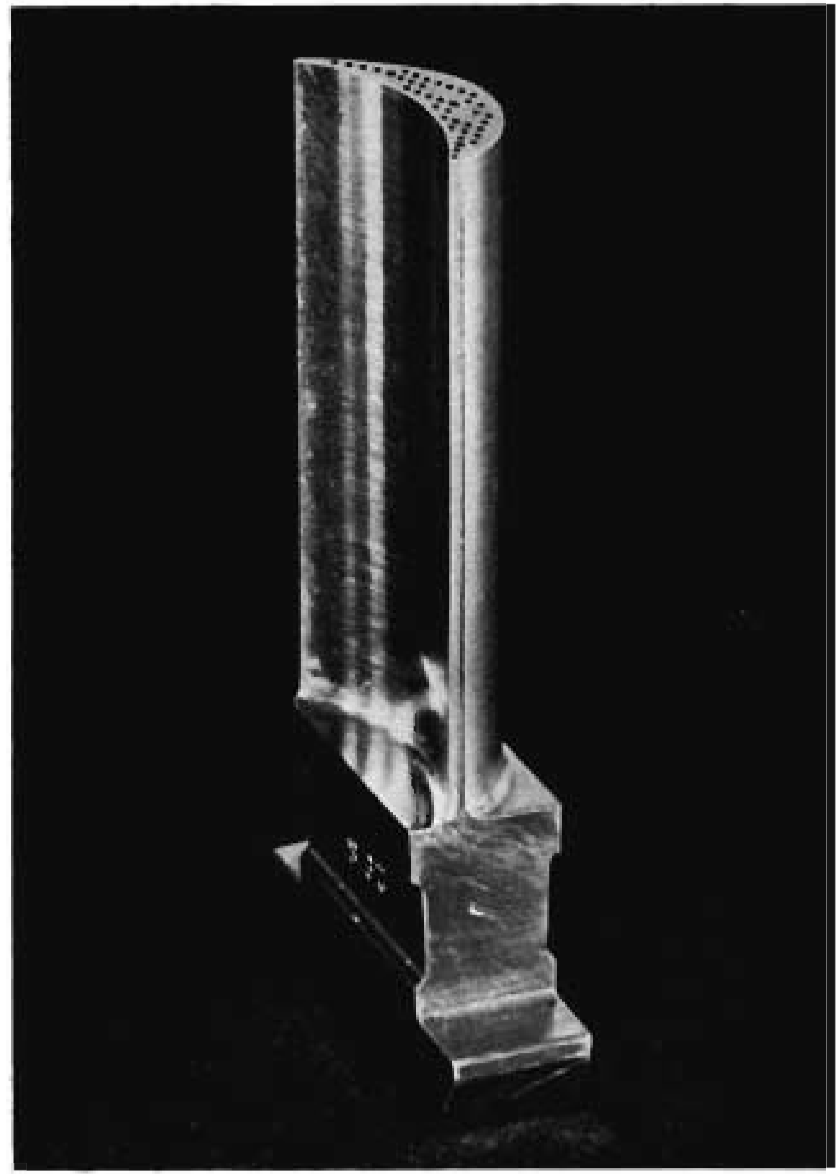

FIG. 4. Air-cooled rotor blade (A.C.I.R.).

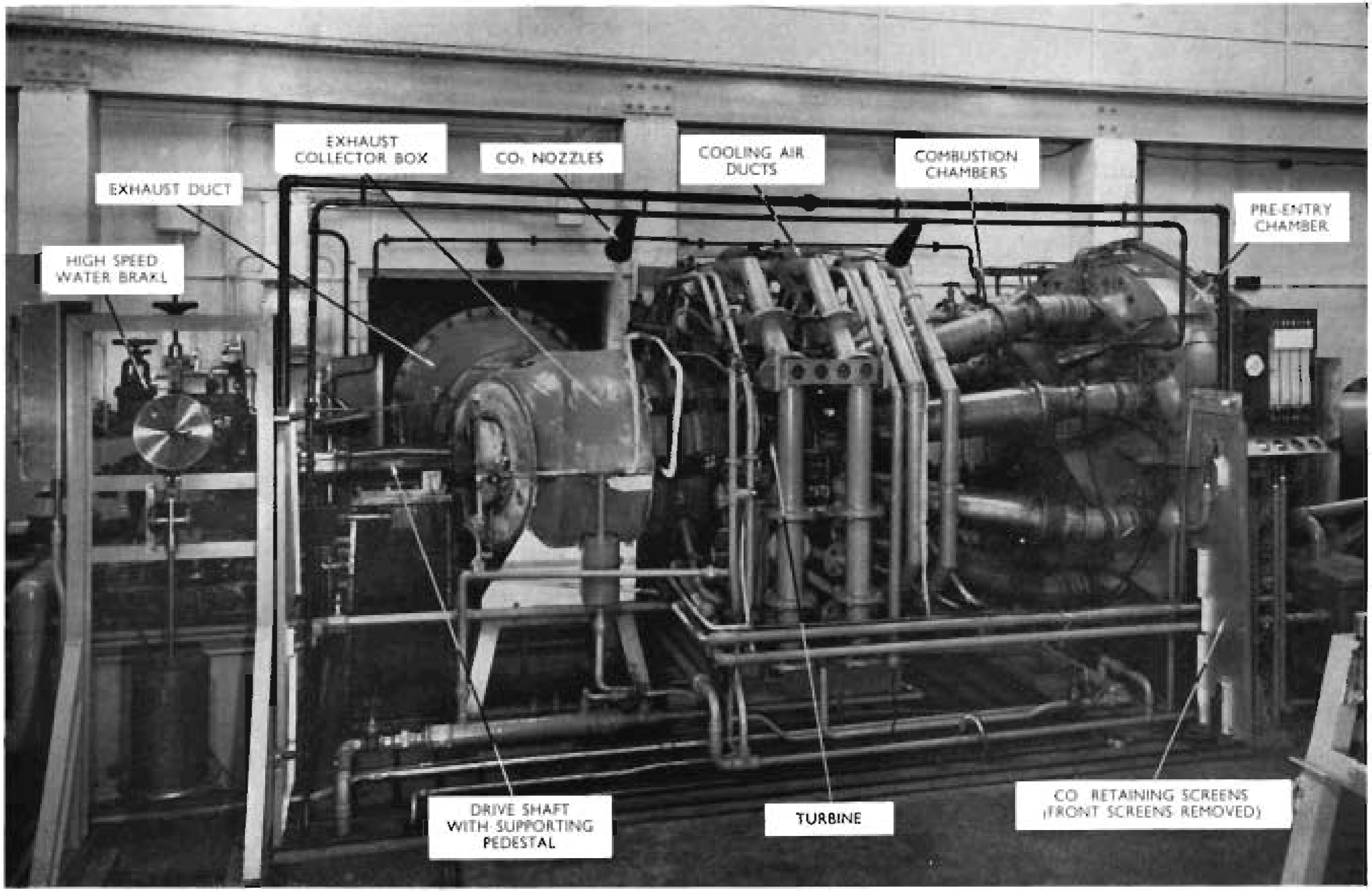


FIG. 5. Turbine test rig.

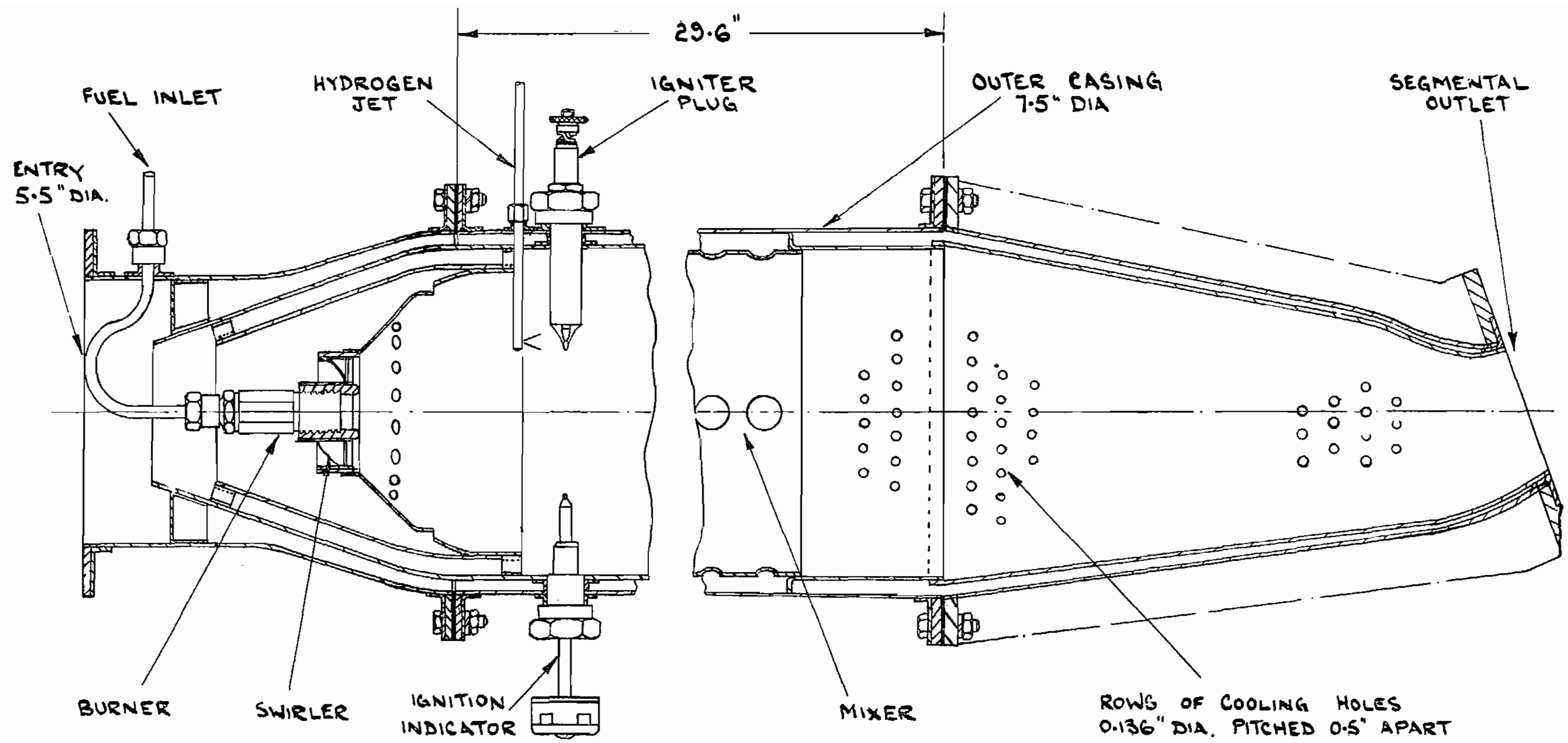


FIG. 6. High temperature combustion chamber.

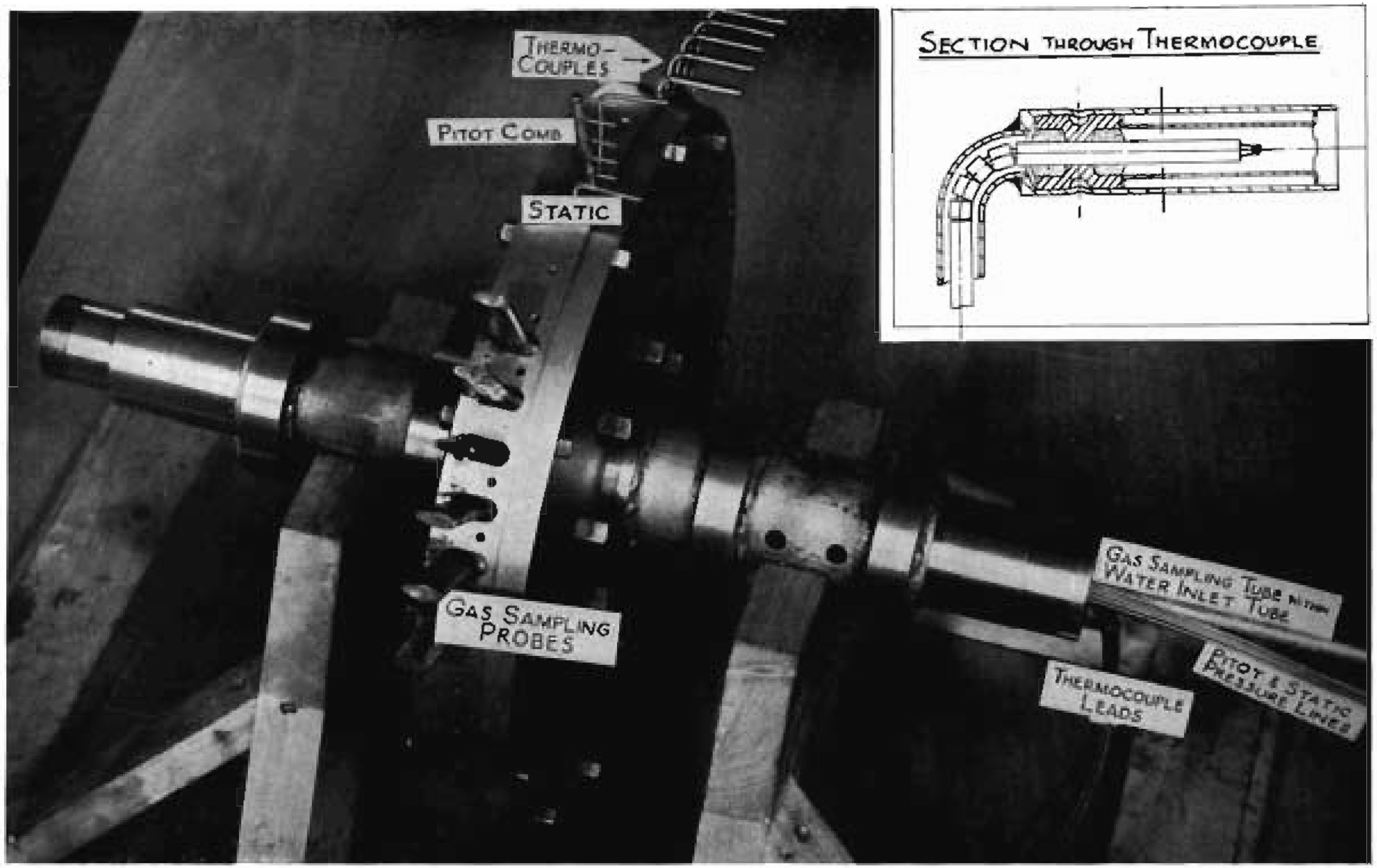


Fig. 7. Dummy rotor with traversing instruments installed.

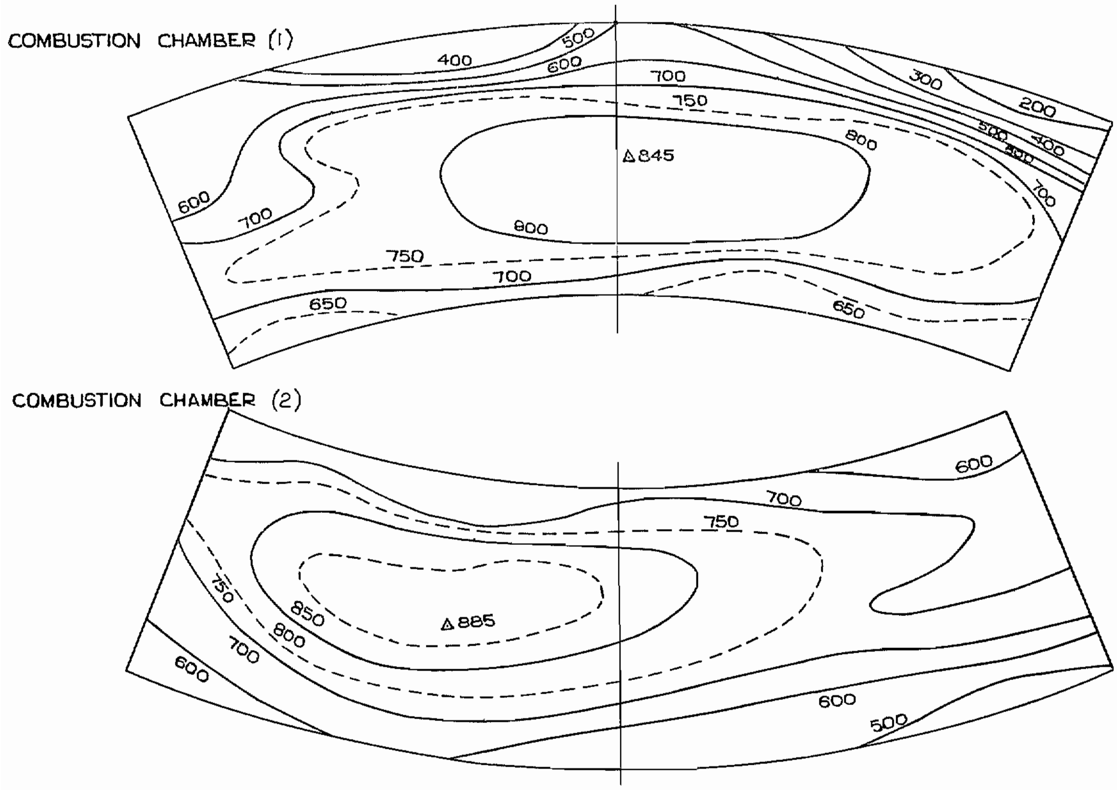


FIG. 8. Gas temperature distribution in turbine inlet annulus (deg C).

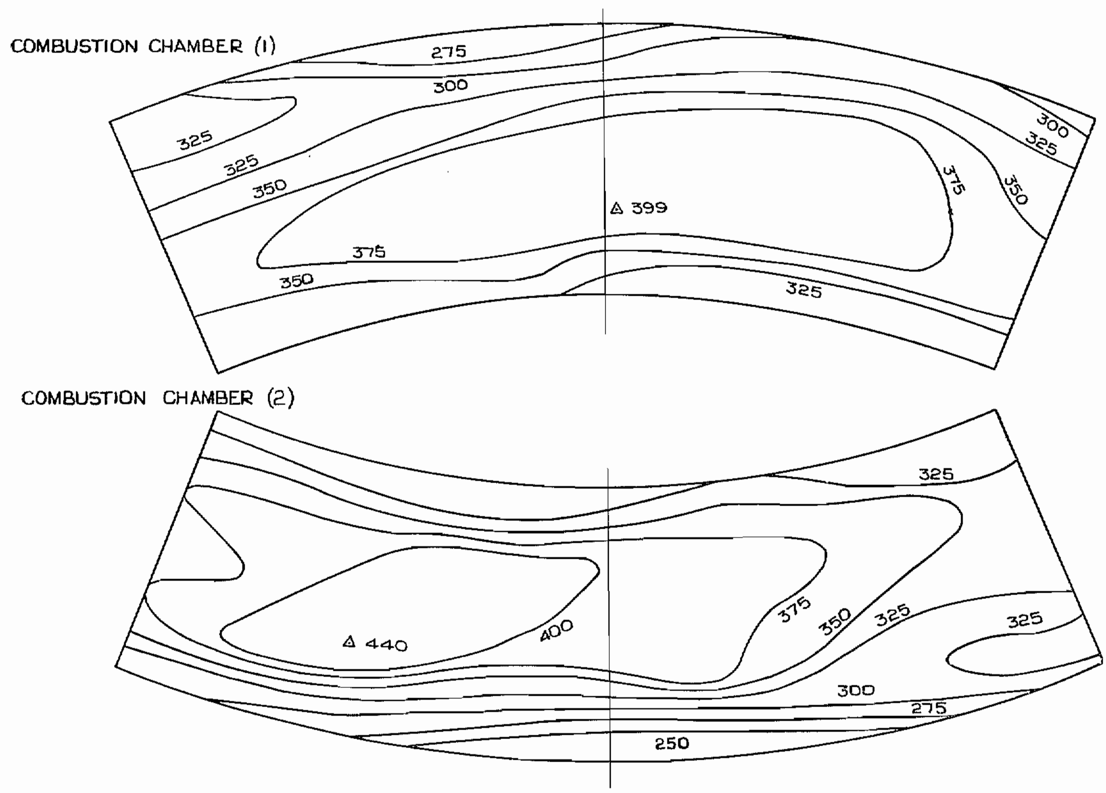


FIG. 9. Gas velocity distribution in turbine inlet annulus (ft./sec.)

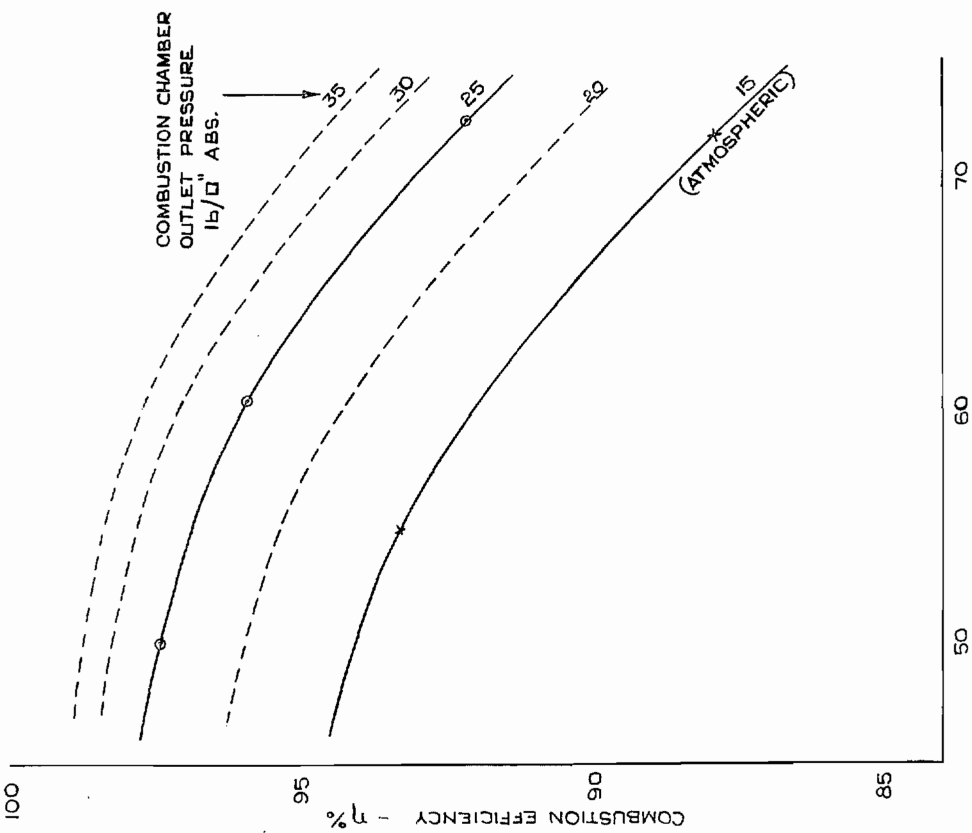


FIG. 10. Relationship between combustion efficiency air/fuel ratio and pressure.

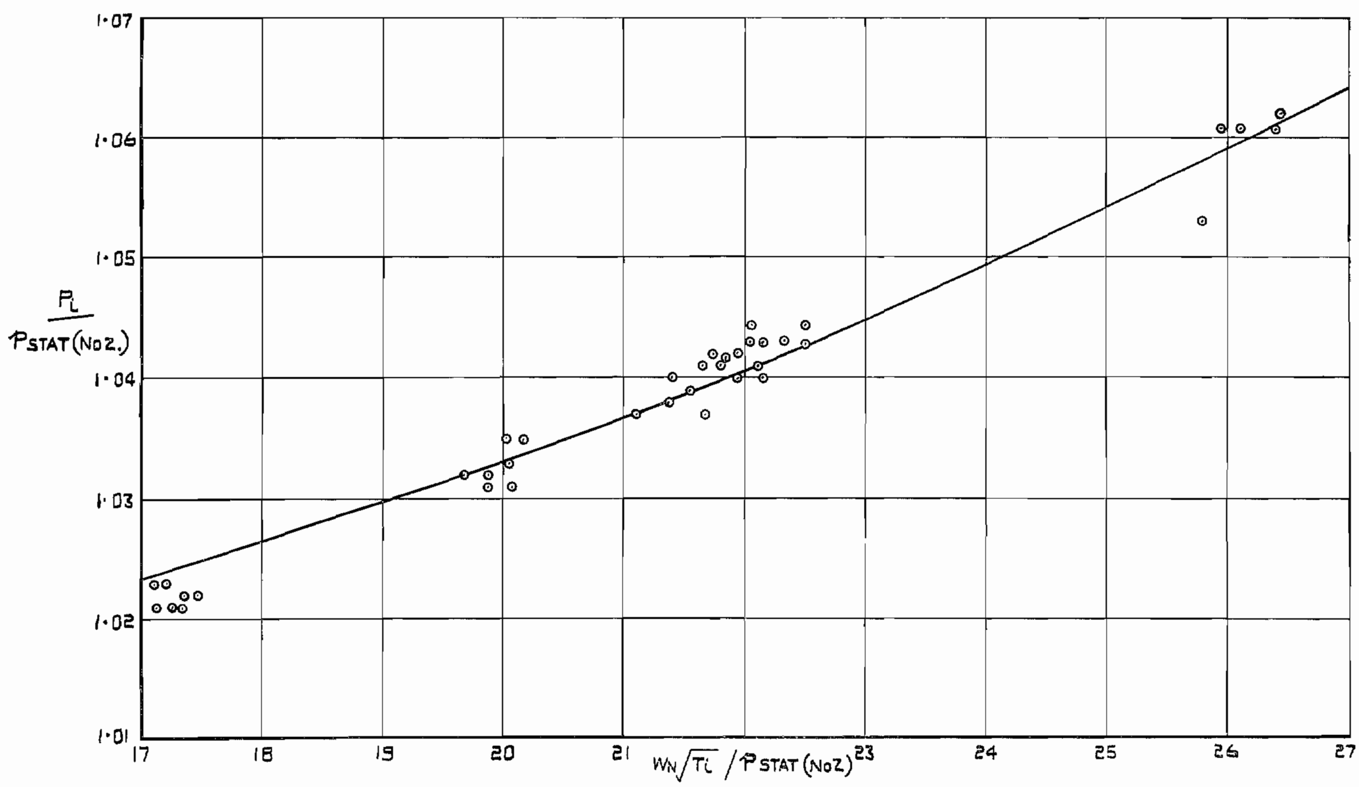


FIG. 11. Calibration between nozzle static press. measurement and turbine inlet total press.

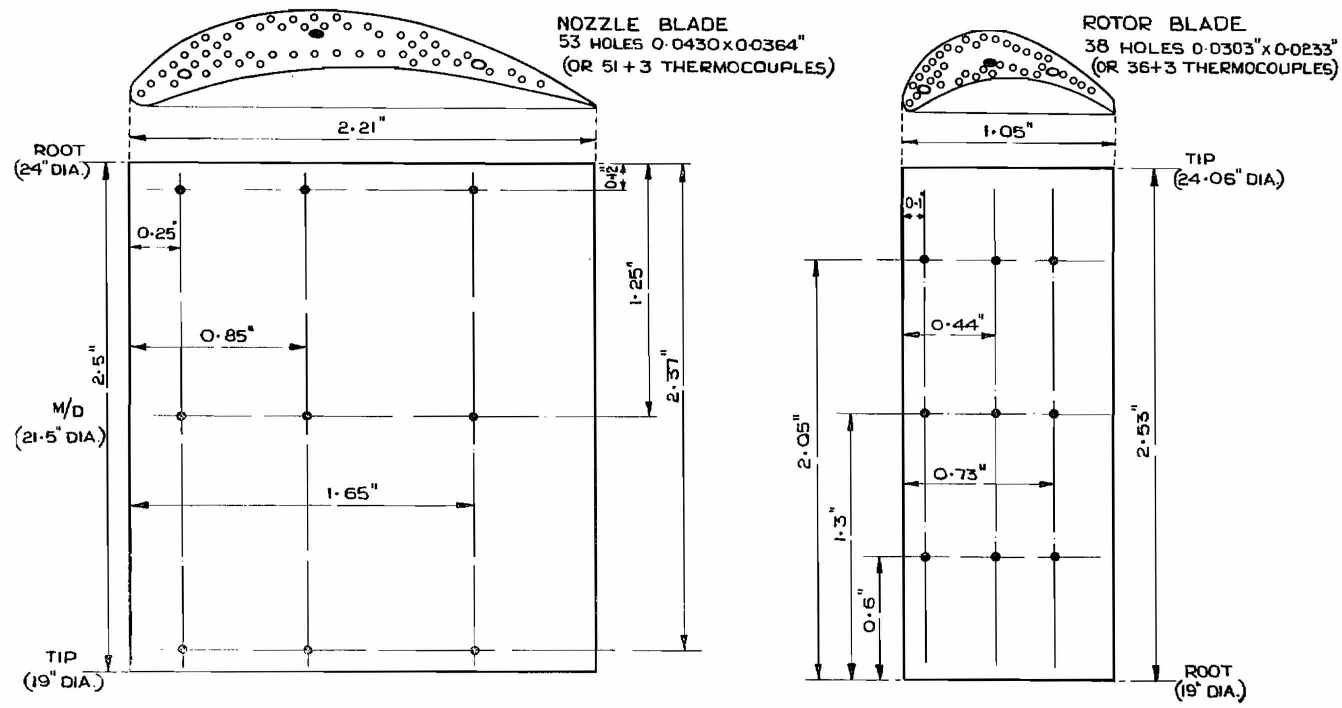


Fig. 12. Location of thermocouples in nozzle and rotor blades.

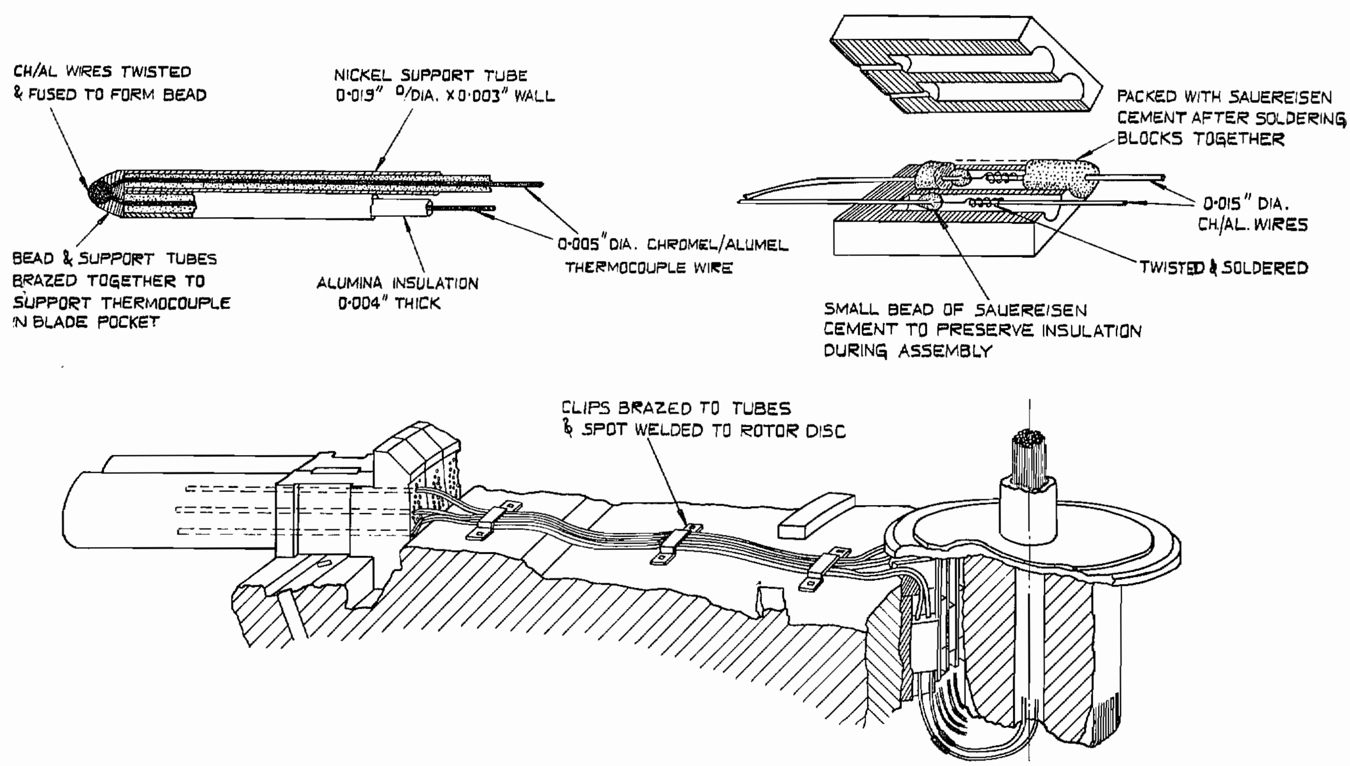


Fig. 13. Diagrammatic sketch of rotor blade thermocouples.

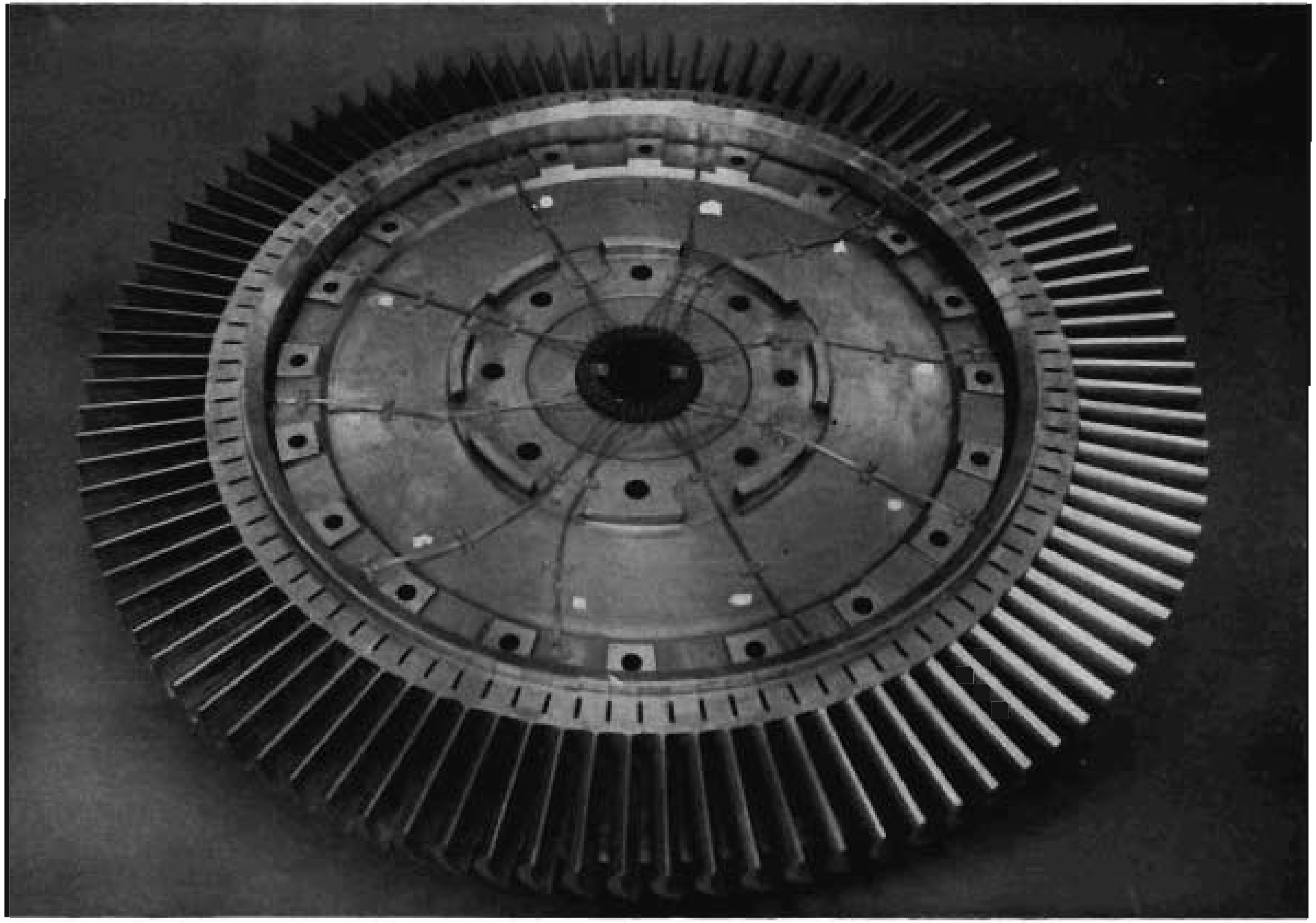

FIG. 14. Installation of rotor blade thermocouples.

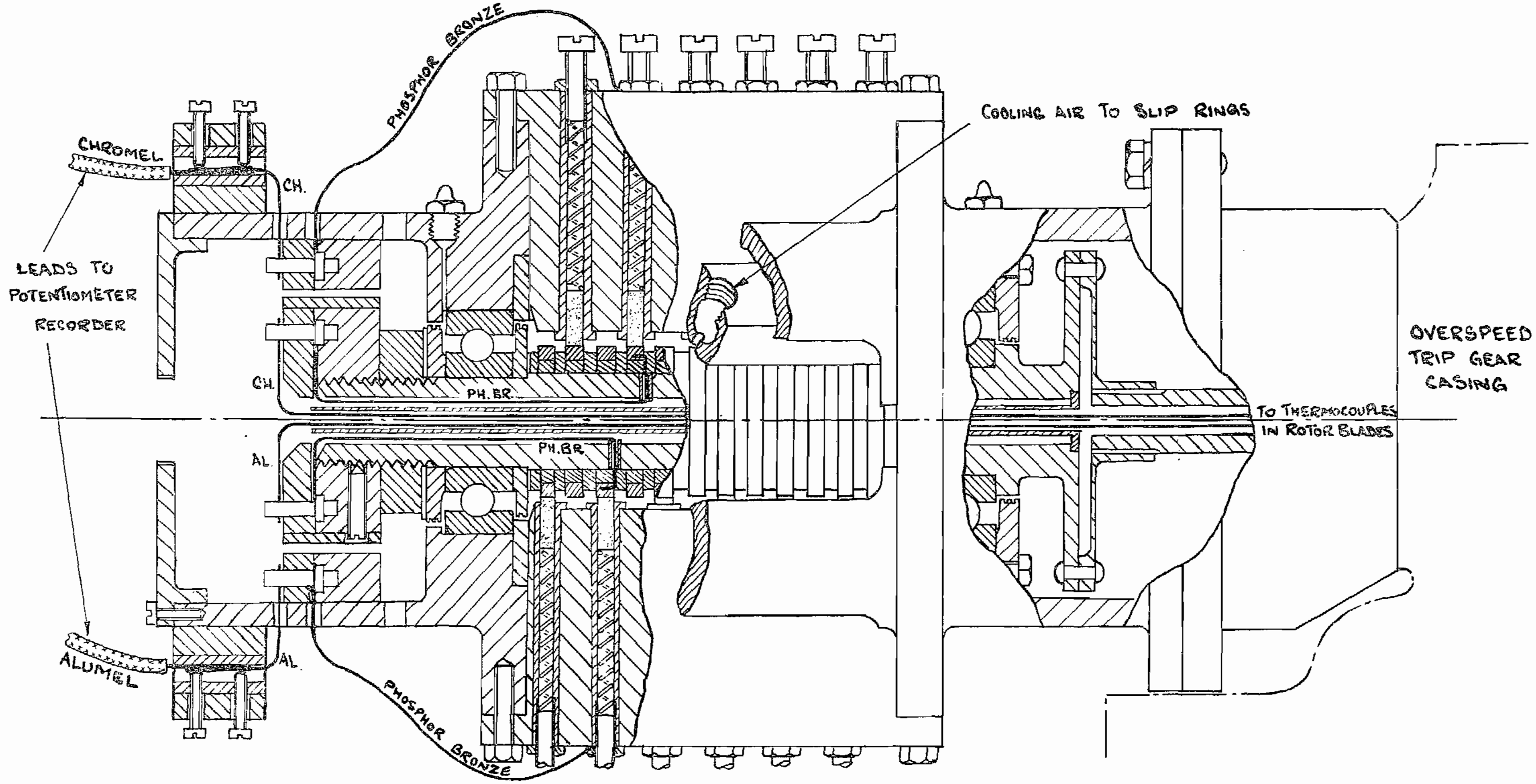


FIG. 15. Brush-type slip-ring unit

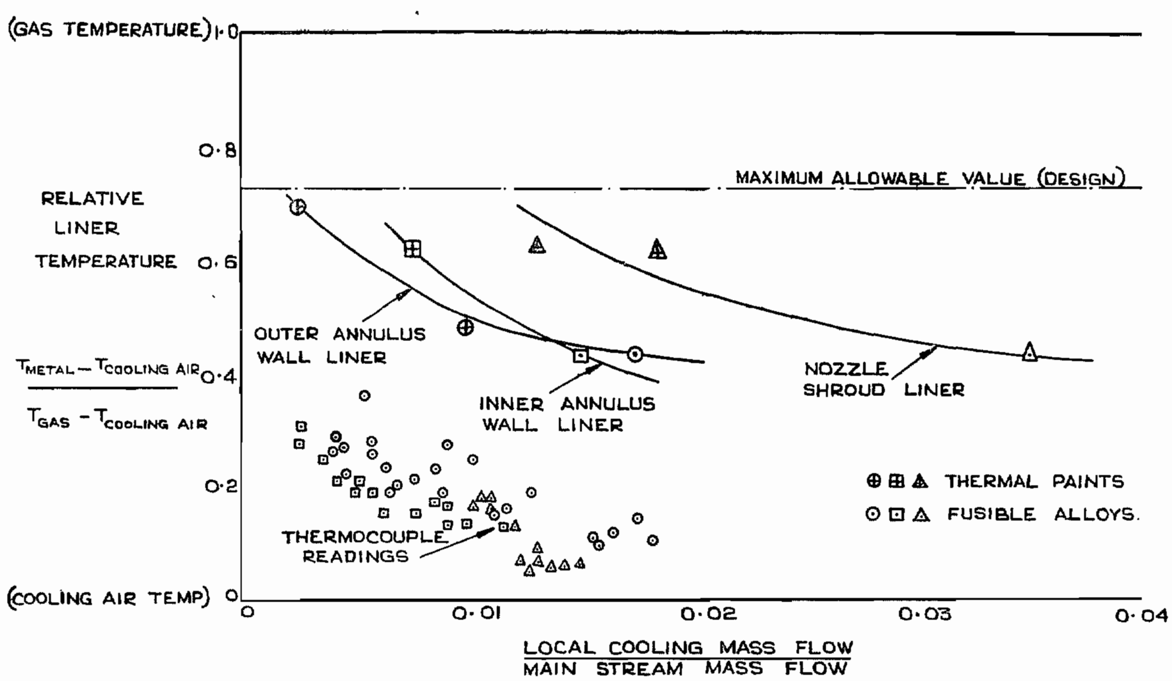


FIG. 16. Variation of annulus wall liner temperatures with cooling air flow.

# PART II

# Cooling Characteristics of Blades having a Multiplicity of Small Diameter Coolant Passages

*By*

D. G. AINLEY, N. E. WALDREN and K. HUGHES

*Summary.*—A thorough examination in an experimental turbine has been made of the cooling characteristics of a set of internally air-cooled nozzle and rotor blades. Particular attention was paid to the rotor blade cooling characteristics and results show that a very substantial reduction in mean rotor blade temperature may be achieved with a cooling flow equal to 2 per cent of the main gas flow. The blades were not uniformly cooled, the blade temperatures being very much higher near the leading and trailing edges than in the mid-chord sections. However, examination of the steady thermal stresses created by the non-uniformity in cooling, and the transient stresses likely to occur during ' thermal shock ', suggest that the non-uniform cooling is not very detrimental. An increase in turbine inlet gas temperature of about 270 deg C above the permissible value for the same rotor blades and same life without cooling appears possible with a cooling flow ratio of 0·02. The results further indicate that when operating with a fixed cooling flow ratio the mean degree of cooling achieved on the present blades is not substantially influenced by changes in the gas flow Reynolds number or, within limits, by substantial changes in blade aerodynamic loading. The results also indicate that cascade tests to investigate cooling characteristics of blades may not be wholly applicable to similar blades operating in an actual turbine stage. This may be due largely to the fact that the amount of heat transferred from the gas to a blade is influenced considerably by the location of the boundary-layer transition points and these in turn may be greatly influenced by the degree and nature of the turbulence in the main gas stream.

1. *Introduction.*—Part I of this report (Ref. 1) gave a general description of an experimental single-stage air-cooled turbine which has been erected and operated at the National Gas Turbine Establishment to facilitate the development of high temperature air-cooled turbine engines. The following report continues with a description of some internally air-cooled nozzle and rotor blades together with an account of some experimental investigations concerning their performance. A preliminary report of this work appears in Refs. 5 and 6.

Before describing the investigations in detail it might be helpful to readers to make a few brief introductory comments regarding the parameters controlling the degree of cooling which might be achieved in an internally air-cooled blade.

The degree of cooling which may be achieved is dependent upon a number of factors, chief among which are (*a*) the temperature difference between the main gas stream and the inlet cooling air and (*b*) the ' conductance ratio ', this being defined as the ratio of the heat input to the blade per unit temperature difference between gas stream and blade to the heat passed to the cooling air per unit temperature difference between blade and cooling air (viz. $h_g S_g / h_c S_c$). Clearly to achieve a high degree of cooling the lowest possible value of conductance ratio is required in conjunction with the largest possible temperature difference between gas stream and cooling air.

The heat input to the blade per unit temperature difference between gas stream and blade is the product of the average gas-to-blade heat transfer coefficient and the external surface area, and this in turn is dependent upon the blade shape, gas flow incidence, gas flow Reynolds number, gas Prandtl number, and to a lesser extent upon the ratio of gas temperature to blade temperature, and also gas stream Mach number. Of these latter parameters the influence of Mach number might be discounted providing (Ref. 2) that the effective temperature (*i.e.*, the temperature governing heat transfer) of the main gas stream outside the surface boundary layer is expressed by the relationship :

$$T_{\text{(effective)}} = T_{\text{(static)}} \left[ 1 + (P_r)^n \frac{\gamma - 1}{2} M_n^2 \right]$$

where $P_r$ = Prandtl number

$M_n$ = Mach number

$n$ = $\frac{1}{2}$ for laminar flow in boundary layer or $\frac{1}{3}$ for turbulent flow in boundary layer.

The relationship between gas-to-blade heat transfer coefficient and the remaining controlling parameters is discussed in some detail in Refs. 3 and 4 and also in section 5.3 of this Report. Once the external blade shape and gas stream operating conditions have been fixed then the conductance ratio will be determined by the internal cooling configuration.

To secure a desirably low value of conductance ratio it is necessary to devise a cooling configuration which combines a large internal cooling surface area with a high value of blade-to-cooling air heat transfer coefficient. At the same time the quantity of cooling-air required must be as small as possible in order to minimise reductions in overall engine efficiency created by cooling air pumping losses and the loss of heat to the cooling air. Furthermore the resulting blade must be sufficiently robust to withstand (i) high centrifugal stresses (currently of the order of 10 tons/sq in.), (ii) thermal stresses which may be created by non-uniformity in the blade cooling and (iii) local scaling losses in regions of high local temperature such as the leading and trailing edge.

When the geometry of the blade and its cooling configuration has been finally determined then the degree of cooling will depend primarily upon the temperature difference between gas stream and inlet cooling air and the ratio of cooling air mass flow to main stream gas mass flow. To a lesser extent the operating Reynolds numbers of the gas and cooling air flows, the ratio of gas temperature to cooling air inlet temperature, and the gas flow incidence on to the blade may also be expected to affect the degree of cooling.

2. *Scope of Reported Tests.*—The present Report records a series of tests made on the experimental single-stage air-cooled turbine to investigate the cooling characteristics of a set of air-cooled nozzle and rotor blades which were designed to meet the requirements enumerated in the previous section. These blades were cooled by passing cool air spanwise from root to tip through a multiplicity of small-diameter passages provided within the blades.

The experimental turbine has been described in detail in Ref. 4. The present series of tests were devoted to investigations at relatively low inlet gas temperatures (650 deg C to 700 deg C) with the object of acquiring a comprehensive knowledge of the heat transfer characteristics of the blading, without undue risk of mechanical failure, before proceeding with further tests to determine the durability of the blading at higher gas temperatures.

Cascade tests (Ref. 7) have previously been carried out on a blade similar to the turbine rotor blade and a secondary objective of the present tests was to compare the cooling characteristics obtained in both the turbine and cascade tunnel in order to indicate the degree to which results of such cascade tests may be applicable to blades operating in actual turbine-stages.

Measurements were also made of the air pressures required to force the cooling flows through the blades, these being important to the extent that in any practical application of an air-cooled turbine to an engine it is clearly desirable that the maximum cooling-air pressures required should not exceed the final compressor delivery pressure.

During the tests the ratio of cooling air to gas mass flow for each row of blades was varied over a range of 0 to 0·03 and the gas flow Reynolds number $R_{eg}$ was varied over a range of $0 \cdot 5 \times 10^5$ to $1 \cdot 6 \times 10^5$ on the rotor blades and $1 \cdot 4 \times 10^5$ to $4 \cdot 6 \times 10^5$ on the nozzle blades. The cooling-air inlet temperature was maintained at roughly 80 deg C to 100 deg C, giving a ratio of absolute gas temperature to absolute cooling-air temperature of approximately 2·6.

3. *Description of the Blading.*—The nozzle and rotor blades, each of which were untwisted and of constant section (*i.e.*, untapered), are illustrated in Fig. 1, and Figs. 3 and 4 of Part I. It is shown in Appendix II that the heat passed to the cooling air (per unit temperature difference between blade and cooling air) in circular cooling passages passing a fixed total quantity of cooling air is given approximately by the relationship.

$$h_c S_c \propto n^{0 \cdot 2} / D^{0 \cdot 8} \qquad \ldots \quad (8)$$

where $n$ = number of passages

$D$ = diameter of passage.

This indicates that to secure a high value of $h_c S_c$ the number of cooling passages should be large and the diameter of the passages small. At the same time it is desirable that the cooling flow Reynolds number $R_{ec}$ should be above the critical value in order to secure turbulent flow with high values of passage heat transfer coefficient. Turbulent cooling flow is also desirable to ensure that the degree of cooling secured in a blade is not adversely affected by an increasing Reynolds number $R_{eg}$ in the main stream gas flow. External heat transfer coefficient is approximately proportional to $(R_{eg})^n$, where $n$ varies between 0·6 and 0·8 for turbine blades (*see* section 5.3). For a fixed ratio of cooling-air mass flow to gas mass flow and fixed values of gas and cooling-air temperatures the ratio $R_{ec}/R_{eg}$ is also approximately constant and, with turbulent cooling flow, the internal heat transfer coefficient varies proportionally to $(R_{ec})^{0 \cdot 8}$. Thus, under turbulent flow conditions, the conductance ratio (and hence blade temperature) might be expected to decrease slightly as $R_{eg}$ is increased. With laminar cooling flow, however, the cooling-air heat transfer coefficient would remain constant and the conductance ratio (and blade temperature) would increase appreciably as $R_{eg}$ increased. Finally the number and size of the cooling passages must be such that when passing the design quantity of cooling air the pressure drop in the system must be less than the available pressure difference between the compressor delivery pressure and the static pressure at the turbine blade tip (where the cooling air is discharged from the blade).

Considerations such as these led to the adoption of 38 cooling passages of 0·03-in. nominal diameter in the rotor blades (99 blades in the row) and 53 cooling passages of 0·04-in. nominal diameter in the nozzle blades (45 blades in the row). A ratio of cooling-air mass flow to gas mass flow for each row of blades of 0·02 was assumed for design purposes.

It will be noted in Fig. 1 of Part I that the cooling air is discharged from both the nozzle blades and the rotor blades at the blade tips and mixed with the main gas stream, there being a radial tip clearance between the blade tip and an adjacent stationary shroud ring on both nozzle and rotor rows.

The constant-section untwisted form was adopted for convenience in manufacture since this form was not expected to influence to any important degree the cooling characteristics of the blading. Some degree of taper to relieve blade-root centrifugal stress could be accommodated with this form of blade in a practical application where operating conditions make this desirable.

The blades were fabricated by a sintering technique (developed by the General Electric Company, Ltd.) employing a tungsten-vitallium powder (64 per cent Co, 30 per cent Cr, 6 per cent W) in which the holes were formed by embodying cadmium wires within the blocks of compacted powder. During sintering the cadmium wires volatilised leaving clean holes in the block. As a result of the high pressure used to compress the powder the cadmium wires were slightly flattened resulting in holes of roughly elliptical cross section in the rotor blades with a ratio of major to minor axis of approximately 1·3 : 1. The final hydraulic mean diameter of the rotor blade passages (4 × hole area/perimeter) has been assessed by inspection as 0·028 in. and the hydraulic mean diameter of the nozzle passages as 0·039 in.

The powder was compressed and sintered in the form of rectangular bars, in order to obtain uniform density of material across the blade section (approximately 98·8 per cent of the theoretical value), from which the final blade and root shapes were formed by machining and grinding.

Vitallium was selected as the blade material since, at the time the work was planned, more experience in the field of powder metallurgy was available on this material than on other suitable heat resistant materials. The creep strength of the sintered material is plotted in Fig. 3. The stress-to-rupture in 100 hours at 750 deg C for the sintered material is about 20 per cent less than that of a cast alloy of nearly identical composition. The fatigue strength of the sintered material at various temperatures is tabulated below :

TABLE 1

| Stress (tons/sq in.) | Endurance (cycles) $\times 10^{-6}$ | | |
|---|---|---|---|
| | 750 deg C | 850 deg C | 900 deg C |
| $0 \pm 16$ | 0·504 | | |
| $0 \pm 14$ | 2·528 | | |
| $0 \pm 12$ | 4·564 | | |
| $0 \pm 11$ | 29·410 | | |
| $0 \pm 10$ | 98·428 | 2·47 | |
| $0 \pm 9$ | | | 3·1 |
| $0 \pm 7$ | | 5·24 | |
| $0 \pm 5$ | | | 105·0 |
| $0 \pm 4$ | | | 2070·0 |

The relevant dimensions and angles of the nozzle and rotor blades are tabulated in Appendix III. The blades combine to form a turbine-stage which at 9,000 r.p.m., 1,300 deg K inlet temperature, and zero mean incidence on to the rotor blades operates with a total head pressure ratio of about 1·65, a work done coefficient $(2K_p \Delta T_W / U_m^2)$ of 4·3, and a mean stage reaction of about 30 per cent.

At the same condition the centrifugal stress in the root section of the rotor blade is estimated as 8·5 tons/sq in. and the maximum gas bending stress is estimated as approximately 1·3 tons/sq in. when the operating Reynolds number of the rotor blading is $1 \times 10^5$.

4. *Description of Tests.*—As previously stated in section 2 the inlet gas temperature to the turbine was maintained at an approximately constant value of 650 deg C to 700 deg C and the cooling air inlet temperature at 80 deg C to 100 deg C throughout the tests. For each test the overall pressure ratio was adjusted to obtain a predetermined value of gas flow Reynolds number.

Now, $R_{eg} = \dfrac{\rho_2 V_2 C}{\mu_2}$ (for notation refer to Appendix I)

$$= \frac{\rho_2 V_2 A_t C}{A_t \mu_2}$$

$$\simeq \frac{C}{A_t} \frac{W_R}{\mu_2} . \qquad \text{(2)}$$

Since viscosity is a function of gas temperature only and since blade chord and total blade passage throat area remain fixed then it is seen from equation (2) that the gas flow Reynolds number is a function of gas mass flow and temperature only and independent of the rotational speed of the turbine. Furthermore, it was found that at constant inlet temperature and constant pressure ratio the turbine gas mass flow remained very nearly constant over a wide range of rotational speeds so that operation of the turbine under these conditions enabled a wide range of operating incidences on to the rotor blades to be covered (by varying the rotational speed) whilst maintaining a constant value of the operating Reynolds number. A range of rotor blade Reynolds number of $0 \cdot 5 \times 10^5$ to $1 \times 10^5$ was covered with atmospheric pressure in the exhaust duct and this range was extended to $1 \cdot 6 \times 10^5$ by throttling the turbine exhaust and running the stage at a higher mean level of pressure. The tests with the unthrottled and throttled outlet overlapped and indicated that the heat transfer characteristics were not noticeably affected by the variations in gas Mach number and turbine rotational speed which accompanied a change in $R_{eg}$ at any given blade incidence.

In a single-stage turbine the mean operating incidence of the gas flow on to the rotor row is approximately a unique function of the stage work-done coefficient, $2K_p \Delta T_w / U_m^2$, and in the following discussion the value of this coefficient is sometimes referred to in lieu of incidence. The relationship between incidence and work done coefficient is plotted in Fig. 4.

At selected values of $R_{eg}$ and $2K_p \Delta T_w / U_m^2$ the ratio of cooling-air mass flow to gas mass flow through the nozzle and rotor blades was varied over a range of approximately 0 to $0 \cdot 03$ in each row and, for each value of cooling flow quantity, measurements of blade metal temperature were made by means of thermocouples placed at nine selected positions in the blades as illustrated in Fig. 2. In any one blade a maximum of 3 couples were installed, these being situated in the same spanwise position but in different chordwise positions. In the nozzle blades measurements at individual points were duplicated in diametrically opposite blades. In the rotor blades the measurements at each of the nine location points in the blades were repeated in three separate blades, both as an insurance against failure of any of the couples and also to provide some indication of any variations that may occur in temperature between different blades under identical overall operating conditions. Since the slip-ring assembly only permitted 6 rotor couples to be used at any one time the tests had to be repeated to secure measurements of blade temperature at all nine positions. Further details of the couple installation and turbine instrumentation are given in Part I.

5. *Discussion of Results*.—5.1. *Cooling of Rotor Blades* ($i \simeq 0$ *deg*, $R_{eg} \simeq 1 \times 10^5$).—The variation of blade temperature at the nine selected positions in the rotor blade with cooling-air quantity is shown in Figs. 5a to 5c, each figure portraying the various blade temperatures measured at one spanwise position along the blade. The test results are plotted on a non-dimensional basis of ' blade relative temperature ' against ' cooling flow ratio '. Blade relative temperature is defined as

$$\frac{\text{Blade temperature} - \text{inlet cooling-air temperature}}{\text{' Effective ' gas temperature} - \text{inlet cooling-air temperature}} .$$

The rotor blade inlet cooling-air temperature was measured at a point just before it entered the hollow rotor shaft. This cooling air is instrumental in cooling the blade roots as well as the blades proper. Since the rotor discs are well cooled by an independent cooling-air supply passing over the outer face of the discs and across the disc rims the blade cooling air will pick up only a negligible quantity of heat in passing from the rotor shaft to the blade roots. Since the gas Mach numbers were generally less than about $0 \cdot 6$ the effective gas temperature was assumed to be equal to the total gas temperature as estimated relative to the moving blades. The true effective gas temperature (as defined in section 1) is actually slightly less than this, but under the operating test conditions the error involved amounts to less than 1 per cent in the estimation of blade relative temperature and has therefore been neglected. Furthermore, in Fig. 5 the gas temperature used is the mass mean gas temperature, designated by $\bar{T}_g$, for the entire gas flow through the rotor row. The cooling flow ratio is defined as the ratio of cooling-air mass flow passing through the cooling passages to the gas mass flow passing over the blades. Due to the introduction of cooling air into the main gas stream from the nozzle row it should be observed that the gas mass flow through the rotor row, $W_R$, is slightly greater than that passing through the nozzle row, $W_N$.

In Fig. 5d the spanwise variation in blade temperature is plotted for a cooling flow ratio of 0·020. Also shown on this Figure is the spanwise variation in gas temperature, estimated from earlier traverses of the gas flow described in Part I.

It will be observed that the highest metal temperatures were measured at the couples located near the leading edge and the lowest temperatures at the mid-chord points. Furthermore, the spanwise variation of temperature is clearly influenced considerably by the gas temperature distribution, difference between the local gas temperatures and the mean gas temperature at a spanwise section located at $0 \cdot 4 \times$ blade height from the blade root amounting to about 10 per cent of the difference between the mean gas temperature and inlet cooling-air temperature. At this section the greatest variation of blade temperatures along the blade chord occurs.

Also shown in Fig. 5d is an estimate of the maximum blade temperatures, occurring at the extreme trailing edges of the blades. This temperature (not directly measured in the turbine) was derived from earlier cascade tests as described in the following paragraph.

In Fig. 6a the measured chordwise variation of blade relative temperature at the mid-span position is plotted for two values of cooling flow ratio. The general form of the distribution remains similar for each cooling flow ratio, but as the cooling flow increases the mean level of blade temperature falls and at the same time the difference in temperature between selected points along the blade chord increases. It is to be noted that, since the chordwise variation in blade temperature at a given span position will be influenced by the local gas temperature in that vicinity rather than the mean gas temperature, the effective gas temperature used to define blade relative temperature in Fig. 6 is the local gas temperature at the mid-span position, designated by $T_g^*$.

The chordwise distribution in temperature may be expressed conveniently by plotting the variation of a parameter $(T_b - T_{bm})/(T_g^* - T_{bm})$ with chordwise position, $x/c$, where $T_{bm}$ is the mean blade temperature at the section considered. In estimating the value of $T_{bm}$ allowance is made for the variation of blade-section thickness along the chord and it was found, by trial and error, that

$$T_{bm} \simeq [T_{b\,(x/c\,=\,0\cdot 1)} + 2T_{b\,(x/c\,=\,0\cdot 42)} + T_{b\,(x/c\,=\,0\cdot 7)}]/4$$

The above defined temperature distribution parameter is plotted in Fig, 6b, showing the approximate insensitiveness of the chordwise distribution, expressed in this manner, to cooling flow ratio. In Fig. 7 the values of $(T_b - T_{bm})/(T_g^* - T_{bm})$ measured on the rotor blade are compared with the distribution measured on a cascade blade (Ref. 7) closely resembling the turbine blade and operating at a similar value of gas incidence, Reynolds number, cooling flow ratio and ratio of gas temperature to cooling-air inlet temperature. The cascade blade had an external profile identical to the turbine blade but a slightly different configuration of cooling holes, as illustrated in the lower half of Fig. 7. As compared with the cascade blade the turbine blade appears to operate relatively hotter along the leading half of the blade chord and cooler along the trailing half of the chord. This might reasonably be attributed to the facts that (*a*) the turbine blade has a slightly larger number of cooling holes in the trailing half of the blade section than the cascade and (*b*) the turbine blade apparently operates with a larger proportion of the boundary layer in a turbulent condition than the cascade; the factors leading to this latter deduction are described later in section 5.3 and as a consequence it may be anticipated that the leading half of the blade section will operate with relatively larger values of gas-to-blade heat-transfer coefficient than the cascade blade.

Thus, using the cascade test results as a guide, it is possible to make a reasonable extrapolation of the turbine-blade temperature measurements to the trailing and leading edges, as shown by the broken line in Fig. 7. This estimated distribution, corresponding strictly to a value of cooling ratio of $0 \cdot 01$, is also shown on Fig. 6b. The turbine results suggest that the values of $(T_b - T_{bm})/(T_g^* - T_{bm})$ when $w_R/W_R = 0 \cdot 02$ should be slightly greater at the trailing edge and slightly less at the leading edge than those corresponding to $w_R/W_R = 0 \cdot 01$ and the distribution has been adjusted accordingly, as shown on Fig. 7b, although the magnitude of this adjustment corresponds to a change in the value of $(T_b - T_{cR})/(T_g^* - T_{cR})$ at the trailing edge of only about $+ 0 \cdot 015$.

The general form of the chordwise temperature distribution, namely high blade-temperatures at the leading and trailing edges and substantially lower temperatures at the mid-chord sections, is common to most forms of cooled blade and is due to the extreme difficulty of extracting a sufficient quantity of heat from the blade near the leading and trailing edges where the local gas-to-blade heat-transfer coefficients are large and the internal space available for cooling-air passages is severely restricted. Typical distributions of local heat-transfer coefficient, represented non-dimensionally as a Nusselt number, round a turbine-blade profile nearly similar to that of the test blade are shown in Fig. 18 (*see* section 5.3 later), from which it may be seen that heat transfer close to the leading-edge stagnation point is about four times as great as the average value for the whole section. The very thin boundary layers coupled with a large value of $dV/dx$ in this region account largely for this phenomenon. It appears possible to alleviate the cooling difficulties to some extent in this region by using blades with rather blunter leading edges which have the twofold benefit of both reducing the magnitude of the gas-to-blade heat-transfer coefficient and also providing a thicker blade section near the leading edge with more space for the provision of extra cooling passages. The trailing edge presents a more difficult problem since a relatively long tapering section is required for the trailing section of a blade to secure high aerodynamic efficiency. The external heat-transfer coefficients are fairly high in this region, due to the turbulent nature of the associated boundary layers, and the provision of sufficient cooling passages within the blade becomes very difficult without excessively weakening the mechanical strength. The low thermal conductivity of heat-resistant materials leads to very little relief of temperature at the trailing edge by conduction of heat along the blade chord to the cooling passages situated nearer the centre of the section.

In the present blades it would appear possible to alleviate the variation in temperature along the chord to a small extent by inserting a few extra passages in the trailing-edge section between $x/c = 0 \cdot 7$ and $x/c = 1 \cdot 0$ and eliminating several of the holes near the mid-chord position.

Such a procedure, to have an appreciable effect, would, however, necessitate a reduction in the total number of passages so that for a given cooling flow ratio a slight reduction in the average degree of cooling would result together with an appreciable increase in the cooling air pressure drop. On the other hand, it is by no means clear that the temperature distributions obtained are likely to have drastic consequences on the ultimate potentialities of this type of cooled blade. In fact it can be argued that within limits such a distribution carries some advantage since the thermal strains created by this form of temperature distribution transfer the major operating stresses to the relatively cool and robust centre-section of the blade chord. At the same time the hot leading and trailing edges must be capable of tolerating the greater degree of oxidation that will occur at these points as compared with the remainder of the blade. A basically 'solid' type of blade, such as those under present investigation, might be expected to be superior in this respect to fabricated blades consisting essentially of a stress carrying outer shell having some form of internal structure (either loose or brazed in) provided to secure efficient heat transfer to the cooling air. A more detailed discussion of the thermal stresses and their possible consequences is deferred to sections 6 and 7 later.

Assuming that the form of the chordwise temperature distribution shown in Fig. 6b is applicable to all spanwise positions the variation of mean blade temperature $T_{bm}$, along the blade span is illustrated in Fig. 8a for cooling flow ratios of 0 to $0 \cdot 025$. In this figure the original definition of blade relative temperature (taking an overall mass mean of gas temperature) has been reverted to.

With no cooling the measured blade temperatures approximate to the gas temperature, the blade temperature being slightly less than the gas temperature towards the blade root, on account of the heat abstracted from the blade root by the disc cooling air, and the blade temperatures being slightly greater than the gas temperature towards the blade tips due to heat being conducted along the blade from the hot mid-span position towards the cooler blade tips. This comparison of gas and metal temperature distribution with no cooling is, of course, only approximate since the gas temperature distribution is derived from earlier tests in which the flow in the unbladed turbine annulus was traversed. Slight changes are to be anticipated due to the presence of the nozzle row and also due to slight variations in fuel spray characteristics of the burners in the combustion chambers which might be expected to occur over a long period of time. In the light of these possible variations this comparison appears remarkably good, and serves to indicate that the thermocouples were registering temperatures very close to the true metal temperatures.

In Fig. 8b the mass average of blade temperature for the entire rotor blade, $\bar{T}_{bm}$, is plotted (on a basic of blade relative temperature) against cooling flow ratio. When the cooling flow ratio is $0 \cdot 02$ an average blade relative temperature of $0 \cdot 63$ is obtained. If the mean gas temperature measured relative to the blades were 1,100 deg C and the cooling-air inlet temperature 200 deg C then this implies that the average blade temperature would be 766 deg C, *i.e.*, an average cooling of 334 deg C.

The temperature-stress relationship in the blade is such that the weakest section occurs at about $0 \cdot 4$ to $0 \cdot 5$ of the blade span from the root (*see* section 7 later). The estimated values of the blade temperatures at the mid-span position when the turbine is operating at full speed (9,000 r.p.m.) with a cooling flow ratio of $0 \cdot 02$, zero incidence, rotor-blade gas-flow Reynolds number of $1 \cdot 0 \times 10^5$, and inlet cooling-air temperature of 200 deg C, is plotted in Fig. 10 for a wide range of turbine inlet mean gas temperature. Uncooled turbines in current aircraft engines operate with maximum blade temperatures in the vicinity of 820 deg C. A cooled blade of the present type manufactured from a material of the same properties would apparently allow an inlet gas temperature of 1,170 deg C (2,140 deg F) if the mean cooled blade temperature were allowed to reach 800 deg C or, on a more conservative basis, an inlet temperature of 965 deg C (1,770 deg F) if the trailing-edge temperature only were allowed to reach 820 deg C. Actually the permissible maximum operating conditions must take into account the thermal stress created by the non-uniform temperature distribution, and also the oxidation resistance of the material, and will lie somewhere between the above values. This problem is discussed more fully later in section 7. The above figures merely serve to give a rough measure of the potentialities of the present form of air-cooled blade as looked at from a highly optimistic and from a highly conservative point of view respectively.

5.2. *Cooling of Nozzle Blades* ($i = 0$ *deg*, $R_{eg} \simeq 4 \cdot 5 \times 10^5$).—A detail analysis of the cooling of the nozzle blades is hampered considerably by the non-uniform distribution in gas temperature upstream of those nozzle blades fitted with thermocouples. Large circumferential variations occur in gas temperature as well as radial variations (for detail information *see* Ref. 1) and furthermore variations in mean delivery temperature from individual combustion chambers occurred from test to test. The circumferential variations were of little consequence in the rotor-blade cooling investigations since the high speed of rotation resulted in the blades being sensitive only to a circumferential mean of gas temperature at any spanwise position. Only mean gas temperatures were evaluated during tests, these being derived from measured values of air flow, fuel flow, and combustion efficiency, so that the gas temperature distribution upstream of the nozzle row had to be estimated from previous tests mentioned in Ref. 1.

The analysis presented here is derived from the tests at the highest test value of Reynolds number (approximately $4 \cdot 5 \times 10^5$ on the nozzle blades). Under these conditions the fuel burner pressures were high and difference in mean outlet temperature between individual combustion chambers least.

The nozzle blades fitted with thermocouples were in two groups, designated 'A' and 'B', with three adjacent blades in each group. The three blades in each group had three couples fitted in each, these measuring temperatures at $x/c = 0 \cdot 11$, $0 \cdot 38$, and $0 \cdot 75$ along the chord. Temperatures at the blade root, mid-span, and tip positions were measured respectively in the three adjacent blades of each group.

The variations of measured blade temperatures, on a blade relative temperature basis, with cooling flow ratio for both groups of nozzle blades are illustrated in Fig. 10.

In general the blade temperatures were higher in group A than in group B, particularly in the top halves of the blades. This effect is largely due to the differences in the gas temperature distributions associated with the two groups. Typical gas temperature distributions in the vicinity of each group of instrumented nozzle blades are shown in Fig. 11. In group A the difference between peak gas temperature and overall mean gas temperature was approximately 24 per cent of the difference between the mean gas temperature and the cooling air inlet temperature. Thus, when the mean gas temperature was, say 900 deg K, the peak gas temperature was approximately 1,030 deg K. As explained in Ref. 4 this relatively poor temperature distribution was obtained as a consequence of the type of design selected for the high-temperature combustion chamber (*viz.*, a 'multi-can' assembly with film-cooled metal liners in the chambers). The results achieved on the present turbine must serve to emphasise the need for designs of high-temperature combustion chamber which have as great a degree of uniformity in outlet temperature distribution as possible.

The chordwise distribution of nozzle blade temperature at the mid-span position in group A is shown in Fig. 12a for various values of cooling flow ratio, the revised definition of blade relative temperature, based on local gas temperature at mid-span, being used. In Fig. 12b the variation of the distribution parameter $(T_b - T_{bm})/(T_g{}^* - T_{bm})$ with chordwise position and cooling flow ratio is shown.

It is clear from Fig. 12 that with low values of the cooling flow ratio the trailing half of the blade section is being relatively better cooled than the leading half and the more usual temperature distribution (high temperatures at leading and trailing edges and lower values at mid chord) is only observed at high values of cooling flow ratio. This effect appears to be largely due to the fact that the nozzle cooling air spills into the main gas stream in a radial clearance space at the blade tip and that, due to the large gas flow static pressure drop in passing through the nozzle row, the local static pressures at the blade tip are much higher near the leading edge of the blade than at the trailing edge. Thus, there is a tendency for a greater proportion of the cooling air to pass down the cooling passages in the trailing half of the blade section than in the leading half. This tendency becomes particularly marked at low values of cooling flow ratio when the frictional pressure losses in the cooling passages are small. In fact, when the cooling flow ratio is $0 \cdot 017$ the gas static pressure just upstream of the nozzle row is approximately equal to the cooling-air inlet total pressure. At this cooling flow ratio there will evidently be very little cooling air passing through the leading-edge cooling passages, whilst at substantially lower cooling flows a reverse flow may commence in the passages near the leading edge ; hot gas passing up the blade from tip to root near the leading edge whilst the externally supplied cooling air could only pass down the centre and trailing-edge sections.

A similar trend, though very much less pronounced, is discernible on the rotor blades when operating at high negative incidences. At zero incidence the effect is only slight (Fig. 6), since the static pressure drop in the main gas stream across the rotor blade tips is then small compared with the cooling-air static pressure drop in the cooling passages. This of course, largely results from the low reaction of the stage. It may be anticipated that the effect will be more pronounced on the rotor blades in high reaction stages. The tendency for the leading-edge cooling passages of the nozzle vanes to be relatively starved of cooling air may be counteracted by shrouding the nozzle blade tips and allowing the cooling air to spill into a space of uniform pressure underneath the shroud ring which in turn, is vented to the space between nozzle and rotor rows. In this way the pressure drop along all the cooling passages may be equalised and the nozzle tip static pressure reduced to the minimum possible value which will still allow the exhausted cooling air to be mixed into the main gas stream and perform useful expansion work in subsequent turbine stages. It will be shown in a later report that the present arrangement of a radial clearance space at the nozzle blade tips also entails a serious penalty in the overall stage efficiency of the turbine.

The spanwise variation of mean blade temperature for various values of cooling flow ratio is shown for both groups of instrumented nozzle blades in Fig. 13.

It may be noted that the spanwise variations in blade temperature differ in the two groups, the differences being associated with differences in gas temperature distribution between the groups. In group B the spanwise variation is a little more uniform and the gas temperature in the vicinity of the blade root a little higher than in group A. Corresponding differences occur between the spanwise variations in blade temperature.

In Fig. 14 the variation of the mass average temperature of the entire nozzle blade with cooling flow ratio is shown. The mean gas temperature used in estimating the blade relative temperatures in this instance was the local mean value of the gas temperature, this being greater in group A than in group B. The difference still remaining between the results obtained from the two groups is presumed to be a reflection of the uncertainty of the local gas temperatures truly appertaining to the relevant tests.

5.3. *Influence of Gas Flow Reynolds Number on the Blade Cooling Characteristics.*—If the cooling flow ratio, gas flow incidence, and the ratio of gas temperature to cooling-air temperature are maintained at constant values while the gas flow Reynolds number $R_{eg}$ is varied then the Reynolds number of the cooling air flow, $R_{ec}$, in the internal blade passages will vary in direct proportion to $R_{eg}$. Now it is well known (Refs. 3, 4) that the gas-to-blade heat-transfer coefficient $h_g$ for a turbine blade varies in proportion to $(R_{eg})^n$ where $n$ normally lies in the range $0 \cdot 8 > n > 0 \cdot 5$, the precise value of $n$ being largely dependent upon the geometrical shape and operating conditions of the blade. Similarly (Ref. 8), when the cooling air passes through passages of constant cross-section and large length/diameter ratio at a Reynolds number exceeding the critical value for turbulent flow, the blade to cooling air heat-transfer coefficient, $h_c$ varies in proportion to $(R_{ec})^{0 \cdot 8}$. Thus, when cooling flow ratio, gas temperature, and inlet cooling air temperature are maintained constant the conductance ratio, $h_g S_g / h_c S_c$, will vary in proportion to $(R_{eg})^{(n - 0 \cdot 8)}$, i.e., somewhere in the range $R_{eg}^{0}$ to $R_{eg}^{-0 \cdot 3}$. Thus it might be anticipated that under these conditions the blade relative temperature will remain constant or decrease slowly as the gas flow Reynolds number is increased. The rate of decrease will be largest when $n$ is smallest and this occurs when the entire boundary-layer flow over the external blade surface is laminar, $n$ then being equal to $0 \cdot 5$. On the other hand if this boundary layer were entirely turbulent then $n$ would be roughly equal to $0 \cdot 8$ and the blade relative temperature would remain constant as the Reynolds number varied.

Since the absolute rates of heat transfer to and from the blade increase as the gas flow and cooling flow Reynolds numbers increase, while at the same time the blade conductivity remains substantially constant, then it may be anticipated that the chordwise temperature gradients in the blade metal will invariably increase as the Reynolds number increases.

In Fig. 15 the measured chordwise distribution of rotor-blade relative temperature at midspan and the distribution parameter $(T_b - T_{bm})/(T_g{}^* - T_{bm})$, is shown for a cooling flow ratio of $0 \cdot 02$ and gas flow Reynolds number of $0 \cdot 6 \times 10^5$, $1 \times 10^5$, and $1 \cdot 6 \times 10^5$. These distributions clearly illustrate the twin effects of a slightly decreasing mean value of blade relative temperature and increasing chordwise temperature gradients as $R_{eg}$ increases. A noticeable decrease in blade relative temperature occurs at the mid-chord position while at the leading and trailing-edge positions only a very slight change occurs.

In Fig. 16 the variation in the average rotor-blade relative temperature (for the entire blade) with $R_{eg}$ is shown, the mean value falling slightly from $0 \cdot 64$ at $R_{eg} = 0 \cdot 6 \times 10^5$ to $0 \cdot 62$ at $R_{eg} = 1 \cdot 6 \times 10^5$. For the conditions of test (cooling flow ratio $= 0 \cdot 02$ and ratio of gas to cooling-air temperature $= 2 \cdot 5$) the Reynolds number of the cooling flow at entry to the cooling passages was approximately equal to $0 \cdot 042 \times R_{eg}$. Thus the cooling flow Reynolds number varied between 2,470 and 6,600 over the test range of $R_{eg}$. Over this range the value of $R_{ec}$ exceeds the critical value of 2,170 so that the flow in the cooling passages is presumed to have been turbulent throughout. Indeed, there is no evidence in the test results to suggest that the cooling flow reverted to a laminar form at the low end of the Reynolds number range.

For comparison with the turbine tests the corresponding results derived from the cascade tests are also shown, the cascade blade exhibiting substantially lower values of blade relative temperature and a greater decrease of blade temperature with increasing gas flow Reynolds number. These differences combined suggest very strongly that the blade tested in the cascade tunnel had a very much more extensive area of laminar boundary layer over the external surface than the turbine blade. This would appear quite probable since there was a long settling length of straight pipe in the cascade test rig between the combustion chamber and cascade section, which would be inducive to a steady inlet flow on to the test blade. In the turbine, however, the eight individual combustion chambers immediately upstream of the stage, combined with the wakes from the nozzle blades, and powerful secondary flows, would produce a highly turbulent and varying gas flow over the individual blades in the rotor which might be expected to lead to a more forward location of transition points. In particular, on the under-surface (or concave surface) of many turbine blades of similar profile form to the present blades, studies of potential flow using an electric tank (Ref. 9) have indicated the presence of a slight opposing pressure gradient situated about $0 \cdot 1$ to $0 \cdot 15$ of the blade chord from the leading edge. With smooth in-flow conditions the boundary layer might in some instances negotiate this region without transition and then remain laminar over nearly the entire under-surface. Large recurrent disturbances in the inflowing stream, however, may well lead to transition at about $0 \cdot 1 \times$ chord from the leading edge and thus render 90 per cent of the boundary layer on the under-surface turbulent.

To substantiate this theory further an approximate estimate of the mean gas-to-blade heat-transfer coefficient for the turbine rotor blades was made and compared with other experimental data and also with theoretical estimates. This approximate estimate was made from a knowledge of the measured values of blade metal temperature and cooling-air inlet temperature combined with the assumption that the mean blade-to-cooling-air heat-transfer coefficient, expressed in the form of a Nusselt number, is given by the relationship

$$\bar{N}_{uc} = 0 \cdot 02 \bar{R}_{ec}^{\,0 \cdot 8}$$

where $\bar{N}_{uc}$ and $\bar{R}_{ec}$ are evaluated taking air conductivity and viscosity values at mean blade temperature and air density at mean cooling-air temperature. This simple relationship is derived from data presented in Ref. 8 for air having a value of Prandtl Number of $0 \cdot 72$. It also accords closely with data given by McAdams (Ref. 10) who shows that the same relationship holds for non-circular passages, provided that hydraulic diameter ($4 \times$ area/periphery) is used as the representative length dimension in $\bar{N}_{uc}$ and $\bar{R}_{ec}$. This enabled a calculation to be made of the heat passed to the cooling air and this, for steady conditions, is equal to the heat passed from the hot gas stream to the cooled surfaces. It was necessary to make a separate estimate of the heat picked up by the cooling air in the blade root, it being assumed that this heat (together with the heat picked up by the disc cooling air in the disc rim) was equal to the heat passed from the hot gas to that area of the disc rim and root platform which is scrubbed by the hot gas stream. The heat-transfer coefficient on these surfaces (the surface area affected being about 14 per cent of the blade surface area) was assumed to be the same as the mean blade heat-transfer coefficient. This value may be rather high but on the other hand the error will be partially balanced out by the fact that the assumed disc rim area heated by the hot gas stream may be rather smaller than the actual heated area. The resulting estimated relationship of gas-to-blade heat-transfer coefficient, expressed in the form of Nusselt number, $N_u$*, with gas flow Reynolds number, $R_e$*, is shown by the shaded area in Fig. 17a. $N_u$* and $R_e$* are evaluated by estimating gas conductivity and viscosity at mean blade temperature and gas density at the arithmetic mean of blade temperature and gas temperature, this procedure being recommended in Ref. 4. Also shown on the same figure is the relationship, estimated in a similar manner, for the cascade tested blade and, for comparison, the experimental values for a typical impulse blade and typical nozzle blade presented in Ref. 4. In addition three theoretical calculations of the $N_u$* vs. $R_e$* relationship were made using the method of Ref. 2 for a blade (having a known surface velocity distribution) which was very similar in form and gas angles to the test rotor blade and assuming (*a*) transition at $x/c = 0 \cdot 5$ on the upper surface and at $x/c = 0 \cdot 1$ on the under-surface, (*b*) transition at $x/c = 0 \cdot 5$ on the upper surface and laminar flow on the under-surface, and (*c*) completely laminar flow. The theoretical relationship made on assumption (*a*) agrees remarkably well with the turbine test data. The theoretical estimates also suggest that the cascade blade probably operated with a laminar boundary layer on the lower surface and transition at $x/c \simeq 0 \cdot 7$ on the upper surface. Incidentally it is of interest to note that the mean Nusselt number of any turbine blade generally lies between the upper and lower limits defined by the Nusselt numbers for flat plates with fully turbulent and fully laminar boundary layers respectively. The actual value of Nusselt number depends primarily upon the proportion of the surface which has a laminar boundary layer and the pressure distribution round the surface is apparently important only in so far as it influences the points of transition. The calculated distributions of heat-transfer coefficient round the rotor blade are shown graphically in Fig. 18a.

A similar comparison of the relationship of $N_u$* with $R_e$* was made for the nozzle blade and is shown in Fig. 17b. The theoretical estimates of the distribution of heat-transfer coefficient round the nozzle blade is illustrated in Fig. 18b. This comparison suggests that the nozzle blade also operated with a turbulent boundary layer on the under-surface and the resulting values of $N_u$* are again rather larger than would have been anticipated from cascade tests. It is suggested that the highly turbulent flow from the combustion chambers immediately upstream of the nozzle row is the primary cause of this phenomenon.

These results all tend to throw some doubt on to the value of cascade tests as a means of ascertaining heat-transfer coefficients to turbine blades. It appears that such tests may be of value primarily in assisting the development of adequate theoretical methods and that such tests should include investigations to determine points of transition. The direct application of cascade tests to turbine operation is only practicable providing that the conditions of turbulence, etc., which determine points of transition are truly representative of the operating conditions of similar blades in an actual turbine stage. Similar reasoning would appear to apply equally well to cascade tests carried out to investigate pressure loss and gas deflection characteristics. It should, however, be added that the above reasoning has taken no account of possible differences in secondary flows between the cascade and turbine tests and consequent effects on average heat-transfer coefficient. In the absence of explicit data regarding the effects of secondary flows on gas-to-blade heat-transfer coefficients the preceding reasoning can only be regarded as tentative, although the over-riding effects, namely higher heat transfer in a turbine stage than in a cascade of similar blades, appears quite definite.

5.4. *Influence of Gas Flow Incidence on Rotor Blade Cooling.*—Fig. 19 shows the measured variation of rotor-blade relative temperature at mid-span over a wide range of stage work done coefficient ($5 \cdot 2 > 2K_p \Delta T_w / U_m^2 > 1 \cdot 8$), corresponding to a mean incidence variation of $-30$ deg to $+7$ deg. The cooling flow ratio, gas flow Reynolds number, gas temperature, and inlet cooling-air temperature were maintained constant at all points. The minimum blade temperatures were obtained at roughly zero incidence, although the temperatures remained substantially unaltered over an incidence range of $-10$ deg to $+7$ deg ($5 \cdot 2 > 2K_p \Delta T_w / U_m^2 > 2 \cdot 6$). At incidences below $-10$ deg the blade temperatures commenced to rise, the mean blade relative temperature increasing from $0 \cdot 71$ at $-10$ deg to $0 \cdot 73$ at $-30$ deg. Broadly this agrees with cascade tests (Ref. 11), it being anticipated that the blade temperatures would show a marked tendency to rise at incidences higher than those obtained in the present tests. It is of interest to note that a very substantial variation in stage work-done coefficient from the ' design ' value (corresponding approximately to zero incidence) can be achieved without any noticeable change in blade relative temperatures when the cooling flow ratio is maintained constant.

5.5. *Cooling-Air Pressure Losses.*—(*a*) *Pressure Losses in the Cooling Passages with Zero Heat Transfer.*—The measured pressure drop of the cooling air passing through the cooling passages, expressed in terms of conventional non-dimensional parameters, is shown in Fig. 20 and compared with values calculated assuming classical pipe friction coefficients for smooth pipe flow. The degree of agreement obtained suggests that the passages in the present blades may be regarded as smooth and that the length/diameter ratios are such that entry length effects may be ignored. For a given mass flow through a passage of fixed length the pressure drop (with turbulent flow) is approximately proportional to (passage diameter)$^{4.8}$. It was difficult to determine precisely, by inspection, the diameter of the very small cooling passages and the 10 per cent discrepancy between measured and calculated losses in the nozzle blade is probably largely attributable to an error in the estimation of passage diameter.

Since both the rotor and nozzle blades discharged the cooling air into a small radial clearance space between the blade tip and an adjacent shroud ring it was important to determine the influence of the magnitude of this clearance on the blade pressure losses. This effect was determined in a stationary experiment in which a surface representing the shroud ring was gradually moved up towards the tip of the blade while the mass flow of cooling air passing through the blade was maintained constant and the overall pressure drop between the blade inlet cooling-air pressure and the ambient pressure in the space outside the blade was measured for successively smaller clearances between the blade tip and shroud. The results from this experiment are plotted in Fig. 21. The end clearance on the rotor blade could be reduced from infinity to approximately 0·018 in. with only a 5 per cent increase in overall pressure drop. As the clearance was reduced below this value the overall pressure drop commenced to increase sharply. This implies that the turbine rotor tip clearance must be maintained at a value greater than 0·018 in. to prevent undue restriction to the escape of the cooling air. This clearance amounts to only 0·75 per cent of the blade height and larger clearances are normally required for mechanical reasons.

The nozzle blade has a considerably larger chord than the rotor and a radial clearance greater than about 0·032 in. is required to prevent an increase of more than 5 per cent in overall cooling-air pressure above the nominal unrestricted loss.

(*b*) *Losses in Rotor-Blade Cooling System.*—Under normal turbine operating conditions the pressure drop in the rotor blade for a given cooling flow ratio and operating Reynolds number will differ from the losses in a stationary blade with no heat transfer (as enumerated in the previous section) due to (i) the heating up of the cooling air as it passes through the hot blade, and (ii) the pumping effect created by the rotation of the discs and blades. If the ratio of gas temperature to cooling-air temperature is increased while the cooling flow ratio is maintained constant then the ratio of mean cooling-air density to mean gas density will increase. This leads to a reduction in the ratio of mean cooling-air velocity to mean gas velocity and consequently to a reduction in the ratio of cooling-air pressure drop in the blade passages to gas pressure drop in the turbine stage. It is convenient to express the cooling-air pressure drop non-dimensionally in the form,

$$(P_{cR} - \bar{p}_{sR})/(P_i - \bar{p}_{sR})$$

where $P_{cR}$ is the inlet total pressure of cooling air (measured in the present instance at the point where the rotor blade cooling air is fed into the hollow rotor shaft—*see* Fig. 1 of Part I)

$\bar{p}_{sR}$ mean static pressure at the rotor blade tip

$P_i$ total pressure of gas flow at inlet to the turbine.

When the value of this ratio is greater than unity then $P_{cR} > P_i$ and in a gas-turbine engine this would necessitate compressing the cooling air to a pressure in excess of the compressor delivery pressure (assuming that the pressure loss in the cooling-air duct connecting the compressor outlet to the turbine is approximately equal to the combustion chamber pressure loss in the main gas flow). The measured relationship between $(P_{cR} - \bar{p}_{sR})/(P_i - \bar{p}_{sR})$ and cooling flow ratio is plotted in Fig. 23 for various values of rotational speed and gas to cooling-air temperature ratio. The decrease in this pressure drop ratio at a fixed cooling flow ratio when temperature ratio is increased from 1 to 2·5 is clearly discernible. Also, when the temperature ratio remains constant, a reduction in the pressure drop ratio as rotational speed is increased may be observed, this of course being due to the increase in pumping force as the blade speed increases. It is to be noted that the maximum rotor cooling flow ratio that may be achieved without the cooling-air inlet pressure exceeding the turbine inlet total pressure is 0·017 on the present blade and disc arrangement. It must be emphasised that the loss measured in the present instance includes not only the blade passage loss but also the pressure losses suffered by the cooling air in passing through the entry ports provided in the rotor shaft, along the shaft, and up between the discs to the blade roots. Since the present unit is only an experimental rig in which plenty of excess pressure is available to drive the cooling air to the respective blade rows no attempt was made to provide a clean aerodynamic passage for the rotor cooling air along the hollow shaft and between the discs. The losses in this section were, in fact, about 40 per cent to 60 per cent of the losses in the blade passages themselves. This is demonstrated in Fig. 23b where test values of $(P_{cR} - \bar{p}_{sR})/(P_i - \bar{p}_{sR})$ for a flow ratio of 0·02 are compared with values calculated for the blade passages alone (allowing for the influence of heat transfer and rotation). There is some scatter in the test results but at corresponding values of temperature ratio and rotational speed the 40 per cent to 60 per cent excess of total-cooling-system loss over rotor-blade loss alone is clearly discernible. If the air pressure losses in rotor shaft and disc were reduced to the extent that they were just counterbalanced by the pumping force available from the rotor disc (assuming appropriate 'impeller' vanes are provided) then a flow ratio of 0·0195 could be achieved when $P_{cR} = P_i$. If in addition the cooled blade root were redesigned to reduce the unnecessarily large length of cooling passage in the root itself (in the present blade the root cooling passage has a length equal to half the length of the passage in the blade span) then the flow ratio could be further increased to about 0·021. Such a value would appear to be quite acceptable for a practical application of the present cooled blade configuration to an actual high-temperature cooled engine. It should be added that the above pressure losses apply to a gas flow Reynolds number of $1 \times 10^5$ and that some reduction in loss may be anticipated with increase in Reynolds number, due to the accompanying reduction in pipe-friction coefficient.

(c) *Losses in the Nozzle Cooling System.*—The nozzle-cooling air pressure drop is expressed in a convenient non-dimensional form similar to the rotor-cooling air pressure loss by the expression,

$$(P_{cN} - \bar{p}_{sN})/(P_i - \bar{p}_{sN})$$

where $P_{cN}$ is the inlet total pressure of cooling air measured in the annular header surrounding the nozzle root fixing

$\bar{p}_{sN}$ mean static pressure at nozzle blade tip

$P_i$ turbine gas inlet total pressure.

Since the nozzle blades are stationary then only the gas to cooling-air temperature ratio may be expected to influence the relationship between cooling-air pressure loss and cooling flow ratio. It might be anticipated that (as was found with the rotor cooling air) the ratio $(P_{cN} - \bar{p}_{sN})/(P_i - \bar{p}_{sN})$ would decrease for a given cooling flow ratio as the ratio of gas to cooling-air temperature increased. As will be seen from Fig. 22b this did not in fact occur, the pressure drop ratio showing a tendency to rise slightly as the temperature ratio increased. This effect is attributable to the fact that the thermal expansions of the nozzle blades, the nozzle root clamping ring, and the shroud ring adjacent to the nozzle blade tips combined in such a way that the end clearance between the nozzle blade tips and the adjacent shroud ring decreased as the gas temperature was increased. This end clearance was estimated to vary within the range of 0·020 in. to 0·010 in., these estimates being based on measured temperatures at relevant parts of the turbine structure and hence being only approximate. However, this range of clearance is such that the nozzle-blade cooling-air pressure drop will be perceptibly increased by small decreases in clearance (*see* Fig. 21b) which take place as the gas temperature increases. A comparison of the measured and calculated pressure losses for cooling flow ratios of 0·025 and 0·03 over a wide range of gas to cooling-air temperature is shown in Fig. 23a. Clearly the effect of change in end clearance can be eliminated by increasing the end clearance to a value outside the critical range, although this leads to some sacrifice in turbine efficiency. A better modification, however, as already suggested in section 5.2, would be to pass the nozzle blade tips through the adjacent shroud ring and allow the cooling air to spill into a space underneath the shroud, this space being vented to the axial space between the nozzle shroud ring and rotor disc rim. With the present arrangement it may be seen that a flow ratio of 0·024 to 0·020 (depending upon gas to cooling-air temperature ratio) may be achieved when $P_{cN} = P_i$. The results presented correspond to a Reynolds number of the gas flow through the nozzle blades of roughly $4 \times 10^5$.

6. *Estimate of the Thermal Stresses in the Rotor Blade.*—It is evident that the chordwise temperature distribution in the blades at any spanwise position is such that thermal stresses must be induced, stresses being compressive at the leading- and trailing-edge regions of the blade section and tensile in the centre part of the section. It is of interest to compute the approximate magnitude of these stresses. In order to do this certain simplifying assumptions must be made, these being :

(*a*) that the blade material is perfectly elastic

(*b*) that the coefficient of expansion and modulus of elasticity is constant (in particular, independent of blade temperature)

(*c*) that the blade is long compared with the chord and the temperature distribution remains constant along its length. The assumption of length is made to remove any constraints due to end effects. In fact such end effects will be very localised and would be unlikely to have appreciable influence on the mid-span section of the blade where thermal stresses appear to be most severe

(*d*) that the stresses in directions normal to the span are small compared with stresses in the spanwise direction

(*e*) that the blade is free to bend under the action of the thermal stresses

(*f*) that the temperature distribution along the blade chord is represented by the relationship between $(T_b - T_{bm})/(T_g^* - T_{bm})$ and $x/c$ shown in Fig. 7b for a cooling flow ratio of 0·02.

Making these assumptions it is possible to represent the induced thermal stress at each point in the blade section non-dimensionally by means of the function

$$q_t/E\theta[T_g^* - T_{bm}]$$

where $E$ is the the modulus of elasticity

$\theta$ coefficient of thermal expansion

$T_g^*$ local total gas temperature surrounding the blade at spanwise position considered

$T_{bm}$ mean blade temperature at spanwise position considered

$q_t$ direct stress in spanwise direction.

The underlying theory is outlined in Appendix IV. The chordwise variations of the function

$$q_t/E\theta[T_g^* - T_{bm}]$$

in the rotor-blade sections are plotted in Fig. 24. Also added to this Figure is a scale of stress in tons/sq in. corresponding to :

$$\begin{aligned} T_g^* &= 1{,}100 \text{ deg C} \\ T_{cR} &= 100 \text{ deg C} \\ T_{bm} &= 730 \text{ deg C} \\ w_R/W_R &= 0{\cdot}02 \\ E &= 20 \times 10^6 \text{ lb/sq in.} \\ \theta &= 18 \times 10^{-6} \text{ in./in. deg C.} \end{aligned}$$

These values are representative of a section situated at a distance of $0{\cdot}4 \times$ span from the root (where chordwise temperature gradients are most severe) when the turbine is operated at full speed (9,000 r.p.m.) with a mean turbine inlet gas temperature of approximately 1,350 deg K. Under these conditions the thermal stress is seen to vary from approximately 16 tons/sq in. compressive stress at leading and trailing edges to 12 tons/sq in. tensile stress at a point on the under-surface situated $0{\cdot}4 \times$ chord from the leading edge. The influence of these thermal stresses upon blade life and the possible effects of plastic yield in the material are discussed in the next section.

In addition to the steady thermal stresses it is desirable to have some knowledge of the variations in temperature distribution (and hence thermal stress) that are likely to occur under ' thermal shock ' conditions when the gas temperature is suddenly reduced. An approximate calculation of the change in chordwise temperature distribution at mid span has been made assuming that the gas temperature is suddenly reduced to a value equal to the cooling-air temperature, the gas mass flow remaining approximately constant and the cooling flow ratio remaining constant and equal to an initial assumed value of 0·025. The calculations neglect the influence of chordwise conduction of heat in the blade material during the rapid cooling process and so may be expected to give a slight over-estimate of the chordwise temperature gradients encountered.

The results of this calculation are presented in terms of convenient non-dimensional parameters in Fig. 25. Also added is a representative temperature scale corresponding to an initial gas temperature of 1,100 deg C and a cooling-air temperature of 100 deg C. These calculations clearly indicate a tendency for the blade trailing edge to cool very much more rapidly than the remainder of the blade. Now direct thermal stress at any local position of the blade is roughly proportional to the difference between the local metal temperature at the point considered and the mean temperature for the whole section at the same blade span position. It is to be noted particularly from Fig. 24, therefore, that during the cooling process the trailing edge must undergo a momentary *change* of stress of approximately twice the magnitude of the estimated elastic stress that occurs under steady initial operating conditions. Thus, if a compressive thermal stress of 16 tons/sq in. exists at the trailing edge before the rapid cooling commences then during the cooling process the trailing-edge stress will momentarily be reversed to a tensile value of about 16 tons/sq in. before it eventually becomes zero when the blade is fully cooled to a uniform value. If it is supposed that the blade has operated for a long period under the initial conditions and that the actual compressive stress in the trailing edge is reduced, due to local yield in the material, from 16 tons/sq in. to, say, 5 tons/sq in., then during the ' shock ' cooling process the trailing edge will momentarily reverse to a tensile value of 27 tons/sq in. before settling down to a final residual tensile stress of 11 tons/sq in. At the same time it should be noted that the maximum transient tensile stress fortunately occurs when the trailing-edge temperature has fallen by about four fifths of the ultimate temperature drop (*viz.*, difference between initial temperature and cooling-air temperature).

It is of interest to observe that the large momentary tensile stress occurring during ' shock ' cooling is limited in its severity by the poor internal cooling of trailing-edge region. This poor cooling results in (i) an initial compressive stress which must be ' taken up ' during cooling before the stress becomes tensile and (ii) a relatively slower rate of cooling in the trailing-edge section than would occur if the local internal cooling was made sufficiently vigorous to bring the trailing-edge temperatures during normal operation to values nearer those occurring at the mid-chord position. Thus, if by some internal modifications the chordwise temperature distribution was flattened then, it might be anticipated that during ' shock ' cooling a higher momentary tensile stress would be obtained in the trailing edge with a more serious attendant danger of cracking. Thus it would seem that some degree of non-uniformity (chordwise) in the cooling might be beneficial. The limits to which this applies however are by no means clear at the present time.

7. *Discussion of Permissible Operating Temperatures of the Rotor Blade.*—Leading from the preceding analysis of the blade cooling characteristics and the estimates of thermal stresses likely to be induced it becomes possible to speculate upon the maximum temperatures at which the rotor blade might be expected to work for a chosen blade life. In order to do this it is first necessary to identify the weakest portion of the blade.

Fig. 26a shows the variation in mean centrifugal stress at full speed (9,000 r.p.m.) along the blade span and also the mean tensile stress for 1 per cent creep in 1,000 hours that might be permitted at each spanwise position when the turbine operates with a rotor cooling flow ratio of $0 \cdot 02$ and an inlet gas temperature of 1,070 deg C (1,960 deg F). This figure indicates that the weakest section along the blade span occurs at roughly the mid-span position. The centrifugal stress is the largest mean stress at any spanwise position (the mean thermal stress being zero) and since gas bending stresses are small as compared with the centrifugal stresses the above conclusion would not be substantially modified by taking gas bending stresses into account.

It should be noted further that the local thermal stresses are greatest in the mid-span region of the blade.

Fig. 26b shows the variation of thermal stress + centrifugal stress along the blade chord at the mid-span position together with the stresses for 1 per cent creep in 1,000 hours that might be permitted at each chordwise position when the turbine operates with a rotor cooling flow ratio of $0 \cdot 02$ and an inlet gas temperature of 1,070 deg C. Assuming that the compressive stresses at the leading and trailing edges are unlikely to lead to blade failure (through buckling) then it is seen that the weakest chordwise section at mid span occurs at a distance of about $0 \cdot 4 \times$ chord from the leading edge. The thermal stress at each chordwise position is taken in this instance as the arithmetic mean of the values occurring on the upper and lower surfaces.

Now the centrifugal stress remains independent of the gas temperature whereas the thermal stresses increase as the gas temperature is increased (in proportion to the difference between gas temperature and mean blade temperature). The variation of the mid-span thermal stresses with turbine inlet temperature at (*a*) the trailing edge, (*b*) the lower surface at $0 \cdot 4 \times$ chord from the leading edge, and (*c*) the mean value at $0 \cdot 4 \times$ chord from leading edge, are shown in Fig. 26c. In Fig. 26d the relationship between the mean centrifugal + thermal stress and turbine inlet gas temperature at mid-span and $x/c = 0 \cdot 4$ is shown together with the local value occurring on the lower surface of the blade at the same spanwise and chordwise location. Also shown are the permissible stresses for rupture in 1,000 hours and 100 hours with sintered tungsten vitallium alloy. If no yield occurred in the blade material then the maximum permissible inlet gas temperature for 1,000 hours life would apparently be 1,000 deg C. Since, however, local yield in the material must take place, then the mean value of stress shown is probably more representative and an inlet temperature of 1,090 deg C would then appear possible for 1,000 hours life. This value may still be conservative since the high compressive thermal stresses at the leading and trailing edges will lead to fairly rapid yield in these regions and this will in turn lead to a substantial reduction in thermal stress at all chordwise positions. This will create residual tensile stresses at the leading and trailing edges and residual compressive stresses at the mid-chord position when the turbine is inoperative, but the magnitude of these residual stresses would appear to be well within the safe stress region of the material at low temperatures. To compare with these figures it is estimated that without any cooling (and with the same blade material) the maximum permissible inlet gas temperature for 1,000 hours life would be approximately 820 deg C. Thus the application of cooling apparently results in a permissible increase in the inlet gas temperature of about 270 deg C.

It remains to conjecture upon the possibility of failure of the blade when the inlet gas temperature is suddenly reduced from 1,090 deg C to a value equal to the cooling-air temperature (say 100 deg C). Now the calculated elastic thermal stress at the trailing edge is 16·5 tons/sq in. (compressive) when the gas temperature is 1,090 deg C, so that during the rapid cooling a change of stress of approximately 33 tons/sq in. may be expected (*see* section 6). If no yield has occurred in the blade material then this will lead to a momentary tensile stress of approximately 16·5 tons/sq in. when the trailing edge has attained a temperature of roughly 300 deg C. Since short-time tensile strengths of 45 tons/sq in. and 20 tons/sq in. at room temperature and 850 deg C respectively have been obtained with the present blade material then failure would seem unlikely. Stresses due to ' shock ' cooling become more severe, however, at the trailing edge if the material has yielded under the steady running conditions. Now the total thermal + centrifugal + bending stress at the mid-span position of the trailing edge (no yield) is approximately $(-16{\cdot}5 + 4{\cdot}5 + 0{\cdot}7) = -11{\cdot}3$ tons/sq in. (compressive). If it be assumed that after a long period of running the material has yielded to such an extent that this local stress has become zero and if it is assumed further that the rate of deceleration of the rotor when the gas temperature is reduced is such that the centrifugal + bending stress is reduced to 1 ton/sq in. by the time the trailing-edge tensile stress reaches its momentary maximum value, then this latter stress will become approximately $(16{\cdot}5 + 11{\cdot}3 + 1) = 28{\cdot}8$ tons/sq in. Since, again, this stress occurs when the trailing-edge temperature is approximately 300 deg C, and since, in addition, the blade material has a reasonable degree of ductility (6 per cent elongation at room temperature), then it still appears probable that the blade may negotiate the ' shock ' cooling without failure. Thus, it might be anticipated from the preceding reasoning that the present rotor blades may have a life of the order of 1,000 hours when operating at an inlet gas temperature of 1,090 deg C. At the same time it must be emphasised that this figure is merely speculative and tacitly assumes that the material is homogeneous and ignores stress concentrations which may occur in the vicinity of the cooling holes and the trailing edge. The real limits to permissible operating temperatures remain to be determined by experiment in a further series of tests.

At an inlet gas temperature of 1,090 deg C the maximum metal temperature, attained at the mid-span position of the trailing edge, is predicted from Fig. 10 to be 920 deg C. The scaling loss of the present sintered material has not been determined but the material is broadly similar to an American material known by the name ' Stellite ' and available information indicates a very high resistance to scaling at temperatures in region of 900 deg C. It is anticipated, therefore, that this is unlikely to prove a limiting factor in the present design. In any case it is evident that the major stress carrying portion of the blade is the relatively cool central ' backbone ' and that quite severe oxidation at the leading and trailing edges might be permitted before any major failure becomes imminent.

At this stage it appears quite impossible to predict the possible magnitude of vibration stresses. However, the gas bending stresses are relatively small and the fatigue properties of the material up to 900 deg C are fairly good (*see* Table in section 3). Even with a turbine inlet temperature of 1,090 deg C the bending fatigue factor (defined as the ratio of fatigue stress, for $10^7$ cycles endurance, to steady gas bending stress) is about 6, so that unless a fundamental resonant frequency is encountered the possibilities of a fatigue failure would seem remote. On the other hand the creation of small cracks during ' shock ' cooling in regions of local stress concentration might conceivably initiate such a failure.

8. *Conclusions.*—The cooling characteristics of a type of air-cooled nozzle and rotor blade having a multiplicity of small-diameter cooling passages passing spanwise through the blade have been thoroughly examined at relatively low gas temperatures in an experimental single-stage turbine. Greatest attention was paid to the operation of the cooled rotor blades and the principal effects observed on them were :

(*a*) At a gas flow Reynolds number of $1 \times 10^5$ and a cooling flow ratio of $0 \cdot 02$ the average blade temperature was less than the mean surrounding gas temperature by an amount equal to 37 per cent of the difference in temperature between the gas stream and the inflowing cooling air.

(*b*) The degree of cooling achieved in the turbine rotor blade was about 18 per cent less than that anticipated from previous tests in a cascade tunnel on a blade nearly identical to the turbine blade. Analysis of the test results, supported by some theoretical calculations of gas-to-blade heat-transfer, indicates that this phenomenon may be caused through the turbine blade operating with a more extensive turbulent boundary layer on the blade surfaces than the cascade, this presumably being attributable to the much larger degree of intense turbulence present in the turbine stage as compared with the cascade tunnel. The sensitivity of the gas-to-blade heat-transfer coefficient to a change in the relative proportions of turbulent and laminar boundary layer on the blade surface clearly indicates a necessity for exercising considerable caution in the application of cascade test results to actual turbine operation.

(*c*) The degree of cooling achieved with a given cooling flow ratio remains substantially insensitive to changes in gas flow Reynolds number. This is largely a consequence of the high proportion of turbulent boundary layer that is believed to exist on the blade surface, combined with turbulent flow in the cooling air passages.

(*d*) The degree of cooling achieved with a given cooling flow ratio remains substantially constant over a wide range of turbine blade loading, although at low blade loadings, corresponding to mean gas flow incidences on to the rotor blade of less than $-10$ deg the degree of cooling slightly decreases. It is anticipated that the degree of cooling would also decrease slightly at higher blade loadings than could be obtained on the experimental rig (corresponding to incidences in excess of $+10$ deg).

(*e*) The chordwise distribution of blade temperature is far from uniform, the leading and trailing edges running relatively hot as compared with the mid section of the blade chord. When the mid portion of the blade chord near the mid-span section (chordwise temperature variations being greatest near the mid span section) is cooled by an amount equal to 42 per cent of the difference in temperature between the surrounding gas and the incoming cooling air (at a gas flow Reynolds number of $1 \times 10^5$) the leading and trailing edges are only cooled by an amount equal to 20 per cent of the same temperature difference. This relatively poor distribution is associated with the fundamental difficulties of extracting a sufficient amount of heat from the trailing and leading edges where the local external heat-transfer coefficients are large and the internal space for cooling-air passages severely restricted. This difficulty is accentuated by the low thermal conductivity of heat-resistant materials. It is conjectured that the chordwise distribution of temperature in the present type of blade could possibly be improved to a small extent by repositioning the cooling passages in the blade section, although a sacrifice in the mean degree of cooling or alternatively an increase in the cooling air pressure loss may also be necessary. On the other hand a cursory examination of the probable thermal stresses created by the non-uniformity of cooling and their effect on the maximum permissible operating temperatures suggest that the present form of blade is unlikely to suffer catastrophically from the non-uniform cooling. Indeed, some degree of non-uniformity appears desirable since it induces compressive strains in the relatively weak leading and trailing edges and also tends to reduce the severity of the momentarily high tensile stresses that can be created in these regions during ' shock ' cooling of the blades.

(*f*) Increase in gas flow Reynolds number with a constant cooling flow ratio leads to an increase in the chordwise blade temperature gradients, this increase being due to the increase in heat-transfer coefficients accompanying an increase in Reynolds number whilst the thermal conductivity of the material remains constant.

(*g*) It is speculated that the present rotor blades, constructed from a sintered cobalt-chromium-tungsten alloy, may have a possible life of the order of 1,000 hours when operating with a turbine inlet gas temperature of 1,090 deg and a cooling flow ratio of 0·02. This compares with an inlet temperature of 820 deg C for the same blades without cooling and the same blade life.

(*h*) The cooling-air pressure loss in the rotor blade is such that in a gas-turbine engine, paying due attention to the minimising of spurious losses in the cooling-air ducting, a rotor cooling flow ratio of approximately 0·02 could be achieved with a maximum cooling-air pressure equal to the compressor delivery pressure.

Adequate analysis of the cooling characteristics of the nozzle blades was hampered by a large degree of non-uniformity of the temperature distribution in the incoming gas flow, although the results serve to indicate a few outstanding points :

(i) Even though the potential cooling ability of the air cooled configuration is reasonably good the local peaks of high gas temperature in the inflowing gas stream were so large that with a cooling flow ratio of 0·025 the temperature of the hottest blades along the leading edges between the mid span and tip sections were only slightly below the mean gas temperature. These results must serve to emphasise the importance of securing as uniform a distribution of gas temperature at the turbine inlet as possible.

(ii) The system here adopted of discharging the nozzle cooling air at the blade tips into a small radial clearance space between the blade tips and the adjacent annulus wall of the turbine is not to be recommended. The static pressure drop occurring along the blade chord from the leading- to the trailing-edge results in the cooling passages near the leading edge being relatively starved of cooling air as compared with the passages near the trailing edge. This accentuates the already difficult task of cooling the nozzle blade leading edges.

(iii) The present nozzle cooling-air pressure losses are such that, with adequate radial clearance at the blade tips, a cooling flow ratio of about 0·024 can be achieved with an inlet cooling-air pressure equal to the turbine inlet total gas pressure.

(iv) The test results indicated that the gas-to-blade heat-transfer coefficients were about 50 per cent higher than might have been anticipated from cascade data. As with the rotor blades it is conjectured that this is attributable to a much higher proportion of the turbine nozzle blade surface operating with a turbulent boundary layer than similar blades previously tested in cascade tunnels.

---

## REFERENCES


| *No.* | *Author* | *Title, etc.* |
|---|---|---|
| 1 | D. G. Ainley and N. E. Waldren .. | Investigations on an experimental air-cooled turbine. Part I: General description of turbine and experimental technique. (Part I of this report.) |
| 2 | H. B. Squire .. .. .. .. | Heat transfer calculation for aerofoils. R. & M. 1986. November, 1942. |
| 3 | A. G. Smith .. .. .. .. | Heat flow in the gas turbine. *Proc. I.Mech.E.* Vol. 159. 1948. |

## REFERENCES—*continued*


| No. | Author | Title, etc. |
| --- | --- | --- |
| 4 | S. J. Andrews and P. C. Bradley .. | Heat transfer to turbine blades. Power Jets Memo. M.37. A.R.C. 12,078. October, 1948. |
| 5 | J. Reeman and R. W. A. Buswell .. | An experimental single-stage air-cooled turbine. Part I: Design of the turbine and manufacture of some experimental internally cooled nozzles and blades. *Proc. I.Mech.E.* Vol. 167. 1953. |
| 6 | D. G. Ainley .. .. .. .. | An experimental single-stage air-cooled turbine. Part II: Research on the performance of a type of internally air cooled turbine blade. *Proc. I.Mech.E.* Vol. 167. 1953. |
| 7 | A. G. Smith and R. D. Pearson .. | The cooled gas turbine. *Proc. I.Mech.E.* Vol. 163. 1950. |
| 8 | L. V. Humble, W. H. Lowdermilk and L. G. Desman | Measurements of average heat transfer and friction coefficients for subsonic flow of air in smooth tubes at high surface and fluid temperatures. N.A.C.A. Report 1020. 1951. |
| 9 | T. J. Hargest .. .. .. .. | The theoretical pressure distributions around some conventional turbine blades in cascade. R. & M. 2765. March, 1950. |
| 10 | W. H. McAdams .. .. .. .. | *Heat transmission.* 2nd Ed. McGraw Hill Book Co. 1942. |
| 11 | K. Bammert and H. A. Hahnemann .. | Heat transfer in gas surrounding cooled turbine blades. M.O.S. Report G.D.C. 2466. |


---

## APPENDIX I

### *Notation*

| | |
| --- | --- |
| $A$ | Blade section area |
| $A_t$ | Blade passage throat area |
| $C$ | Blade chord |
| $D$ | Hydraulic diameter of cooling passages |
| $E$ | Modulus of elasticity |
| $f$ | Skin-friction coefficient |
| $h_c$ | Coefficient of heat transfer between blade and cooling air (heat flow/unit time/unit temperature difference) |
| $h_g$ | Coefficient of heat transfer between gas stream and blade |
| $i$ | Gas flow incidence on to blade |
| $k_m$ | Specific heat of blade material |
| $K_p$ | Specific heat of gas at constant pressure |
| $l$ | Distance measured along blade span from blade root |
| $L$ | Total blade height |
| $M$ | Mass of blade per unit span |
| $M_n$ | Mach number |
| $N$ | Turbine rotational speed, r.p.m. |

| | |
|---|---|
| $N_u$ | Local gas flow Nusselt number based on blade chord and gas thermal conductivity at blade temperature $\left(\text{i.e., } N_u = \frac{\text{local heat-transfer coefficient} \times \text{blade chord}}{\text{gas thermal conductivity}}\right)$ |
| $N_u^*$ | Mean gas flow Nusselt number for blade |
| $N_{uc}$ | Cooling-air Nusselt number based on passage hydraulic diameter and air viscosity at blade temperature |
| $\bar{N}_{uc}$ | Mean value of $N_{uc}$ along blade span |
| $o$ | Blade passage throat width |
| $\bar{p}_{sN}$ | Mean static pressure at nozzle blade tip |
| $\bar{p}_{sR}$ | Mean static pressure at rotor blade tip |
| $P_i$ | Total pressure of gas flow at inlet to turbine |
| $P_{cN}$ | Total pressure of nozzle cooling air at entry |
| $P_{cR}$ | Total pressure of rotor cooling air at entry |
| $P_r$ | Prandtl number |
| $R_{eg}$ | Gas flow Reynolds number based on blade chord, outlet velocity relative to blade, and density and viscosity based on gas static temperature and pressure at blade outlet |
| $R_e^*$ | Gas flow Reynolds number based on blade chord, gas outlet velocity relative to blade, density evaluated at average of blade and gas temperatures, and viscosity evaluated at blade temperature |
| $R_{ec}$ | Cooling-air Reynolds number based on passage hydraulic diameter, mean cooling air velocity and density at bulk mean cooling air temperature, and viscosity at blade temperature |
| $\bar{R}_{ec}$ | Mean value of $R_{ec}$ along blade span |
| $s$ | Blade pitch |
| $S_c$ | Total surface area of cooling passages in one blade per unit blade height |
| $S_g$ | Total surface area washed by gas stream on one blade per unit blade height |
| $t$ | Blade thickness, or time |
| $t_e$ | Blade trailing-edge thickness |
| $T_b$ | Blade temperature |
| $T_{bm}$ | Mean blade temperature at a given spanwise position |
| $\bar{T}_{bm}$ | Mean temperature of whole blade (excluding root) |
| $T_{cR}$, $T_{cN}$ | Inlet cooling-air temperature (total) to rotor and nozzle blade respectively |
| $T_g$ | Gas total temperature measured relative to blade under consideration |
| $T_g^*$ | Circumferential mean of gas temperature relative to rotor blade at given spanwise position, or local gas temperature at given spanwise position adjacent to nozzle blade under consideration |
| $\bar{T}_g$ | Overall mass mean of total gas temperature relative to blade row under consideration |

| | |
|---|---|
| $\bar{T}_{ge}$ | Mass mean of total gas temperature over two blade pitches adjacent to nozzle blade under consideration |
| $T_i$ | Mass mean of total gas temperature at turbine inlet |
| $\Delta T_w$ | Gas total temperature drop through stage corresponding to the stage work output to drive shaft |
| $U_m$ | Mean diameter rotor blade speed |
| $V_0$, $V_2$ | Absolute outlet gas velocity from nozzle blade and relative outlet gas velocity from rotor blade respectively |
| $w_N$ | Cooling-air mass flow to nozzle row |
| $w_R$ | Cooling-air mass flow to rotor row |
| $W_N$ | Gas mass flow through nozzle row |
| $W_R$ | Gas mass flow through rotor row |
| $x$ | Distance along blade chord measured from the leading edge |
| $\beta_i$ | Nozzle blade inlet angle (measured relative to axial component of gas flow) |
| $\beta_1$ | Rotor blade inlet angle |
| $\lambda_g$ | Gas thermal conductivity |
| $\lambda_c$ | Cooling-air thermal conductivity |
| $\theta$ | Thermal conductivity of blade metal |
| $\rho_0$ | Gas density downstream of nozzle blade |
| $\rho_2$ | Gas density downstream of rotor blade |
| $\mu_0$ | Gas viscosity downstream of nozzle blade |
| $\mu_2$ | Gas viscosity downstream of rotor blade |
| $\mu_c$ | Viscosity of cooling air at entry conditions to blade cooling passages |

## APPENDIX II

### *Variation of Heat Transfer between Blade and Cooling Air with Number and Size of Cooling Holes*

When a fixed quantity of cooling air, $w$, passes through a blade it is desired to estimate the relationship between the total heat transfer per unit blade height per unit temperature difference between blade and cooling air ($h_c S_c$) and the number, $n$, and diameter, $D$, of the cooling passages.

Now, for air, the heat-transfer coefficient between the blade and cooling air is given approximately by (McAdams, Ref. 8) the expression

$$N_{uc} = 0 \cdot 02 (R_{ec})^{0 \cdot 8} \qquad \ldots \qquad (1)$$

where $N_{uc}$ = Nusselt number $= h_c D/\lambda_c$

$R_{ec}$ = Reynolds number $= \rho_c V_c D/\mu_c$

($V_c$ = cooling-air mean velocity in passage and $\mu_c$ = cooling-air viscosity).

Now $$R_{ec} = \rho_c V_c(\pi D^2/4)/\mu_c(\pi D/4)$$
$$= (w/n)/(\mu_c \pi D/4).$$

Therefore equation (1) becomes
$$h_c D/\lambda_c = 0 \cdot 02\ (4w/nD\pi\mu_c)^{0 \cdot 8}$$
therefore $$h_c = 0 \cdot 02\lambda_c(4w/nD\pi\mu_c)^{0 \cdot 8}/D$$
therefore $$h_c S_c = 0 \cdot 02\lambda_c(4w/nD\pi\mu_c)^{0 \cdot 8}\pi Dn/D$$
if $w$, $\lambda_c$, $\mu_c$, are fixed then :

$\underline{h_c S_c \propto n^{0 \cdot 2}/D^{0 \cdot 8}}$, which is the relationship required.

---

## APPENDIX III

*Blade Details*

(*a*) *Nozzle blade* (*see* Fig. 1)

| | |
|---|---|
| Blade height, $L$ | $= 2 \cdot 50$ in. |
| Blade chord, $c$ | $= 2 \cdot 21$ in. |
| Blade pitch at mean diameter | $= 1 \cdot 495$ in. |
| Pitch/chord | $= 0 \cdot 677$ (mean diameter) |
| Blade opening at mean diameter, $o$ | $= 0 \cdot 585$ in. |
| Thickness/chord, $t/c$ | $= 0 \cdot 1404$ |
| Trailing-edge thickness/blade pitch | $= 0 \cdot 021$ (mean diameter) |
| $\cos^{-1}$ (opening/pitch) | $= 67 \cdot 05$ deg (mean diameter) |
| Blade inlet angle, $\beta_i$ | $= 0$ deg |
| Number of cooling holes per blade | $= 53$ |
| Hydraulic mean diameter of cooling holes | $= 0 \cdot 039$ in. |

(*b*) *Rotor blade* (*see* Fig. 1)

| | |
|---|---|
| Blade height, $L$ | $= 2 \cdot 65$ in. |
| Blade chord, $c$ | $= 1 \cdot 05$ in. |
| Blade pitch, $s$ | $= 0 \cdot 68$ in. (mean diameter) |
| Pitch/chord | $= 0 \cdot 6475$ (mean diameter) |
| Blade opening, $o$ | $= 0 \cdot 353$ in. (mean diameter) |
| Thickness/chord, $t/c$ | $= 0 \cdot 234$ |
| Trailing-edge thickness/blade pitch | $= 0 \cdot 0294$ (mean diameter) |
| $\cos^{-1}$ (opening/pitch) | $= 58 \cdot 7$ deg (mean diameter) |
| Blade inlet angle, $\beta_1$ | $= 45 \cdot 0$ deg |
| Number of cooling holes per blade | $= 38$ |
| Hydraulic mean diameter of cooling holes | $= 0 \cdot 028$ in. |

## APPENDIX IV

### *Estimation of Thermal Stress*

The estimation of thermal stress, making the simplifying assumptions listed in section 6, is straightforward and the method is merely outlined in the following paragraphs. Only direct tensile and compressive stresses normal to a chordwise section of the blade are considered.

Assume that initially the blade is at a uniform temperature and is entirely free of any residual stress, then suppose that the blade temperatures are altered to give a known non-uniform distribution along the blade chord. Consider any blade section as shown in Fig. 27 and designate the position of any local region $\delta A$ by co-ordinates $y$, $z$ relative to the $y$, $z$-axes, which, for convenience, are chosen to coincide with the major and minor principal axes of the section.

Suppose, now, that under the non-uniform temperature distribution the blade is free to expand but that it is constrained from bending. Under this condition (the blade being long and the blade temperatures at a given value of $y$ and $z$ being constant along the span) plane sections across the blade will remain plane and parallel to one another.

Consider two cross-sections of the blade which under the initial uniform temperature, $T_b'$, were distance $l$ apart and under the non-uniformly heated condition are a distance ($l$ and $\delta l$) apart.

At a point $y$, $z$ let the temperature be $T_b$. Under zero stress at this temperature the length of a section of initial length $l$ will be $l[1 + \theta(T_b - T_b')]$. Since the actual length is $(l + \delta l)$ then the direct tensile strain this elemental section will be

$$\{(l + \delta l) - l[1 + \theta(T_b - T_b')]\}/l[1 + \theta(T_b - T_b')]$$
$$\simeq \{(\delta l/l) - \theta(T_b - T_b')\},$$

if $\theta(T_b - T_b')$ is small compared with unity.

The tensile thermal stress $q_t'$, at the point $y$, $z$ will then be given by :

$$q_t' = E\{[\delta l/l] - \theta[T_b - T_b']\}. \quad \ldots \quad (1)$$

Now since the blade is free to expand as a whole without restraint then,

$$\iint_A q_t' \, dy \, dz = 0 \, . \quad \ldots \quad (2)$$

Therefore $\iint_A E(\delta l/l) \, dy \, dz - \iint_A E\theta(T_b - T_b') \, dy \, dz = 0 \, .$

Since $E$, $\theta$, and $\delta l/l$ are constant for all values of $y$ and $z$ then,

$$\delta l/l = \theta \iint_A (T_b - T_b') \, dy \, dz/A \quad \ldots \quad (3)$$

where $A$ is the total cross-sectional area of blade section.

Suppose $\bar{T}$ is a temperature such that $\delta l = l\theta[\bar{T} - T_b']$ then equation (1) gives

$$q_t' = E\theta[\bar{T} - T_b] \quad \ldots \quad (4)$$

and equation (3) gives

$$\bar{T} = \iint_A T_b \, dy \, dz/A, \quad \ldots \quad (5)$$

i.e., $\bar{T}$ is the area mean temperature of the non-uniformly heated blade section $= T_{bm}$.

Equation (4) can be rewritten as

$$q_t' = E\theta(T_g^* - T_{bm})\{(T_{bm} - T_b)/(T_g^* - T_{bm})\} \, . \quad \ldots \quad (6)$$

Now it has been demonstrated in section 5.1 that the variation of $(T_b - T_{bm})/(T_g^* - T_{bm})$ across a blade section of a cooled blade remains approximately constant over a wide range of operating conditions ; in particular it remains independent of the actual values of gas temperature and cooling-air temperature when the cooling flow ratio and gas flow Reynolds numbers are fixed. For convenience let the value of $(T_b - T_{bm})/(T_g^* - T_{bm})$ at any point $y$, $z$ be designated by the symbol, $\phi$.

Then at any point $y$, $z$:

$$q_t' = -E\theta[T_g^* - T_{bm}]\phi \quad \ldots \quad (7)$$

Since it has been assumed that bending of the blade span has been fully constrained, then the distribution of stress $q_t'$ over the blade cross-section will create bending moments about the $y$- and $z$-axes. The moment about the $y$-axis will be:

$$\begin{aligned} M_y &= \iint_A z q_t' \, dy \, dz \\ &= -E\theta[T_g^* - T_{bm}]\iint_A z\phi \, dy \, dz \\ &= -E\theta[T_g^* - T_{bm}]\Psi_y \quad \ldots \quad (8) \end{aligned}$$

where $\Psi_y = \iint_A z\phi \, dy \, dz$, and is constant for a given distribution of $\phi$ over a given blade section.

Similarly the moment about the $z$-axis will be given by

$$M_z = -E\theta[T_g^* - T_{bm}]\Psi_z \quad \ldots \quad (9)$$

where $\Psi_z = \iint_A y\phi \, dy \, dz$.

Applying the principle of superposition of stress, then if moments equal to $-M_y$ and $-M_z$ are applied externally to the constrained blade the resultant bending moments in the blade cross-section will disappear and thus the stresses in the blade section when the blade is allowed freedom to bend under the action of the thermal stresses can be calculated. The externally applied moments $-M_y$ and $-M_z$ will lead to bending stresses in the blade section at any point $x$, $y$ of magnitude

$$q_b = -(M_y z/I_y) - (M_z y/I_z) \quad \ldots \quad (10)$$

where $I_y$, $I_z$ are the moments of area of the blade section about the principle axes $y$ and $z$ respectively.

Thus,
$$q_b = +E\theta[T_g^* - T_{bm}]\{(\Psi_y z/I_y) + (\Psi_z y/I_z)\} \quad \ldots \quad (11)$$

The final resultant stress at any point $x$, $y$ is then given by:

$$\begin{aligned} q_t &= q_t' + q_b \\ &= -E\theta[T_g^* - T_{bm}]\{\phi - [(\Psi_y z/I_y) + (\Psi_z y/I_z)]\} \quad \ldots \quad (12) \end{aligned}$$

or

$$\begin{aligned} q_t/E\theta[T_g^* - T_{bm}] &= -\phi + (\Psi_y z/I_y) + (\Psi_z y/I_z) \\ &= f(y, z). \end{aligned}$$

For a given cooled blade, operating at a predetermined cooling flow ratio and gas flow Reynolds number, $f(y, z)$ remains independent of the actual values of the gas and cooling-air temperatures. When the chordwise temperature distribution, expressed non-dimensionally by the parameter $(T_b - T_{bm})/(T_g^* - T_{bm})$, (*see* section 5.1) is known then the values of $\phi$, $\Psi_y$, $\Psi_z$, $I_y$ and $I_z$ may be determined by numerical or graphical methods and the variation of $q_t/E\theta(T_g^* - T_{bm})$ over the blade section found. To find the stresses corresponding to a particular set of operating conditions then $T_g^*$ must be found from the known form of the gas temperature distribution and the selected value of mean gas temperature. $T_{bm}$ is found from the known relationship between the blade relative temperature $(T_{bm} - T_{cR})/(T_g - T_{cR})$, and the cooling flow ratio, $w_R/W_R$, substituting the selected values of $T_g$, $T_{cR}$, and $w_R/W_R$.



E

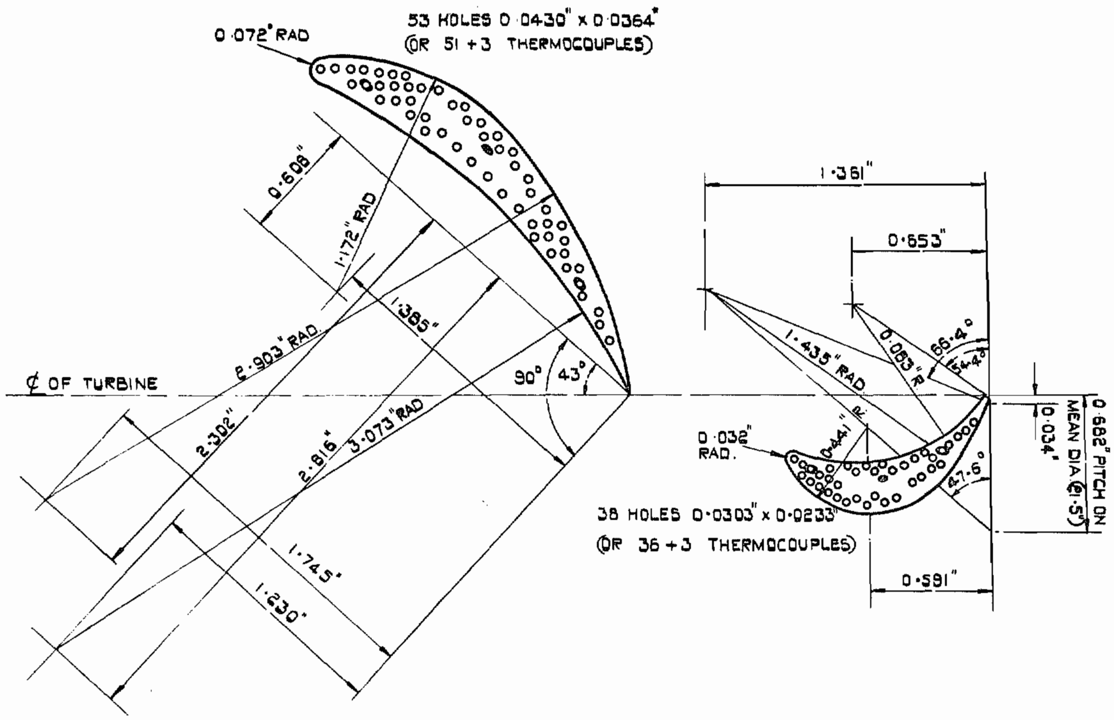


FIG. 1. Cross-section of nozzle blade and rotor blade.

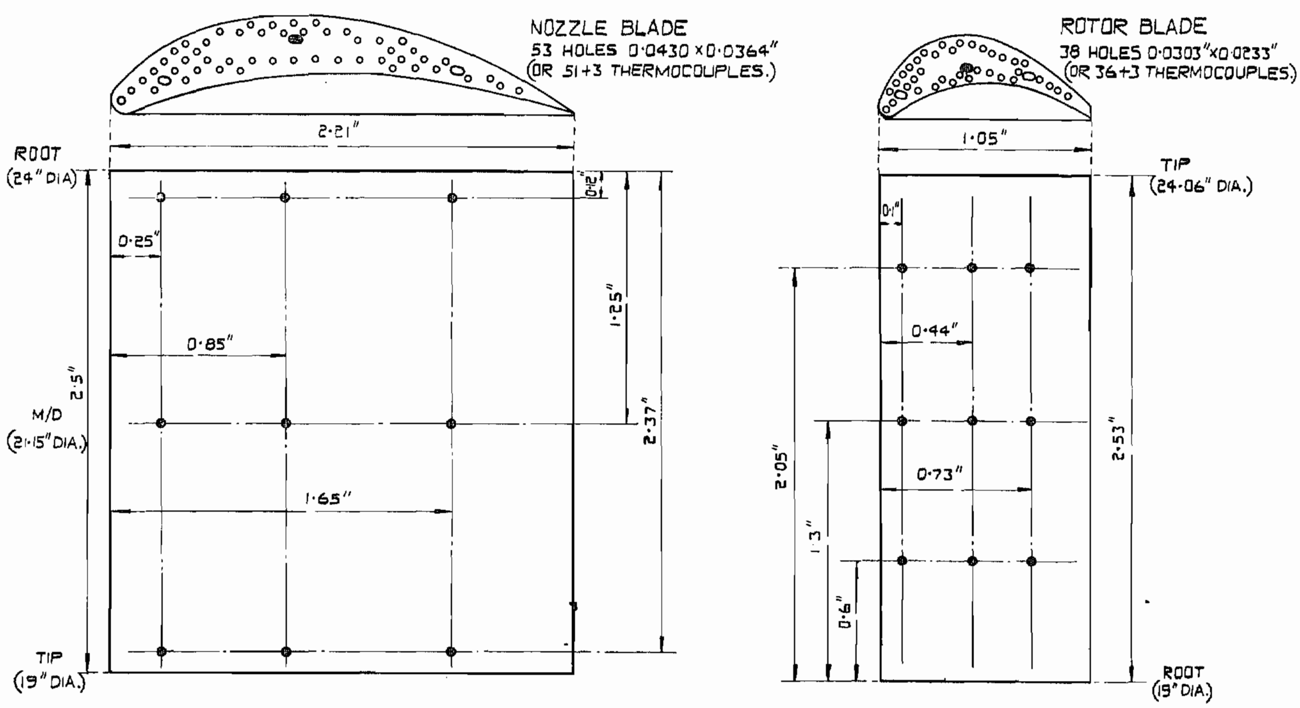


FIG. 2. Location of thermocouples in nozzle and rotor blades.

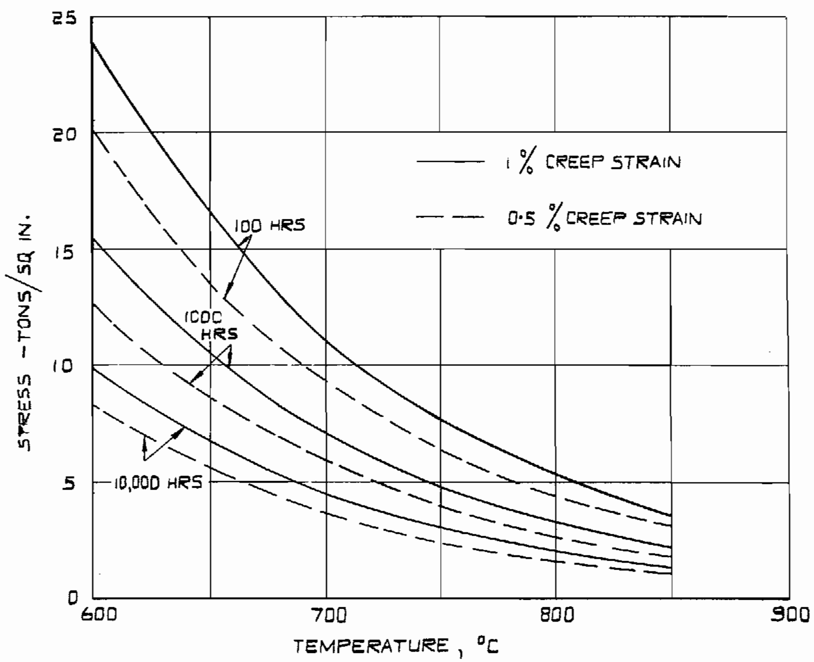


FIG. 3. Creep properties of sintered tungsten vitallium alloy.

Chemical composition :

Nominal = cobalt 64%, chromium 30%, tungsten 6%

Typical = cobalt 63·5%, chromium 29%, tungsten 6·4%, iron 0·13%, aluminium 0·27%, silicon 0·22%, carbon 0·024%.

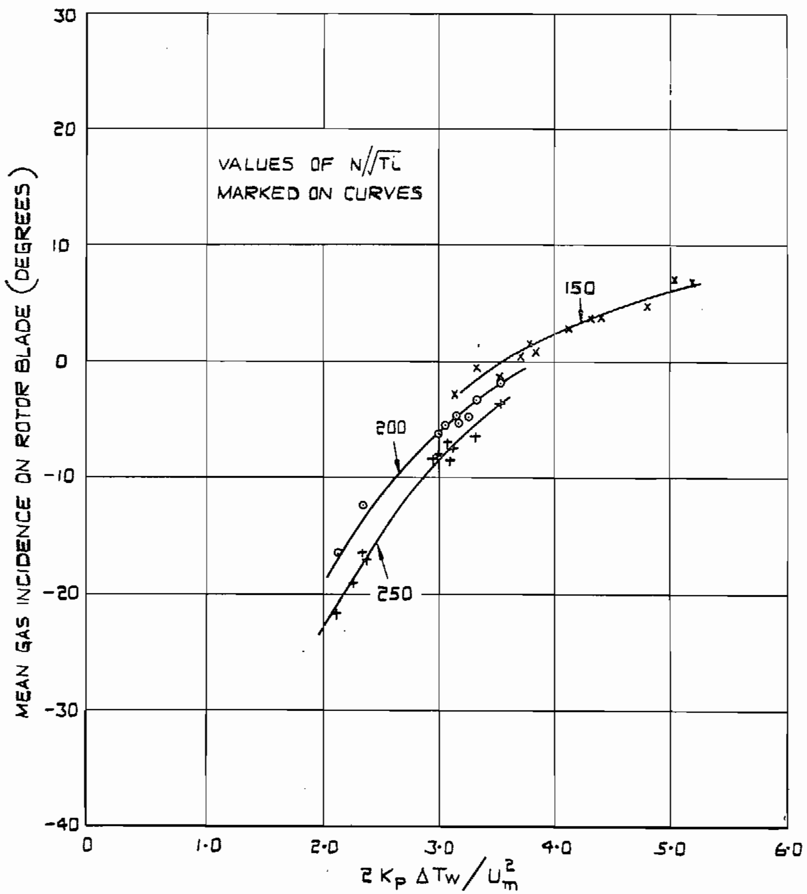


FIG. 4. Variation of mean rotor blade incidence with stage work-done coefficient.

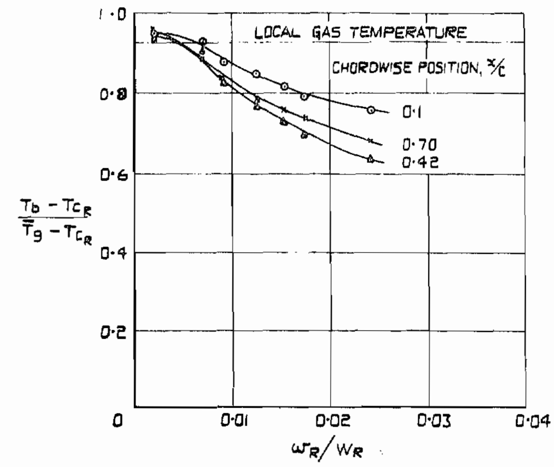


FIG. 5a. Tip section ($l/L = 0 \cdot 81$).

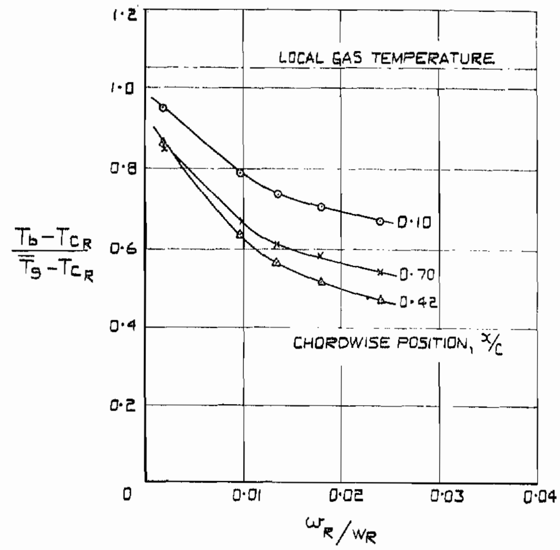


FIG. 5c. Root section ($l/L = 0 \cdot 23$).
Variation of rotor blade relative temperature with cooling-air quantity.
$R_{eg} = 1 \times 10^5$ ; $i = 0$ deg ; $\overline{T}_g/T_{cR} = 2 \cdot 55$.

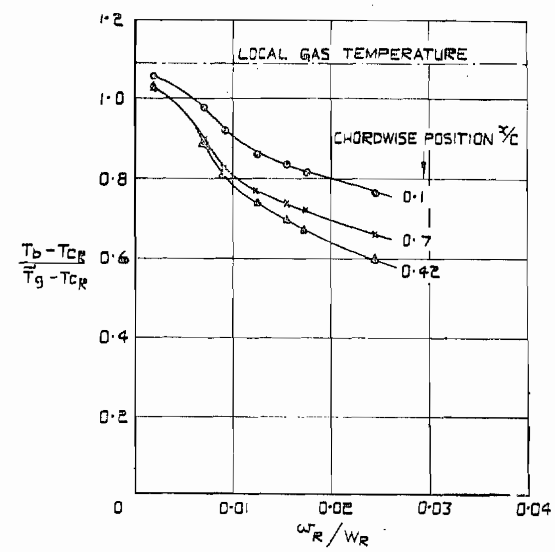


FIG. 5b. Mid section ($l/L = 0 \cdot 51$).

FIGS. 5a and 5b. Variation of rotor blade relative temperature with cooling-air quantity.
$R_{eg} = 1 \times 10^5$; $i = 0$ deg; $\overline{T}_g/T_{cR} = 2 \cdot 55$.

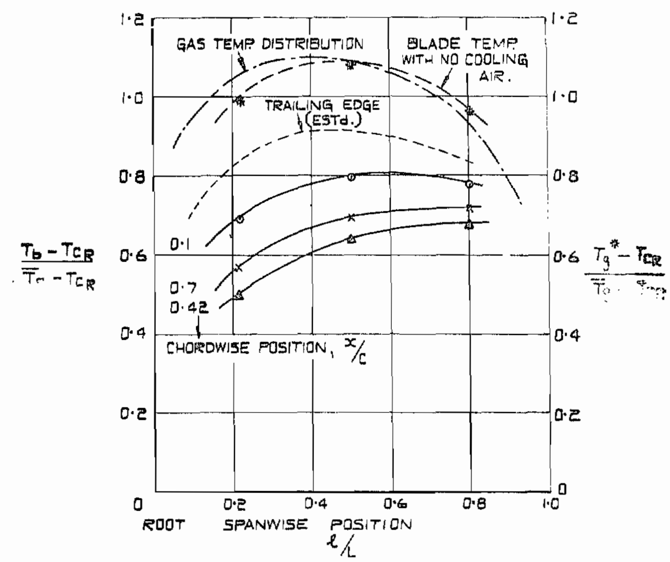


FIG. 5d. Variation of blade relative temperature along blade span.
$R_{eg} = 1 \times 10^5$ ; $i = 0$ deg ; $\overline{T}_g/T_{cR} = 2 \cdot 55$ ; $w_R/W_R = 0 \cdot 02$.

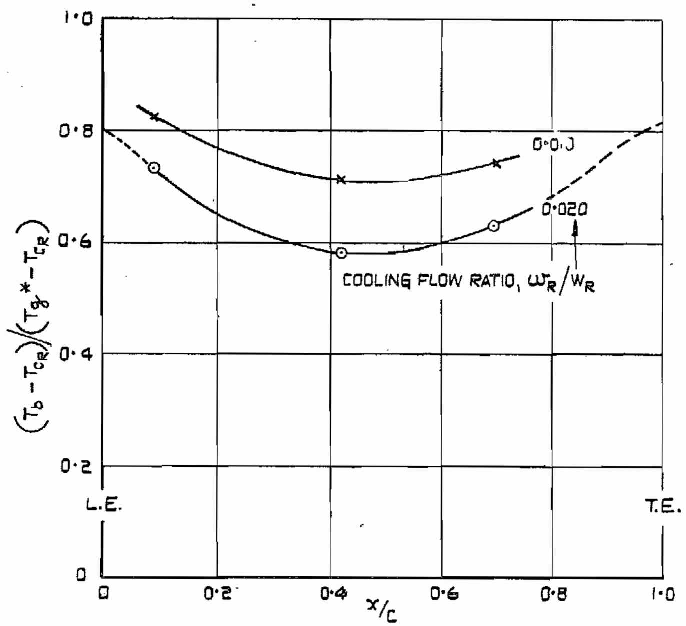


Fig. 6a.

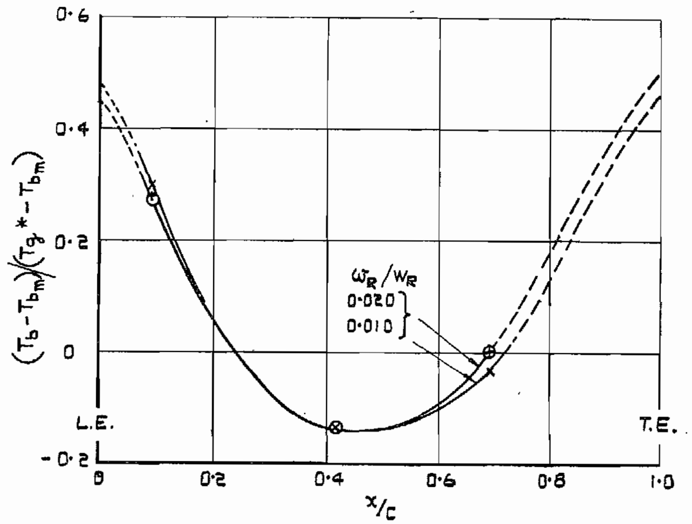


Fig. 6b.

Figs. 6a and 6b. Chordwise temperature distribution in rotor blade at various cooling flow ratios (mid-span).
$R_{eg} = 1 \times 10^5$ ; $i = 0$ deg ; $\overline{T}_g/T_{cR} = 2{\cdot}55$.

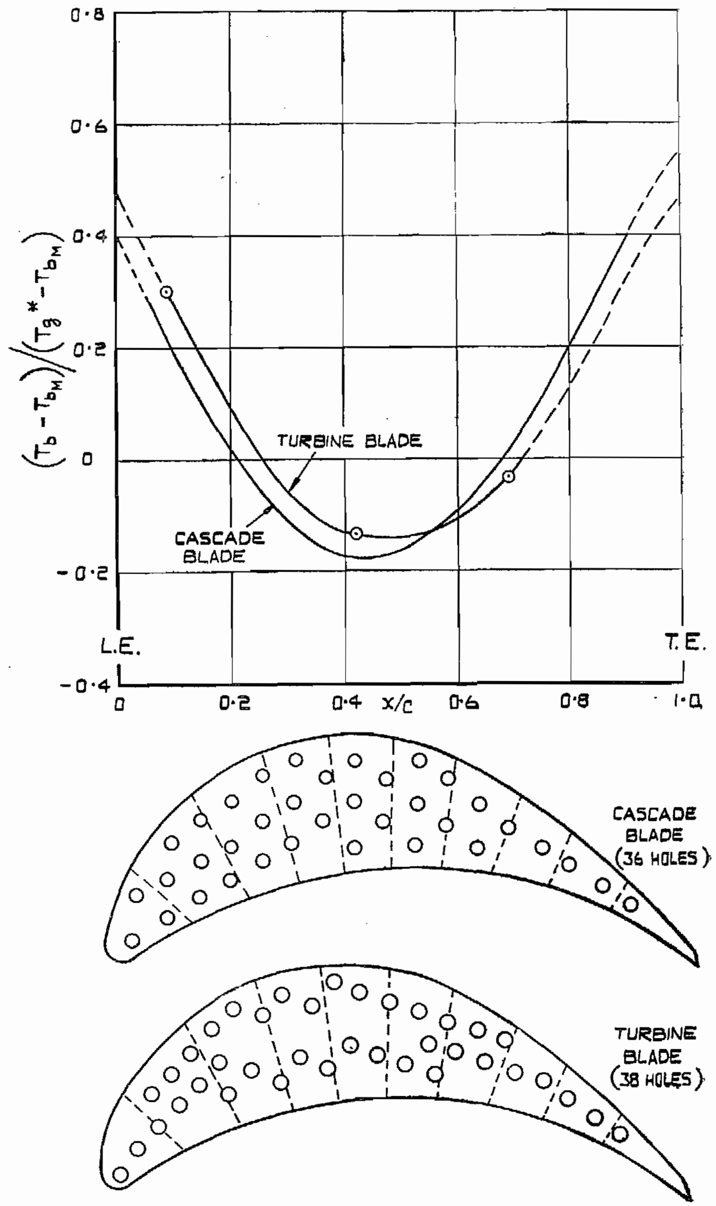


Fig. 7. Comparison of chordwise temperature distributions in turbine and cascade blades.
$R_{eg} = 1 \times 10^5$ ; $w_R/W_R = 0{\cdot}01$ ; $i = 0$ deg ; $\overline{T}_g/T_{cR} \simeq 2{\cdot}6$.

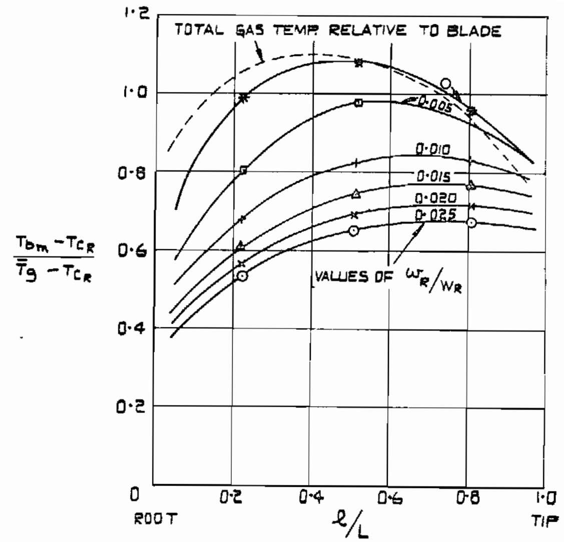


FIG. 8a. Variation of mean rotor blade temperature along blade span.

$R_{eg} = 1 \times 10^5$ ; $i = 0$ deg ; $\overline{T}_g/T_{cR} = 2{\cdot}55$.

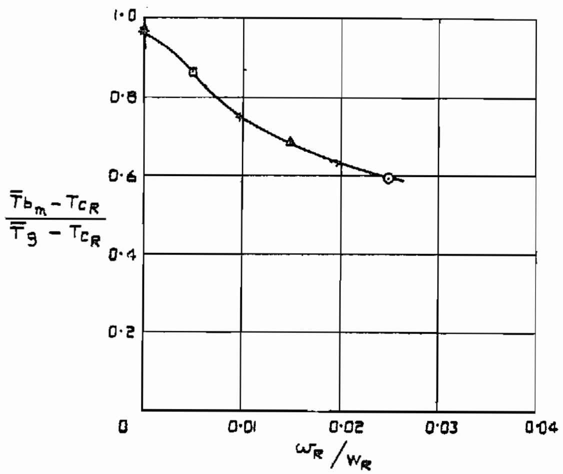


FIG. 8b. Variation of average blade temperature with cooling-air quantity.

$R_{eg} = 1 \times 10^5$ ; $i = 0$ deg ; $\overline{T}_g/T_{cR} = 2{\cdot}55$.

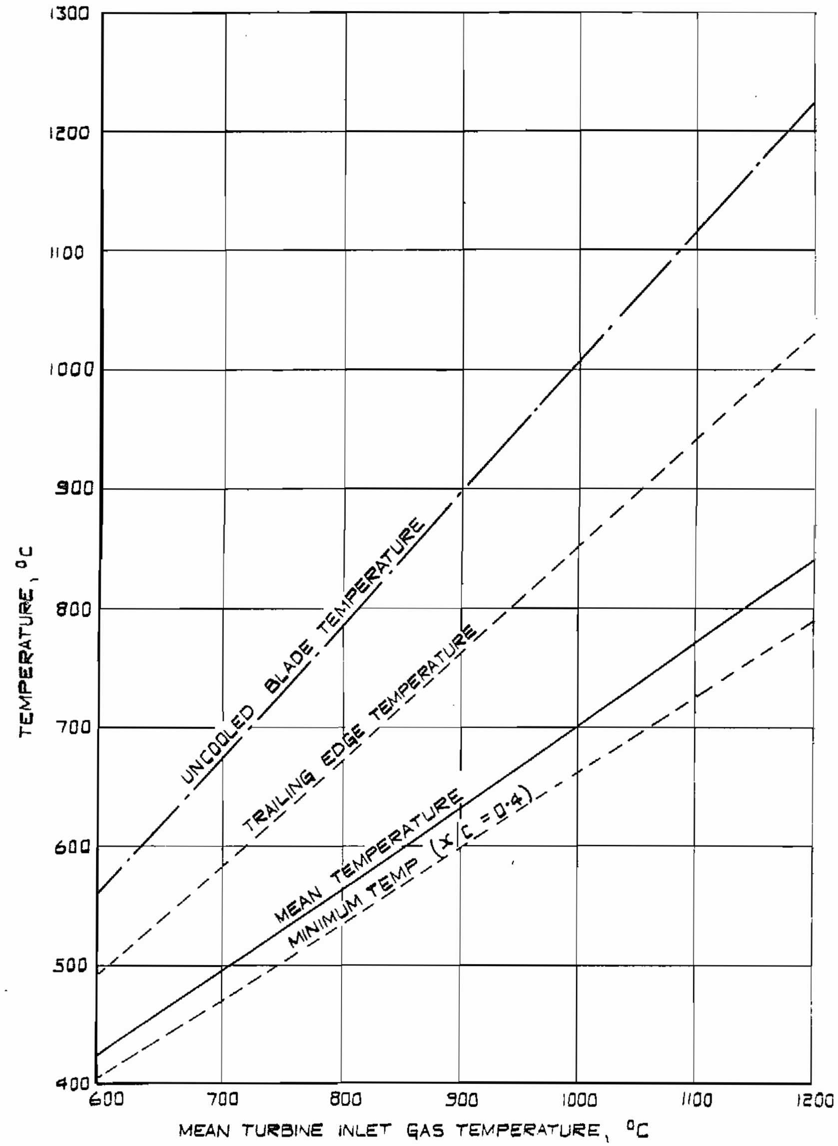


FIG. 9. Estimated variation of rotor blade temperatures at mid-span with turbine inlet gas temperature.

$w_R/W_R = 0{\cdot}02$ ; $N = 9{,}000$ r.p.m.; $i = 0$ deg; $R_{eg} = 1 \times 10^5$;
$T_{cR} = 200$ deg. C.

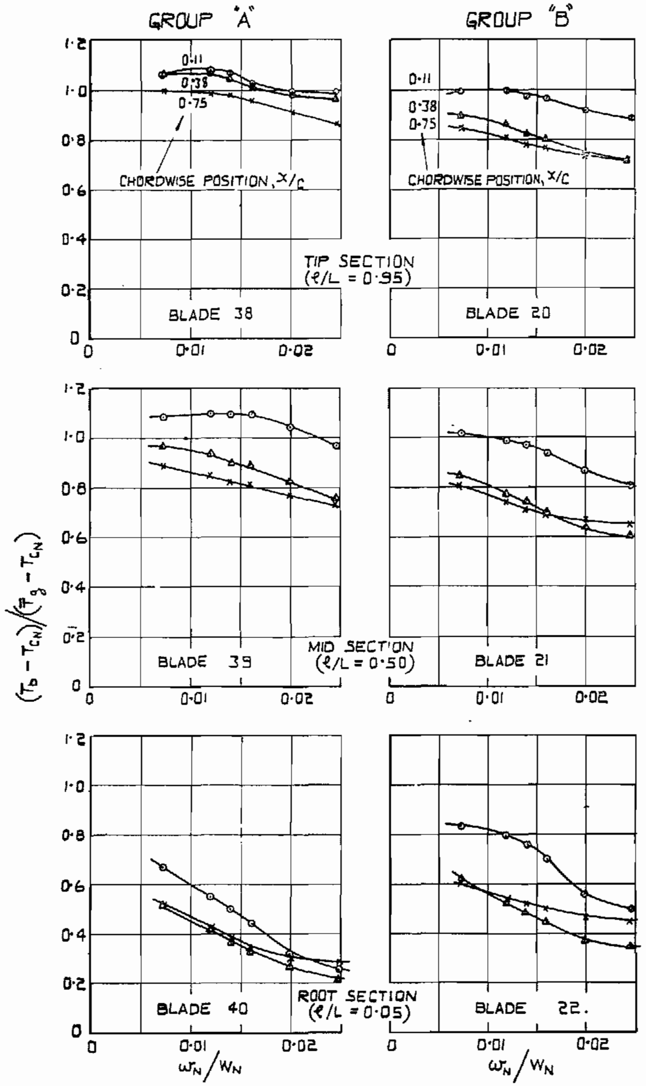


FIG. 10. Variation of nozzle blade relative temperatures with cooling air quantity.

$R_{eg} = 4 \cdot 6 \times 10^5$ ; $\overline{T}_g / T_{cN} = 2 \cdot 50$.

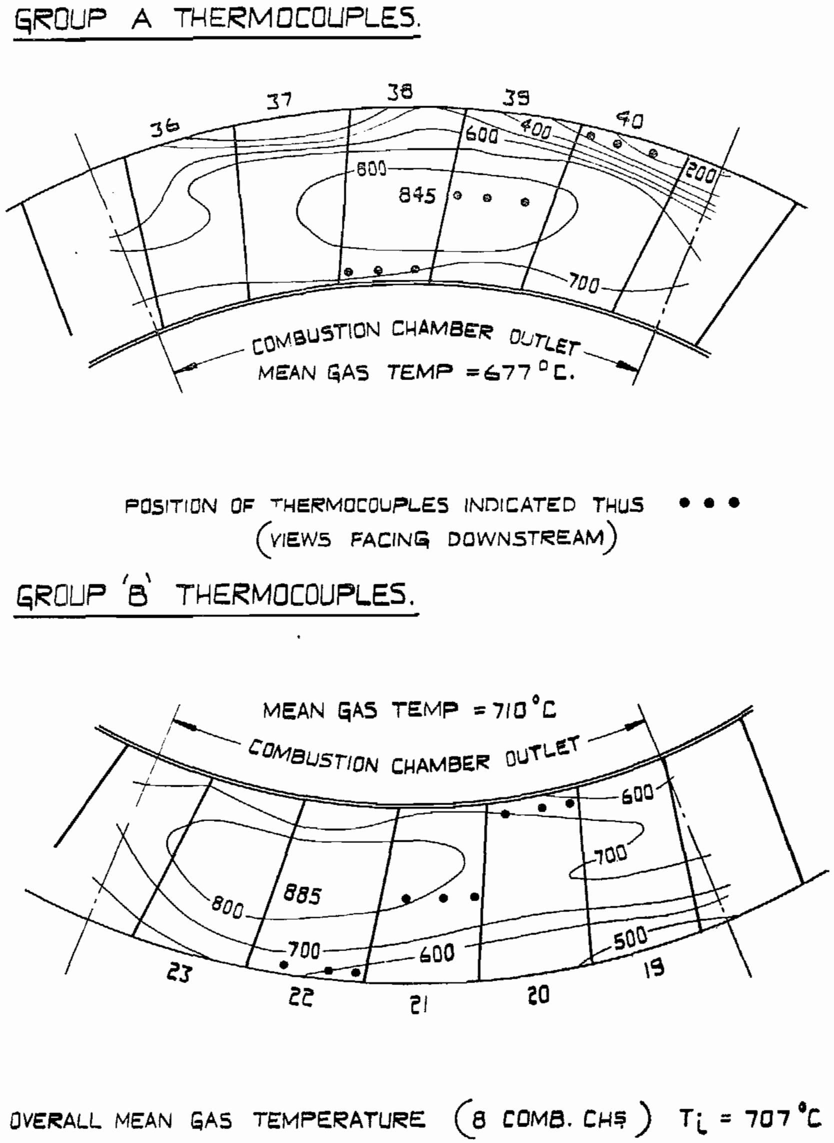


FIG. 11. Location of thermocouples in nozzle blades with typical gas temperature distribution superimposed.

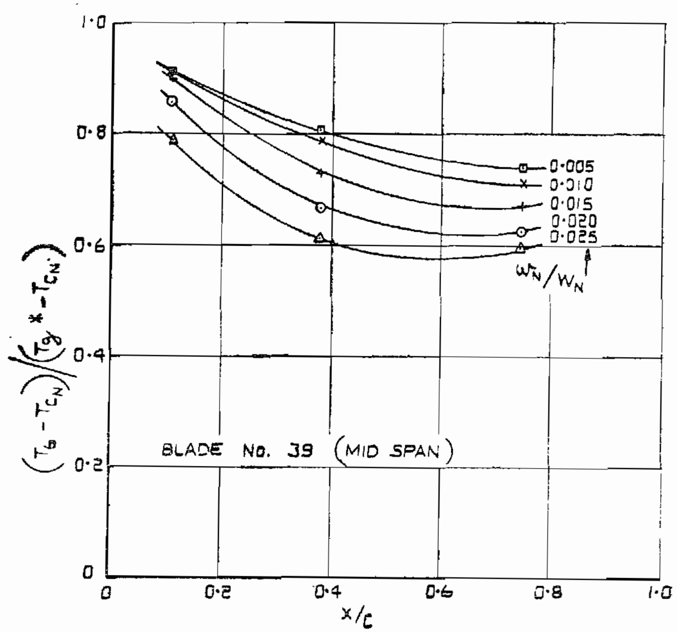


FIG. 12a.

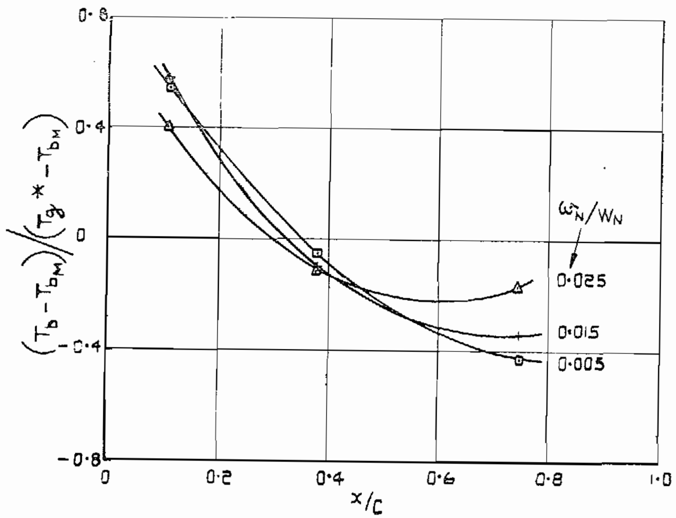


FIG. 12b.

FIGS. 12a and 12b. Chordwise temperature distribution in nozzle blade at various cooling flow ratios (mid-span) Group A. $R_{eg} = 4{\cdot}6 \times 10^5$ ; $\overline{T}_g/T_{ex} = 2{\cdot}50$.

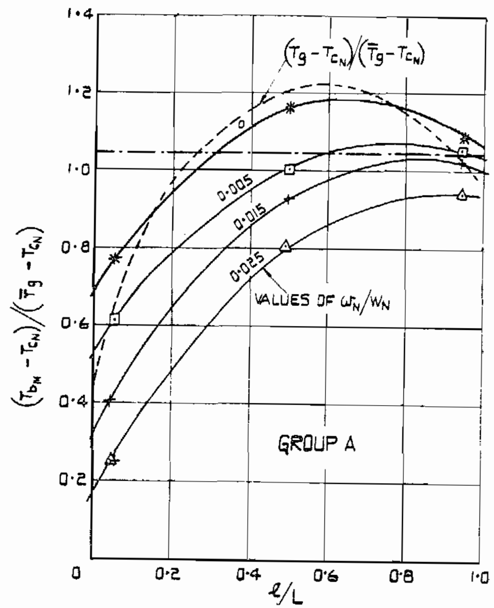


FIG. 13a.

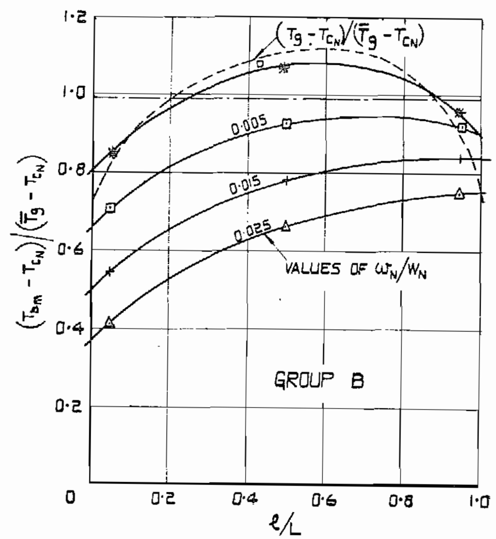


FIG. 13b.

FIGS. 13a and 13b. Variation of mean nozzle blade temperature along span. $R_{eg} = 4{\cdot}6 \times 10^5$ ; $\overline{T}_g/T_{ex} = 2{\cdot}50$.

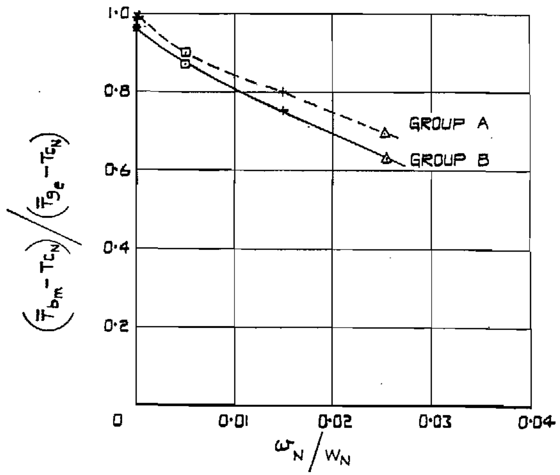


FIG. 14. Variation of average nozzle blade temperature with cooling-air quantity.
$R_{eg} = 4 \cdot 6 \times 10^5$; $\overline{T}_g/T_{cN} = 2 \cdot 50$.

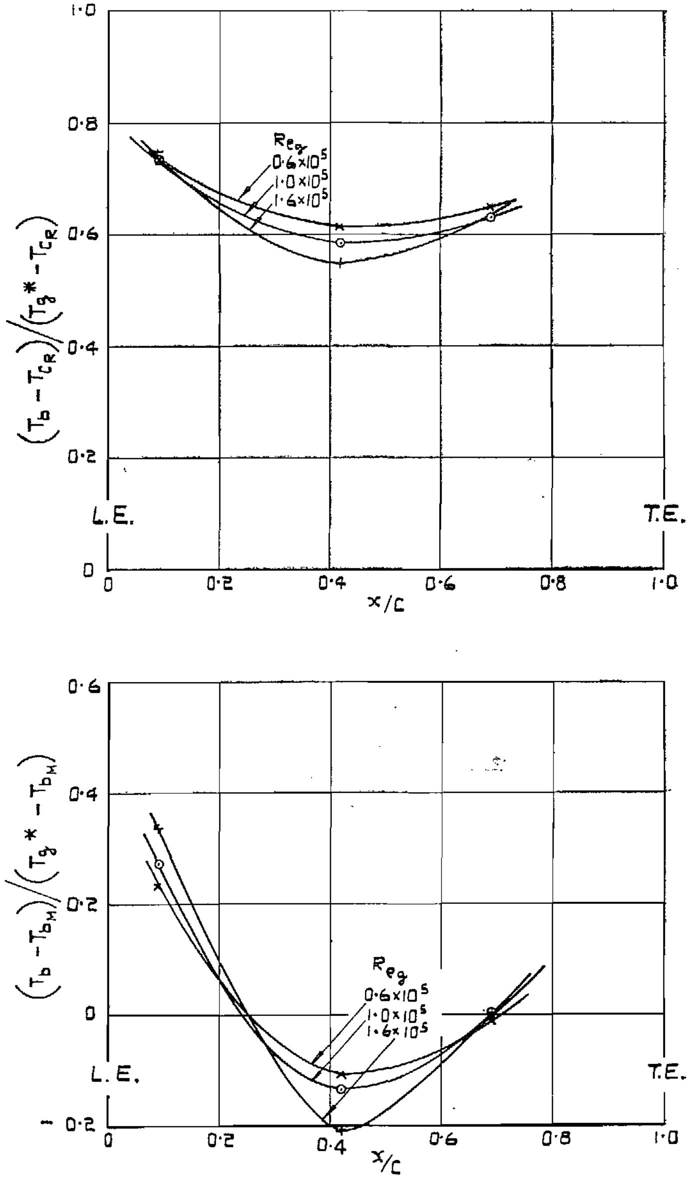


FIG. 15. Chordwise temperature distribution in rotor blade at various gas flow Reynolds number (mid-span).
$w_R/W_R = 0 \cdot 020$ ; $i \simeq 0$ deg ; $\overline{T}_g/T_{cR} \simeq 2 \cdot 5$.

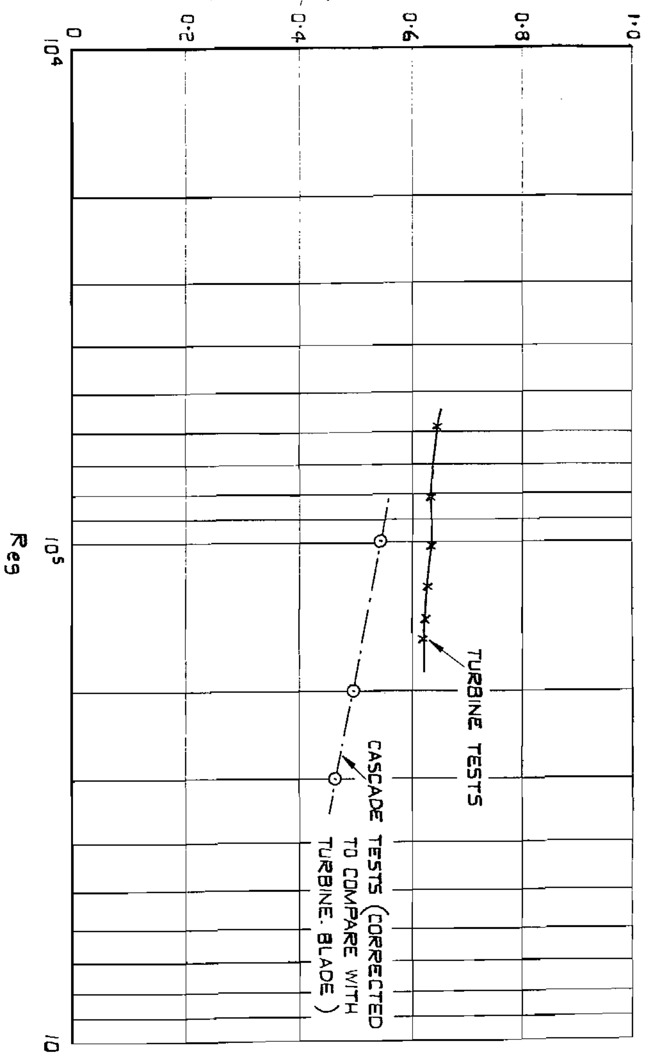


FIG. 16. Variation of average rotor blade metal temperature with gas flow Reynolds number. $w_R/W_R = 0{\cdot}020$ ; $i \simeq 0$ deg ; $\overline{T}_g/T_{cR} \simeq 2{\cdot}5$ ; $R_{e\,c} \simeq 0{\cdot}042\, R_{eg}$.

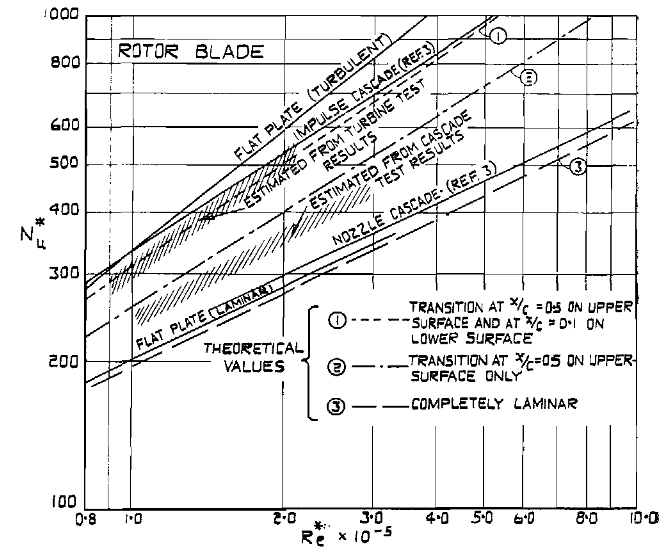


FIG. 17a.

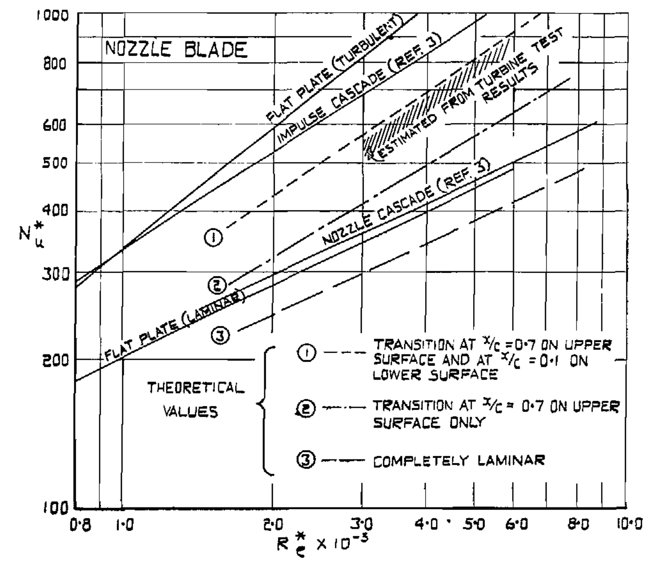


FIG. 17b.

FIGS. 17a and 17b. Relationship between external heat-transfer coefficient and Reynolds number for rotor and nozzle blades and comparison with other data.

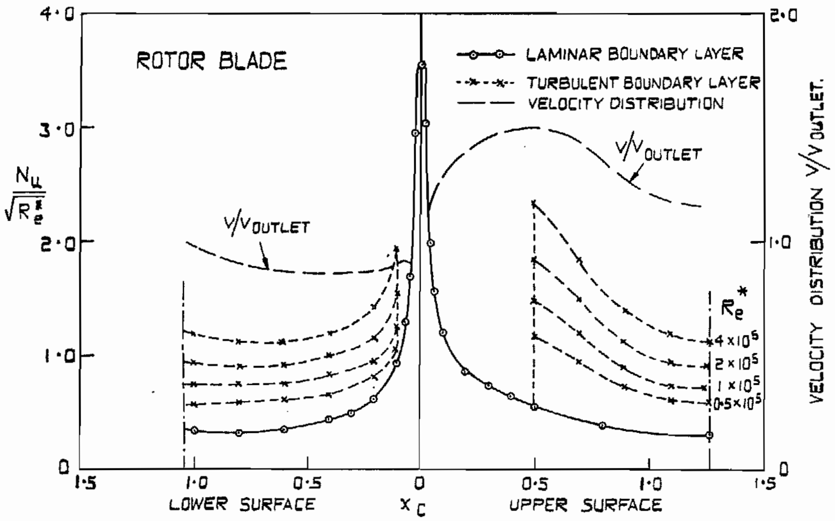


Fig. 18a.

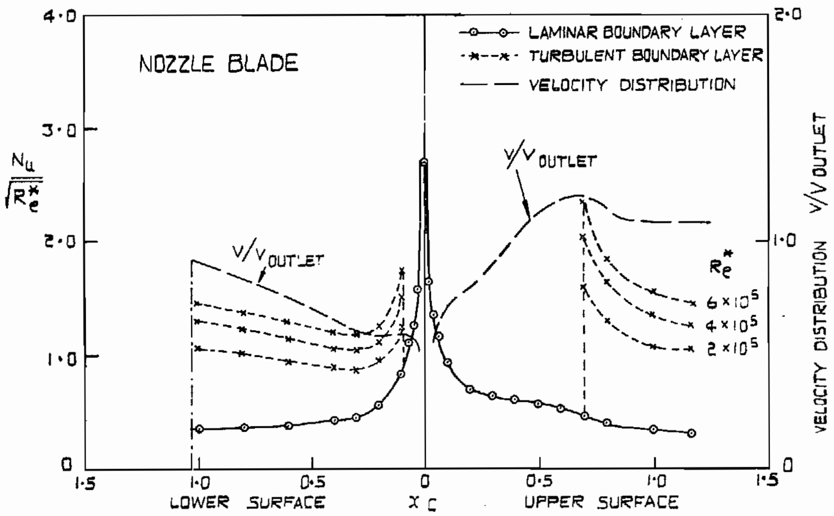


Fig. 18b.

Figs. 18a and 18b. Calculated variation of heat-transfer coefficient around rotor and nozzle blade sections.

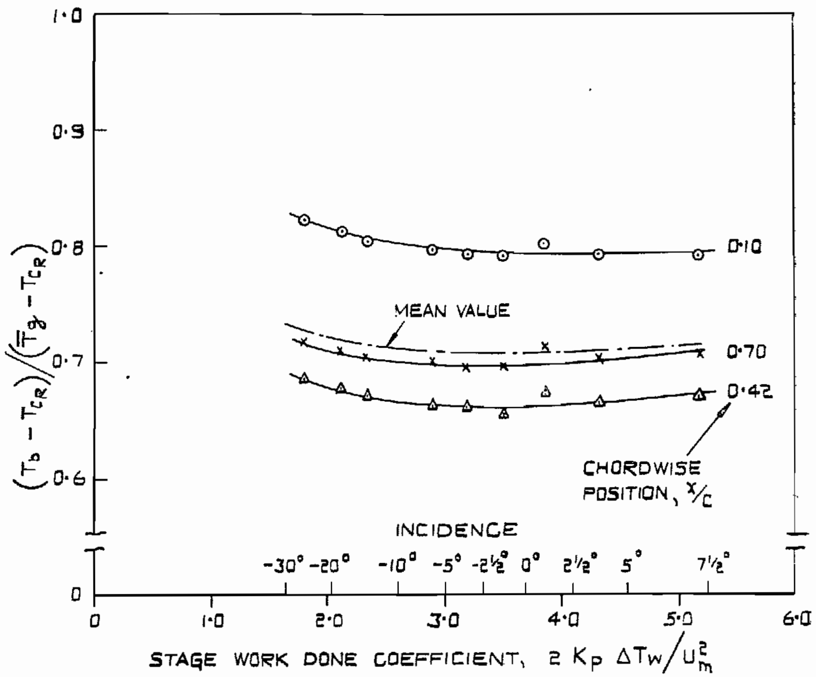


Fig. 19. Variation of relative rotor blade temperatures with gas incidence angle (constant cooling flow ratio).
$w_R/W_R = 0{\cdot}018$ (constant) ; $R_{eg} = 0{\cdot}81 \times 10^5$ ; $\overline{T}_g/T_{cR} = 2{\cdot}64$ ; mid-blade section

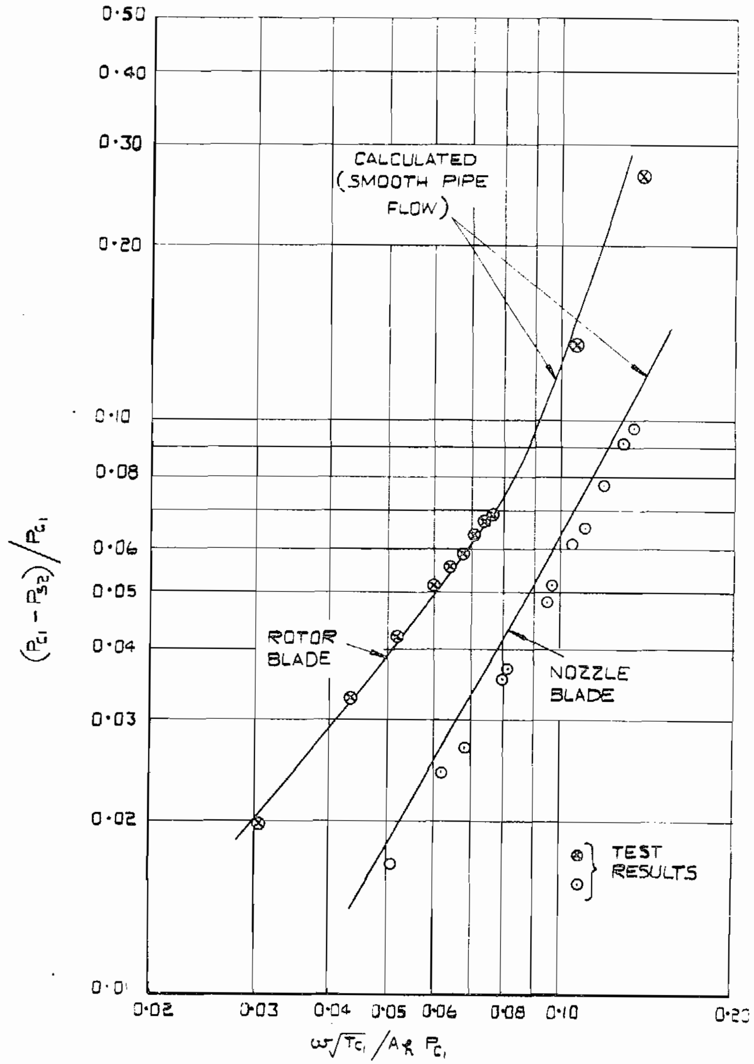


FIG. 20. Pressure losses in blade cooling-air passages (no heat transfer).

$P_{s\,2}$ = Static pressure at blade tip $\simeq$ 14·7 lbs/sq in.
$T_{c\,1}$ = Cooling-air temperature $\simeq$ 295 deg $K$.
$P_{c\,1}$ = Total pressure of cooling air entering blade root.
$w$ = Cooling-air mass flow to blade.
$A_h$ = Total cross-sectional area of blade cooling passages.

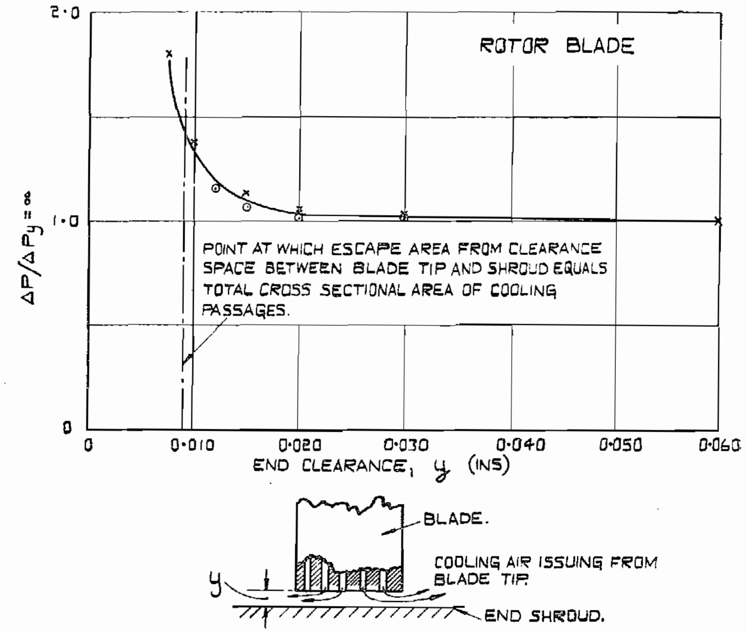


FIG. 21a.

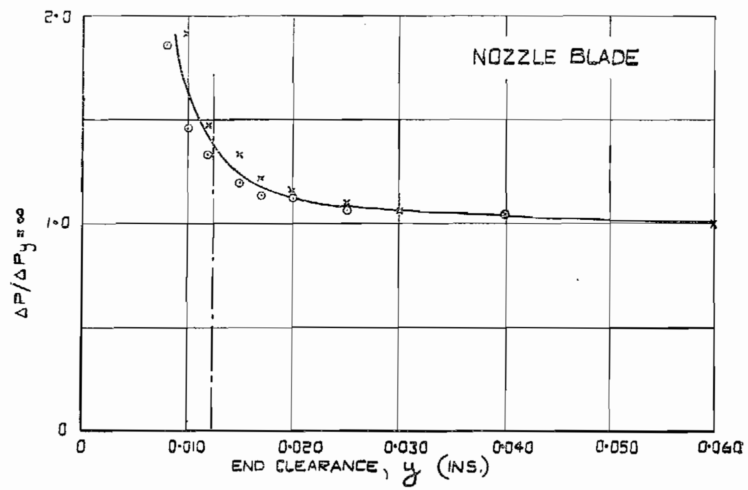


FIG. 21b.

FIGS. 21a and 21b. Effect of radial tip clearance on blade cooling-air pressure drop, $\Delta P$.

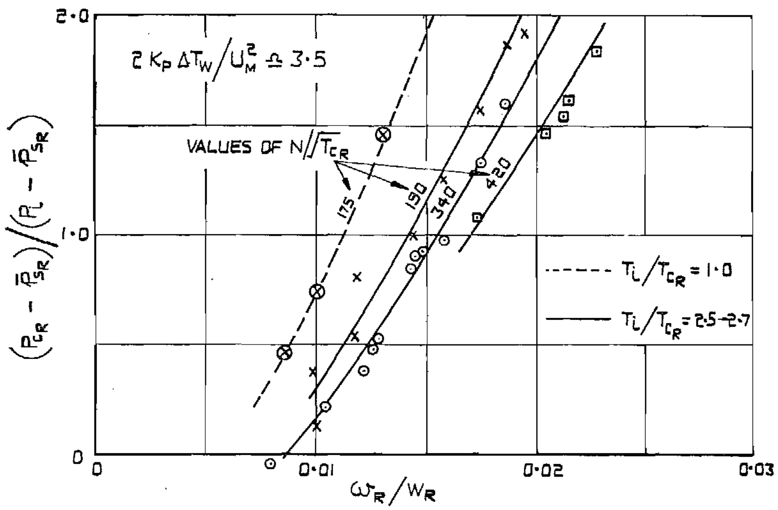


FIG. 22a. Rotor row.

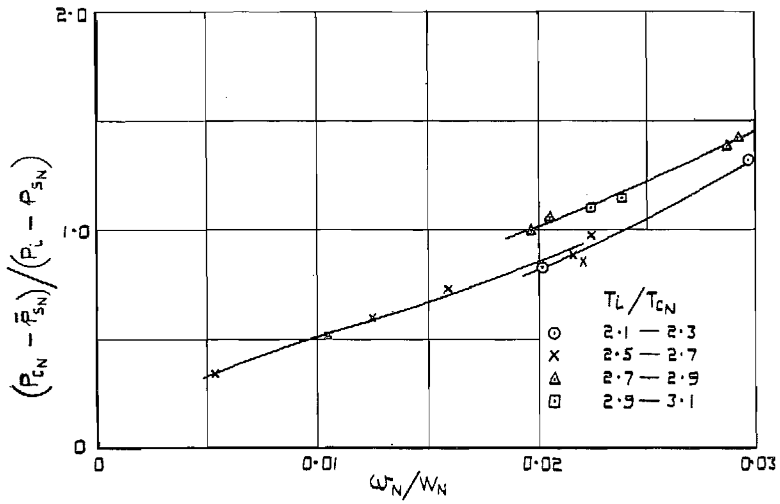


FIG. 22b. Nozzle row.

FIGS. 22a and 22b. Variation of cooling-air pressure drop with cooling-air quantity.

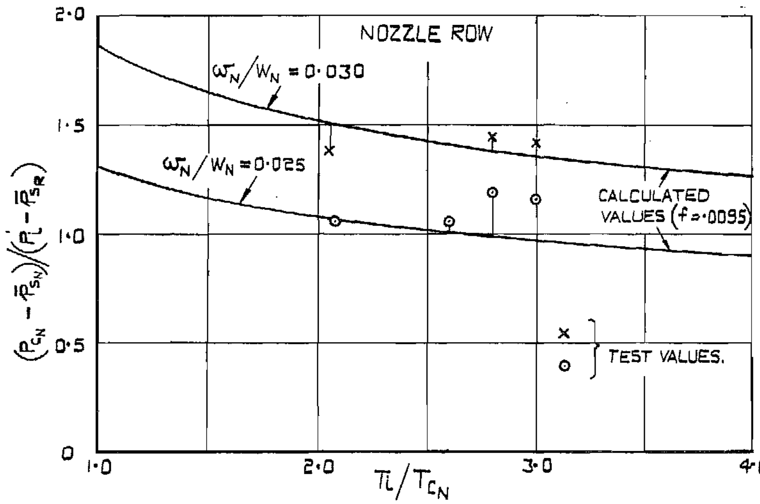


FIG. 23a.

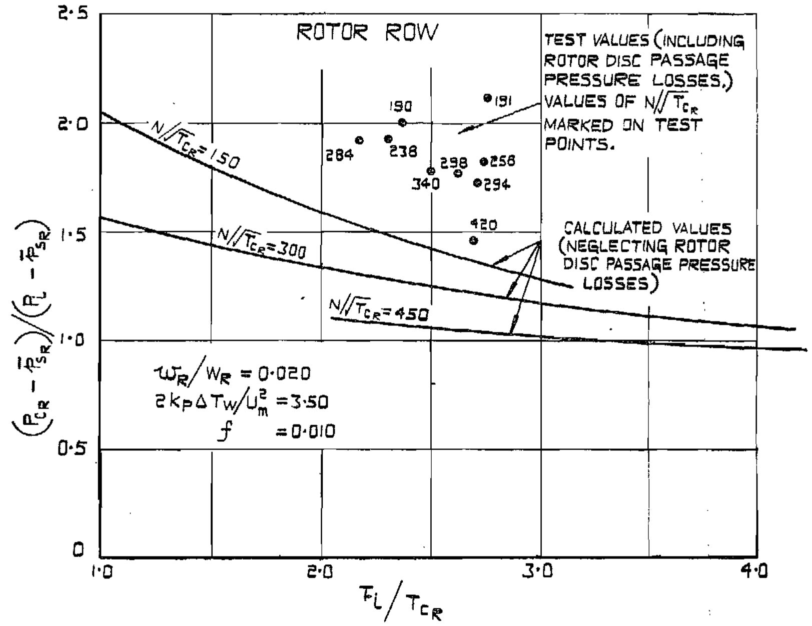


FIG. 23b.

FIGS. 23a and 23b. Pressures required to force cooling air through nozzle and rotor blade tows.

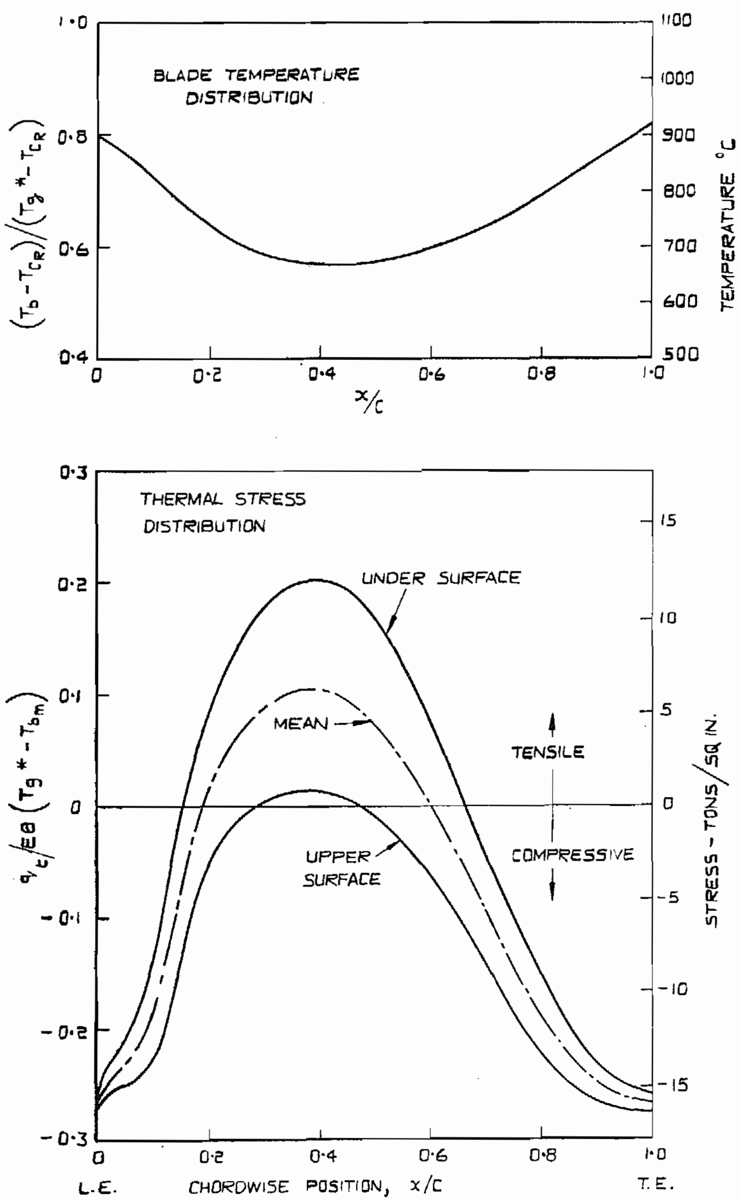


FIG. 24. Estimated direct thermal stresses in rotor blade section due to non-uniform cooling.

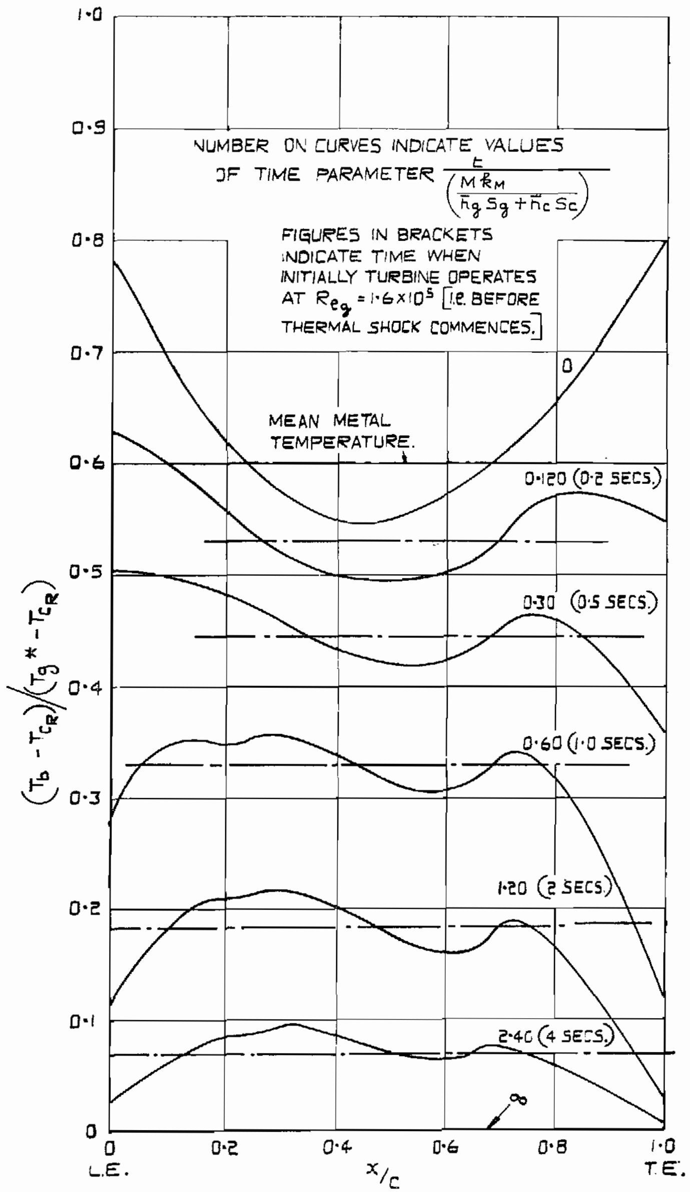


FIG. 25. Approximate estimate of variation in rotor blade chordwise temperature distribution (mid-span) while undergoing 'shock' cooling. $w_R/W_R = 0{\cdot}025$.

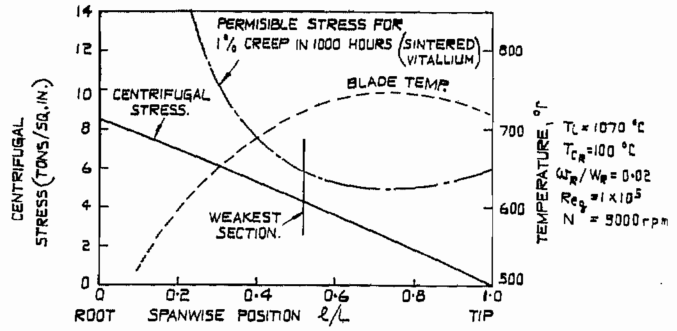


FIG. 26a.

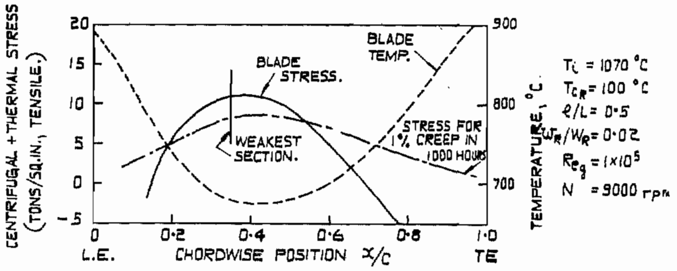


FIG. 26b.

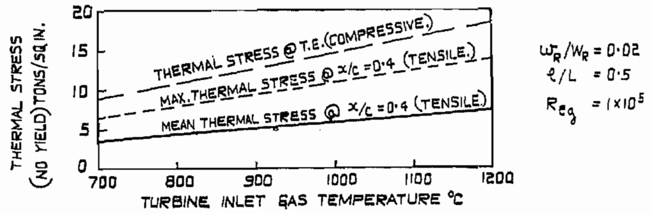


FIG. 26c.

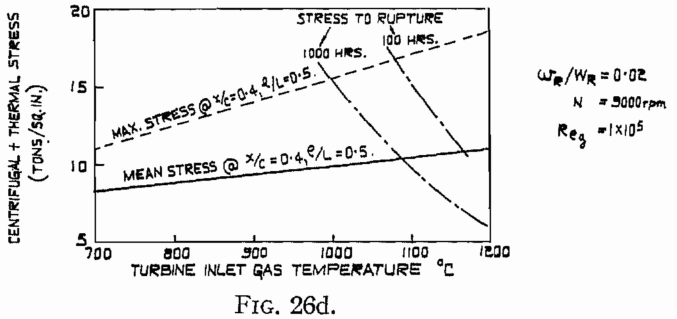


FIG. 26d.

FIGS. 26a to 26d. Comparison of rotor blade stresses with permissible operating stresses for blade material (sintered tungsten-vitallium).

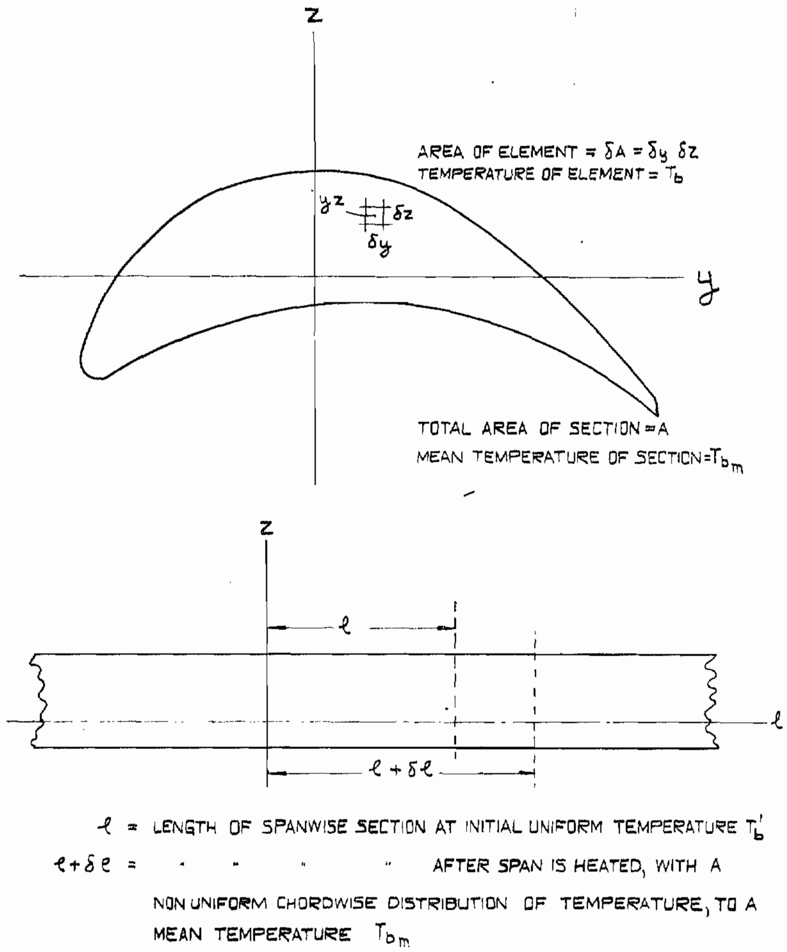


FIG. 27. Calculation of thermal stress.



J4369 Wt.20/9036 K7 6/56 D&Co. 34/263

PRINTED IN GREAT BRITAIN

# Publications of the Aeronautical Research Council

## ANNUAL TECHNICAL REPORTS OF THE AERONAUTICAL RESEARCH COUNCIL (BOUND VOLUMES)

1939 Vol. I. Aerodynamics General, Performance, Airscrews, Engines. 50*s*. (51*s*. 9*d*.)
Vol. II. Stability and Control, Flutter and Vibration, Instruments, Structures, Seaplanes, etc. 63*s*. (64*s*. 9*d*.)

1940 Aero and Hydrodynamics, Aerofoils, Airscrews, Engines, Flutter, Icing, Stability and Control, Structures, and a miscellaneous section. 50*s*. (51*s*. 9*d*.)

1941 Aero and Hydrodynamics, Aerofoils, Airscrews, Engines, Flutter, Stability and Control, Structures. 63*s*. (64*s*. 9*d*.)

1942 Vol. I. Aero and Hydrodynamics, Aerofoils, Airscrews, Engines. 75*s*. (76*s*. 9*d*.)
Vol. II. Noise, Parachutes, Stability and Control, Structures, Vibration, Wind Tunnels. 47*s*. 6*d*. (49*s*. 3*d*.)

1943 Vol. I. Aerodynamics, Aerofoils, Airscrews. 80*s*. (81*s*. 9*d*.)
Vol. II. Engines, Flutter, Materials, Parachutes, Performance, Stability and Control, Structures. 90*s*. (92*s*. 6*d*.)

1944 Vol. I. Aero and Hydrodynamics, Aerofoils, Aircraft, Airscrews, Controls. 84*s*. (86*s*. 3*d*.)
Vol. II. Flutter and Vibration, Materials, Miscellaneous, Navigation, Parachutes, Performance, Plates and Panels, Stability, Structures, Test Equipment, Wind Tunnels. 84*s*. (86*s*. 3*d*.)

1945 Vol. I. Aero and Hydrodynamics, Aerofoils. 130*s*. (132*s*. 6*d*.)
Vol. II. Aircraft, Airscrews, Controls. 130*s*. (132*s*. 6*d*.)
Vol. III. Flutter and Vibration, Instruments, Miscellaneous, Parachutes, Plates and Panels, Propulsion. 130*s* (132*s*. 3*d*.)
Vol. IV. Stability, Structures, Wind tunnels, Wind Tunnel Technique. 130*s*. (132*s*. 3*d*.)

## ANNUAL REPORTS OF THE AERONAUTICAL RESEARCH COUNCIL—

1937 2*s*. (2*s*. 2*d*.) 1938 1*s*. 6*d*. (1*s*. 8*d*.) 1939–48 3*s*. (3*s*. 3*d*.)

## INDEX TO ALL REPORTS AND MEMORANDA PUBLISHED IN THE ANNUAL TECHNICAL REPORTS, AND SEPARATELY—

April, 1950 - - - - - - R. & M. No. 2600. 2*s*. 6*d*. (2*s*. 8*d*.)

## AUTHOR INDEX TO ALL REPORTS AND MEMORANDA OF THE AERONAUTICAL RESEARCH COUNCIL—

1909–January, 1954 - - - - R. & M. No. 2570. 15*s*. (15*s*. 6*d*.)

## INDEXES TO THE TECHNICAL REPORTS OF THE AERONAUTICAL RESEARCH COUNCIL—

| | | |
|---|---|---|
| December 1, 1936 — June 30, 1939. | R. & M. No. 1850. | 1*s*. 3*d*. (1*s*. 5*d*.) |
| July 1, 1939 — June 30, 1945. - | R. & M. No. 1950. | 1*s*. (1*s*. 2*d*.) |
| July 1, 1945 — June 30, 1946. - | R. & M. No. 2050. | 1*s*. (1*s*. 2*d*.) |
| July 1, 1946 — December 31, 1946. | R. & M. No. 2150. | 1*s*. 3*d*. (1*s*. 5*d*.) |
| January 1, 1947 — June 30, 1947. - | R. & M. No. 2250. | 1*s*. 3*d*. (1*s*. 5*d*.) |

## PUBLISHED REPORTS AND MEMORANDA OF THE AERONAUTICAL RESEARCH COUNCIL—

| | | |
|---|---|---|
| Between Nos. 2251–2349. - - | R. & M. No. 2350. | 1*s*. 9*d*. (1*s*. 11*d*.) |
| Between Nos. 2351–2449. - - | R. & M. No. 2450. | 2*s*. (2*s*. 2*d*.) |
| Between Nos. 2451–2549. - - | R. & M. No. 2550. | 2*s*. 6*d*. (2*s*. 8*d*.) |
| Between Nos. 2551–2649. - - | R. & M. No. 2650. | 2*s*. 6*d*. (2*s*. 8*d*.) |

*Prices in brackets include postage*

HER MAJESTY'S STATIONERY OFFICE

York House, Kingsway, London W.C.2; 423 Oxford Street, London W.1; 13a Castle Street, Edinburgh 2; 39 King Street, Manchester 2; 2 Edmund Street, Birmingham 3; 109 St. Mary Street, Cardiff; Tower Lane, Bristol 1; 80 Chichester Street, Belfast, *or through any bookseller*

S.O. Code No. 23-2975